APPLICATION OF RECYCLED CONCRETE AGGREGATE FOR STABILIZING LATERITE SOIL

BY

SYAIFULLOH QOIMUDDIN

A THESIS SUBMITTED IN PARTIAL FULFILLMENT OF THE REQUIREMENTS FOR THE DEGREE OF MASTER OF SCIENCE (ENGINEERING AND TECHNOLOGY)

SIRINDHORN INTERNATIONAL INSTITUTE OF TECHNOLOGY

THAMMASAT UNIVERSITY

ACADEMIC YEAR 2024

Ref. code: 25676522040077WTA

THAMMASAT UNIVERSITY

SIRINDHORN INTERNATIONAL INSTITUTE OF TECHNOLOGY

THESIS

BY

SYAIFULLOH QOIMUDDIN

ENTITLED

APPLICATION OF RECYCLED CONCRETE AGGREGATE
FOR STABILIZING LATERITE SOIL

was approved as partial fulfillment of the requirements for
the degree of Master of Science (Engineering and Technology)

on December 2, 2024

Chairperson

(Associate Professor Pulpong Pongvithayapanu, Ph.D.)

Member and Advisor

(Associate Professor Amin Eisazadeh Otaghsaraei, Ph.D.)

Member

(Associate Professor Ganchai Tanapornraweekit, Ph.D.)

Director

(Professor Pruettha Nanakorn, D.Eng.)

Ref. code: 25676522040077WTA

Thesis Title	APPLICATION OF RECYCLED CONCRETE AGGREGATE FOR STABILIZING LATERITE SOIL
Author	Syaifulloh Qoimuddin
Degree	Master of Science (Engineering and Technology)
Faculty/University	Sirindhorn International Institute of Technology/ Thammasat University
Thesis Advisor	Associate Professor Amin Eisazadeh Otaghsaraei, Ph.D.
Academic Years	2024

ABSTRACT

The increasing urgency for sustainable development, driven by challenges such as global warming and extreme weather, necessitates innovative solutions in construction practices. Construction and demolition waste (CDW) recycling is a pivotal strategy to address environmental concerns while conserving natural resources. This study investigates the use of recycled concrete aggregate (RCA) and lime as stabilizers for improving the engineering properties of laterite soil (LS), a material commonly employed in road construction in Thailand but often deficient in required subgrade properties. RCA, a byproduct of demolition waste, offers potential as a sustainable alternative to natural aggregates.

A series of laboratory tests, including compaction, unconfined compressive strength (UCS), direct shear, California Bearing Ratio (CBR), and permeability tests, were conducted on various mix designs comprising LS, RCA, and lime. The results demonstrated that incorporating 45% RCA and 6% lime yielded the highest UCS and CBR values, meeting the Department of Highways (DOH) standards for subbase materials. UCS tests revealed a 7.1-fold strength increase in lime-treated mixtures after 56 days of curing, with the formation of calcium silicate hydrate (C-S-H) gels confirmed through FESEM and EDS analyses. This microstructural improvement was attributed to the pozzolanic reactions and cementitious properties of RCA and lime.

Ref. code: 25676522040077WTA

Furthermore, the addition of RCA enhanced soil gradation, reduced plasticity, and increased permeability, while lime mitigated water absorption and further stabilized the soil structure. These findings highlight the efficacy of RCA and lime in transforming laterite soil into a sustainable and cost-effective construction material, contributing to environmentally responsible infrastructure development in Thailand and beyond.

Keywords: Laterite soil, Recycled concrete aggregate, Lime, Compaction, UCS, Shear strength, CBR, Permeability test.

Ref. code: 25676522040077WTA

ACKNOWLEDGEMENTS

First and foremost, I would like to extend my deepest gratitude to my thesis advisor, Assoc. Prof. Dr. Amin Eisazadeh, for his unwavering support, insightful guidance, and encouragement throughout my research journey. It has been a privilege to work under his mentorship and benefit from his vast expertise. I am also profoundly thankful to Associate Professor Ganchai Tanapornraweekit, Ph.D., the chair of my thesis committee, for his invaluable advice on material selection, data analysis, and presentation, which significantly enriched the quality of my work.

I wish to express my sincere appreciation to Associate Professor Pulpong Pongvithayapanu, Ph.D., my external committee member, for his thoughtful feedback and recommendations, which added depth and impact to this research. I am extremely grateful to Sirindhorn International Institute of Technology (SIIT) for their generous support through the "Excellent Foreign Students" (EFS) Scholarship Program. This financial assistance, along with access to advanced test facilities, was instrumental in the successful completion of my research.

I owe a special acknowledgment to my family and friends for their unwavering love and encouragement during this demanding academic journey. Their prayers, advice, and both emotional and financial support have been a source of strength and inspiration throughout this process. Lastly, I dedicate this achievement to Almighty Allah (S.W.T), whose blessings and guidance have sustained me through every challenge, allowing me to accomplish this significant milestone in my academic career. Alhamdulillah!

Syaifulloh Qoimuddin

Ref. code: 25676522040077WTA

TABLE OF CONTENTS

Ref. code: 25676522040077WTA

Ref. code: 25676522040077WTA

Ref. code: 25676522040077WTA

LIST OF TABLES

Ref. code: 25676522040077WTA

Ref. code: 25676522040077WTA

LIST OF FIGURES

Ref. code: 25676522040077WTA

Ref. code: 25676522040077WTA

Ref. code: 25676522040077WTA

LIST OF SYMBOLS/ABBREVIATIONS

Symbols/ Abbreviations	Terms
A	Cross-sectional area of the specimen
AASHTO	American Association of State Highway and Transportation Officials
Al	Aluminum
Al_2O_3	Aluminum Oxide
ASTM	American Society of Testing and Materials
BA	Bottom Ash
BrO_2	Bromine (II) Oxide
c	Cohesion
Ca	Calcium
C-A-H	Calcium Alumina Hydrates
CaO	Calcium Oxide
$Ca(OH)_2$	Calcium Hydroxide
CB	Crushed Brick
CBR	California Bearing Ratio
C_c	Coefficient of Gradation
CDW	Construction Demolition Waste
CF	Coir Fiber
CL	Lean Clay
CO_2	Carbon (II) Oxide
C-S-H	Calcium Silica Hydrates
C_u	Coefficient of Uniformity
Dr	Relative Density
DS	Direct Shear
DOH	Department Of Highway
EDS	Electron Dispersive X-ray Spectroscopy
FA	Fly Ash
Fe_2O_3	Iron (III) Oxide

Ref. code: 25676522040077WTA

FESEM	Field Emission Scanning Electron Microscopy
Fɣ	Unit Weight Factor
g	Acceleration due to gravity
GGBS	Ground Granulated Blast-furnace Slag
GP	Glass Powder
GP-GC	Poorly graded gravel with clay
Gs	Specific Gravity
ICL	Initial Consumption Lime
k	Permeability Coefficient
K_2O	Potassium Oxide
L	Lime
L	Longitudinal dimension of the specimen
LL	Liquid Limit
LS	Laterite Soil
MDD	Maximum Dry Density
MDUW	Maximum Dry Unit Weight
MgO	Magnesium Oxide
MH-OH	Silty Clay
ML	Silt
ML-OL	Silty Soil
MnO_2	Magnesium (II) Oxide
MSW	Municipal Solid Waste
OH-	Hydroxyl ion
OLC	Optimum Lime Content
OMC	Optimum Moisture Content
P	Water Pressure applied
pH	Hydrogen Potential
PI	Plasticity Index
PL	Plastic Limit
Q	Rate of water flow

Ref. code: 25676522040077WTA

RAP	Recycled Asphalt Pavement
RA	Recycled Aggregate
RC	Recycled Concrete
RCA	Recycled Concrete Aggregate
SC	Clayey Sand
SC-SM	Clayey Sand with Silt
SEM	Scanning Electron Microscopy
Si	Silicon
SM	Silty Sand
SiO_2	Silicon (II) Oxide
SO_3	Sulphur (III) Oxide
SP	Poorly Graded Sand
TiO_2	Titanium Oxide
UCS	Unconfined Compressive Strength
USCS	Unified Soil Classification System
ρ	Density of water
ϕ’	Friction Angle

Ref. code: 25676522040077WTA

CHAPTER 1
INTRODUCTION

1.1 Background of the Study

With the accelerating pace of urbanization and technological development, global consumption patterns have resulted in a significant rise in solid waste production. Construction and Demolition Waste (CDW), has emerged as a significant contributor to this problem, presenting both environmental and economic difficulties (Hoang et al., 2020; Jain et al., 2017). In Thailand, CDW generation increased dramatically from an average of 1.1 million tons between 2002 and 2005 to 7.2 million tons by 2014 (Kofoworola & Gheewala, 2009; Thongkamsuk et al., 2017). This surge highlights the need for sustainable waste management strategies, particularly in the context of road infrastructure development (Nghiem et al., 2020). CDW, which includes waste created from the renovation, construction, and demolition of buildings, is often disposed of in landfills, contributing to the already strained landfill capacities (Reis et al., 2021).

Several countries have documented the vast amounts of waste generated from construction and demolition. Australia, for example, produces over 3.3 million tons of demolition concrete, 1.3 million tons of demolition bricks, and 8.7 million tons of excavated rock annually (Rahman et al., 2015). Similarly, Spain's construction sector generates approximately 72 tons of waste daily, while across the European Union (EU), about 900 million tons of CDW are produced each year (Arulrajah et al., 2012; Arulrajah et al., 2013). Asian countries also face challenges in managing CDW; China generated 1.6 billion tons in 2016, while Myanmar and Vietnam produced 9.49 and 8.8 million tons, respectively (Makul et al., 2021; Zhang et al., 2021).

Given the escalating production of CDW and the limited capacity of landfill sites, especially in urban areas, there is an increasing need for sustainable waste management solutions. Crushed Brick (CB), Recycled Concrete Aggregate (RCA), and Reclaimed Asphalt Pavement (RAP) have emerged as common materials in geotechnical applications (Arulrajah et al., 2014). In Thailand, the management of CDW, particularly in densely populated regions like Bangkok, has become critical due

Ref. code: 25676522040077WTA

to rapid urbanization and the growing number of construction projects (Chinda et al., 2012).

Although many governments have implemented regulations to manage solid waste, Thailand's existing framework lacks adequate enforcement and a permanent disposal system for construction waste (Yukalang et al., 2017), Table 1.1 highlights the overburdened capacity of landfills in Thailand. The use of RCA in road construction offers a potential solution by reducing the reliance on natural aggregates while promoting sustainability (Chinda et al., 2012; Kofoworola & Gheewala, 2009; Tanthanawiwat et al., 2024).

Due to the abundance of CDW and its ability to reduce reliance on limited natural aggregate resources, utilizing construction waste in pavement base and subbase layers is regarded as an effective and eco-friendly option (Arulrajah et al., 2013; Ok et al., 2020). In road construction, the unbound base and subbase layers are essential in distributing wheel loads to the subgrade and bearing the weight transferred from the surface, which typically consists of existing soil (Blankenagel & Guthrie, 2006). Numerous research has explored the mechanical properties of RCA as alternative materials for unbound bases and subbases, with the goal of creating long-lasting and sustainable pavement systems (Bennert & Maher, 2008; Thai et al., 2022).

RCA are known to have higher water absorption capacity, lower specific gravity, and less resistance to abrasion when compared to natural aggregates (Poon & Chan, 2006). Due to concerns about potential performance limitations, RCA are commonly utilized as materials for base and subbase layers in road pavement construction (Arulrajah et al., 2014; Haider et al., 2014). Despite these limitations, RCA have been successfully used in many projects, providing the significant benefit of conserving natural aggregate resources (Tavakol et al., 2020). Research has shown that the use of RCA can improve the stabilization of soils with high liquid limits. Soils with high liquid limits are usually avoided for subgrade filling during construction because of their high natural moisture content, poor load-bearing capacity, and instability when immersed (Ma et al., 2022). Untreated soils are unsuitable for direct use in road surfaces due to risks of engineering failures, such as uneven settlement, slope collapse, or debris flows. However, with appropriate treatment, soils with high liquid limits can still be used effectively for road embankment filling (Arulrajah et al., 2013; Ma et al., 2022).

Ref. code: 25676522040077WTA

Table 1.1 Amount of landfill with capacity overload ((Chinda et al., 2012)).

Region	Location of landfill	Province	Area (m^2)	Amount of waste transferred (tons / day)
North	Maesot	Tak	27.2	70-90
Central	Town Municipality	Ayutthaya	30	80-100
	Provincial administrative organization	Nonthaburi	186	1000-1200
Northeast	Town Municipality	Loei	52	70-90
East	Pattaya	Chonburi	140	330-400
	Maptaphut	Rayong	33	100-120
	Town Municipality	Chanthaburi	117	100-200
	Aranyaprathet	Sakaeo	8	20-35
South	Town Municipality	Chumphon	56	60-80
	City Municipality	Nakhon Sithammarat	200	300-400
	Town Municipality	Phatthalung	65	40-60

1.2 Statement of Problem

Although the use of RCA as a sustainable construction material in Thailand is gaining attention, various challenges persist. There is a lack of clear guidelines and standards for its use, insufficient testing methods, and limited awareness among stakeholders in the construction industry. The enforcement of regulations surrounding CDW management also remains inadequate. Given that Bangkok's soil is predominantly expansive and has a high liquid limit, the need for effective soil stabilization techniques is paramount. Current mechanical stabilization methods are often hindered by the moisture sensitivity of expansive soils, which can lead to swelling and other engineering failures (Kianimehr et al., 2019; Ma et al., 2022; Yaghoubi et al., 2021).

Laterite soils, which are widely used in road construction throughout Thailand, present additional challenges. These soils are characterized by low plasticity and poor

Ref. code: 25676522040077WTA

drainage capacity, which often lead to issues such as shrinkage, swelling, and structural instability under varying moisture conditions. Research has indicated that the engineering characteristics of lateritic soils often fail to comply with the required specifications for road base and subbase layers, resulting in considerable road degradation. This issue is particularly pronounced in rural regions, where inadequate drainage conditions further worsen the problem (Jotisankasa et al., 2020). Common failures include the development of potholes, cracking, and surface deformations, all of which increase maintenance costs and pose safety risks

This study aims to tackle these issues by investigating the potential of RCA combined with lime as a stabilizing agent to enhance the mechanical performance of lateritic soils for applications in road base and subbase layers. Soil improvement through the use of construction waste materials like RCA offers a promising solution to enhancing soil strength while minimizing environmental impact.

1.3 Objectives of the Study

RCA, produced from construction and demolition waste, exhibits a particle size distribution comparable to that of natural aggregates, making it a viable material for pavement construction. This study seeks to evaluate the potential of RCA in stabilizing lateritic soils, with a focus on achieving the following objectives:

1. Evaluate the effectiveness of RCA in the light stabilization of lateritic soils while promoting sustainability by reducing the disposal of construction waste in landfills.
2. Evaluate the influence of RCA and lime on the compaction characteristics of soil mixtures.
3. Measure the changes in unconfined compressive strength (UCS) and shear strength (Direct Shear) when RCA and lime are used as stabilizers.
4. Determine the bearing capacity of stabilized material through California Bearing Ratio (CBR) tests.
5. Conduct microstructural analysis through Field Emission Scanning Electron Microscopy (FESEM) and Electron Dispersive X-Ray Spectroscopy (EDS).

Ref. code: 25676522040077WTA

1.4 Significance of the Study

The rising amounts of construction waste, coupled with diminishing landfill space, are pressing environmental concerns in many countries, including Thailand. This situation has led to serious environmental impacts and has become a major focus of research. The use of waste materials in soil stabilization has gained considerable interest in various geotechnical engineering applications, driven by the rapid increase in construction demolition waste. Researchers are actively investigating methods to reduce waste through its application in soil stabilization.

In this study, the use of RCA and lime as stabilizers in soil not only addresses waste disposal challenges but also offers cost-effective alternatives to natural materials in road construction. This research will contribute to the growing body of knowledge on soil stabilization using construction waste materials, providing valuable insights for geotechnical engineering projects and paving the way for more sustainable construction practices.

1.5 Scope of Work

This research investigated the stabilization of laterite soils through the utilization of recycled concrete aggregates sourced from construction and demolition waste, in combination with lime. The study addressed the following aspects:

I. Materials

- Type of soil : Lateritic Soil (LS)
- Type of stabilizer : Recycled Concrete Aggregate (RCA)
- Type of binding material : Hydrated lime (L)

II. Mixtures

- The Amount of RCA : 0, 5, 15, 30 and 45% by weight of dry soil
- The Amount of lime : 6% by weight of sample
- The amount of water : based on the OMC of mixes.

Ref. code: 25676522040077WTA

III. Laboratory Tests

- Basic laboratory tests consist of the Atterberg limit test (LS), specific gravity determination, particle size distribution through sieve and hydrometer analyses, the Los Angeles abrasion test (RCA), and compressive strength measurement (RCA)
- Standard Compaction Test
- Unconfined Compressive Strength (UCS) Test
- Direct Shear (DS) Test
- California Bearing Ratio (CBR) Test
- Permeability Test

IV. Curing Conditions

- Humid curing at room temperature

V. Curing Periods

- Unconfined Compressive Strength Test: 0, 7, 28 and 56 days
- Direct Shear Test: 0, 28 and 56 days
- CBR Test: 0 and 7 days
- Permeability Test: 28 and 56 days
- FESEM and EDS: 56 days

Ref. code: 25676522040077WTA

CHAPTER 2
LITERATURE REVIEW

2.1 Variety of Soil in Thailand

Thailand predominantly experiences a tropical climate and diverse topography, which ranges from lowlands to mountainous regions, contribute to the presence of various soil types (Bhurtel & Eisazadeh, 2020; Horpibulsuk et al., 2013). Common soils include alluvial soils, rich in minerals and ideal for rice cultivation, as well as lateritic soils, typically found in the central and northeastern regions. Additionally, red and yellow soils are prominent in the north and east, while sandy and clayey soils are present in other areas (Kumar et al., 2022b).

A notable soil type is Bangkok Clay, which occurs primarily along the Chao Phraya River basin, including Bangkok and adjacent provinces like Pathum Thani (Bhurtel & Eisazadeh, 2020; Suksiripattanapong et al., 2022). This clay is characterized by its high smectite content, mixed with illite and montmorillonite (54% to 71%), kaolinite (28% to 36%), and mica (Eisazadeh et al., 2019; Teerachaikulpanich & Phupat, 2003; Vichan & Rachan, 2013). The high-water content in Bangkok Clay makes it highly susceptible to water-induced swelling and shrinkage, with its swelling potential increasing at greater depths, complicating its geotechnical properties. Bangkok Clay exhibits limited shear strength and a strong water affinity, posing substantial construction challenges. When subjected to moisture, it tends to swell, while drying causes shrinkage, resulting in instability within the soil structure (Ratananikom et al., 2015; Teerawattanasuk et al., 2015). As a result, ground improvement techniques are often required before constructing large structures on this soil type.

In contrast, laterite soils (LS) are more commonly utilized, particularly in road construction across central and northeastern Thailand. This soil type possesses good binding properties and sufficient strength when dry, making it suitable for use in pavement layers. However, the engineering characteristics of lateritic soils can vary significantly depending on location, often necessitating stabilization to meet strength requirements, especially for highway construction (Panoottikorn, 2018; Vejchasarn et al., 2021). Stabilization methods, such as lime or cement, are frequently employed to

Ref. code: 25676522040077WTA

enhance the soil's load-bearing capacity and mitigate its susceptibility to moisture-related expansion and contraction. While LS is generally more favorable for construction compared to Bangkok Clay, its variable properties still require careful consideration to meet infrastructure project standard.

In both Bangkok Clay and LS, the application of appropriate soil improvement techniques is critical for improving performance in construction, ensuring the long-term stability and durability of infrastructure projects in Thailand under operational and environmental stresses.

2.2 Laterite Soil

The word "laterite" is originating from the Greek term "later," which means "brick," or, more specifically, "lateritis," which means "brick disease." It is widely attributed to Buchanan et al. (Buchanan, 1807), who first introduced it in 1807 to describe a material that is initially soft and can be easily cut with iron tools but hardens like brick when exposed to air, responding to both atmospheric and moisture conditions (Archwichai et al., 1993; Buchanan, 1807; Vallerga & Van Til, 1970). LS are predominantly found in tropical areas, exhibiting colors ranging from reddish to brick red in shaded regions, with variations from dark brown to rusty red (Abd Rashid et al., 2019; Kumar et al., 2022a; Udoeyo et al., 2006).

Laterite soil forms through extensive weathering and is characterized by high concentrations of alumina and/or iron oxide (Tan et al., 2016). Its cohesive and non-cohesive properties are largely dependent on particle size distribution. LS with a higher proportion of clay and silt exhibit cohesive behavior, whereas those dominated by sand-sized particles are non-cohesive (Kumar et al., 2022a; Oyelami & Van Rooy, 2016). Cohesive LS are notable for their plasticity, stable strength, and susceptibility to erosion and swelling (Tran et al., 2022). In Thailand, where the climate is tropical, laterite soils are widespread across lowland areas and the rocky, mountainous regions of the north (Horpibulsuk et al., 2013).

In Thailand, LS is commonly employed as a primary material for road pavement bases and subbase layers and as backfill material due to its load-bearing capacity (Chantruthai et al., 2017). However, this material is not universally applicable, as various laterite soil types found in tropical regions may fail to meet the necessary

Ref. code: 25676522040077WTA

strength requirements. High-quality laterite soil is often abundant, particularly in protected forest areas (Kheoruenromne, 1987). Nonetheless, due to the limited availability of crushed rock in many parts of Thailand and the environmental concerns associated with rock quarrying, laterite soil is increasingly favored as a viable alternative (Chan & Low, 2010; Chantruthai et al., 2017). Unfortunately, deforestation has resulted in severe environmental challenges, such as increased atmospheric carbon dioxide, altered water cycles, accelerated soil erosion, and biodiversity loss. Consequently, sustainable practices, such as mechanical or chemical stabilization or the incorporation of industrial by-products, are crucial for preserving virgin laterite soil (Meepon et al., 2019; Tam & Tam, 2006).

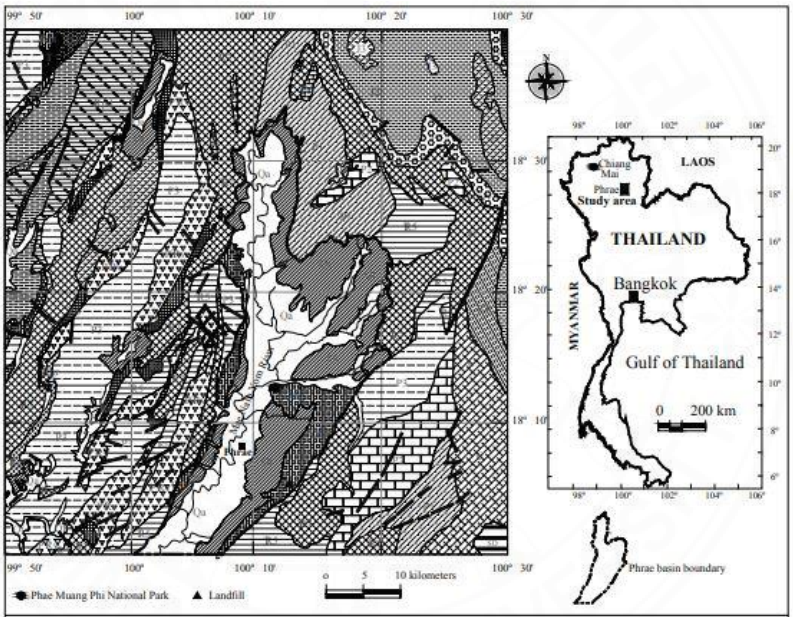

LEGEND

Quaternary	SEDIMENTS Qa Alluvial deposits : gravel, sand, silt, clay, and mud Qt Terrace deposits: gravel, sand, silt, and lateritic soil Qth High terrace deposits : gravel beds, sand, silt and clay with laterite and lateritic soil Qc Colluvial unit: rock fragments,gray, red, covered with clayey sand and laterite	Triassic	TRpt Interbedded black shale, tuff, sandstone and conglomerate
Tertiary	SEDIMENTARY AND METAMORPHIC ROCKS T Interbedded claystone, sandstone and mudstone	Permian	PTR Sandstone, siltstone, shale and conglomerate P3 Interbedded black shale, gray sandstone and limestone P2 Massive limestone, calcareous shale and sandstone P1 Phyllite, gray sanstone, siltstone, quartzite and schist
Jurassic	J3 Arkosic sandstone and shale J2 Sandstone, shale, tuffaceous and conglomerate	Carboniferous	C Quartzite and feldspatite sandstone
Triassic	TR7 Shale and sandstone and limestone TR6 Limestone, gray, massive to bedded; shale and sandstone TR5 Sandstone, siltstone, shale and conglomerate TRpd Sandstone, siltstone, conglomerate and shale TRhh Silicified mudstone, tuffaceous sandstone, shale and siltstone	Silurian	SD Phyllite, phyllitic shist and quartzofeldspatic schist
		Jurassic	IGNEOUS ROCKS Jv Rhyolite, purplish gray, tuffaceous shale and sandstone
		Triassic	TRgr Granite and adamellite
		Permian	PTRv Volcanic rocks : rhyolite, andesite, rhyolitic tuff and andesitic tuff
			fault

Modified from Department of Mineral Resources (1994) and Won-In (2003)

Figure 2.1 Laterite soil distribution map in Thailand,(Soe et al., 2008).

Ref. code: 25676522040077WTA

The northeastern region of Thailand dominates laterite soil production, providing approximately 42% of the total supply, whereas the southern region contributes a comparatively smaller share of 12.23% (Chantruthai et al., 2017). Historically, laterite soil has been employed as a substitute for crushed rock due to its notable load-bearing capacity (Kumar et al., 2022a). The distant location of quarry materials from construction sites often results in higher construction costs (Meepon et al., 2019). Table 2.1 summarizes the standard characteristics of laterite soil, encompassing specific gravity, liquid limit, plasticity index, and CBR values. Laterite soil is characterized by its reddish hue, which is primarily attributed to its high iron oxide content. The liquid limit ranges from 14.33 to 43.40, and the plasticity index varies between 3.50 and 22.56. The specific gravity of fine-grained laterite soil falls between 2.5 and 3.6, with maximum dry density (MDD) values ranging from 17.7 to 22.7 kN/m³, and optimal moisture content spanning from 4.10% to 13.10%.

The gradations requirements for base and subbase materials, as specified by the Department of Highways in Thailand, are detailed in Table 2.2. In Thailand, lateritic soils are categorized into grades A through E, where grade A represents the superior quality and grade E denotes the lowest standard. Soil stabilization is essential for enhancing both the structural integrity and durability of these materials, especially since lower-grade lateritic soils often demonstrate poor load-bearing capacity and are prone to erosion and degradation under changing environmental conditions

Ref. code: 25676522040077WTA

Table 2.1 Typical properties of Laterite soils in Thailand.

Properties of Laterite soil in Thailand	Authors								
	(Hoy et al., 2023)	(Chindaprasirt et al., 2023)	(Suksiripattanapong et al., 2022)	(Meepon et al., 2019)	(Pongsivasathit et al., 2019)	(Chantruthai et al., 2017)			(Phummiphan et al., 2017)
Location	Nakhon Ratchasima	Nakhon Ratchasima	Nakhon Ratchasima	Chachoengsao	Ratchaburi	Songkhla, Thailand			Rayong, Thailand
Color	-	Reddish	-	-	-	Dark Brown	Light Brown	Dark Brown	-
Liquid limit (%)	21	27	31	30	-	23.8	35.5	43.2	27.72
Plastic Limit (%)	8	7	21	19	-	15.47	23.76	24.52	20.9
Plasticity Index (%)	13	20	10	11	-	8.33	11.29	18.68	6.07
Specific Gravity	2.78	2.75	2.73	2.67	2.74	-	-	-	2.58
Maximum dry density (kN/m^3)	21.3	17.1	20.15	19.13	19.91	21.5	17.73	20.32	20.85
Optimum water content (%)	8.07	17.7	9.78	10	8	7	12.5	13	8
Classification AASHTO	-	SP	-	-	A1-A	A-2-4	A-6	A-7-6	A-2-4
USCS	GC	ML	SC	SC	GW	SC	CL	GC	SC-SM
CBR (%)	18	14.7	-	17	-	-	-	-	14.7

***Note: - (not detected)*

Ref. code: 25676522040077WTA

Table 2.2 Gradations of Base and Subbase materials (Department of Highways Thailand).

Sieve Size (mm)	Requirements				
	A	B	C	D	E
50	100	100	-	-	-
25	-	-	100	100	100
9.5	30-60	40-75	50-85	60-100	-
2	15-40	20-75	25-50	40-70	40-100
0.425	8-20	15-30	15-30	25-45	20-50
0.075	2-8	5-20	5-15	5-20	6-20

2.3 Chemical Composition of Lateritic Soil

Laterite soil is characterized by distinct stratified layers, with the upper horizons predominantly containing sesquioxides, especially iron (Fe_2O_3) and aluminum oxides (Al_2O_3), while the lower layers exhibit varying degrees of kaolinization. Upon exposure to atmospheric conditions, the soil undergoes a hardening process. This hardening occurs due to the precipitation, accumulation, and crystallization of iron and aluminum oxides. Water leaching facilitates the downward migration of iron, resulting in iron-rich concentrations in deeper layers (Maignien, 1966; Pereira-De-Oliveira et al., 2019). Table 2.3 details the chemical composition of laterite soil in Thailand as reported by various studies. On average, the soil consists of approximately 62.8% silica (SiO_2), 23.2% alumina (Al_2O_3), and 8.6% iron (Fe_2O_3).

Table 2.3 Chemical composition of Laterite soil.

Authors	Oxide								
	SiO_2	Al_2O_3	Fe_2O_3	CaO	SO_3	TiO_2	K_2O	MnO	MgO
(Chindaprasirt et al., 2023)	61.84	25.08	9.02	0.77	0.06	-	0.96	-	0.98
(Suksiripattanapong et al., 2022)	54.7	22.15	11.3	6.5	-	-	-	-	1.3
(Chindaprasirt et al., 2020)	49.93	45.48	2.52	0.26	0.47	-	0.42	-	0.1
(Pongsivasathit et al., 2019)	73.96	19.06	4.47	0.34	0.06	0.67	0.84	-	0.39
(Phummiphan et al., 2017)	77.81	4.42	10.93	1.13	1.36	1.33	2.33	0.55	-
(Donrak et al., 2016)	58.82	23.06	13.38	1.42	-	0.86	0.82	-	0.84

***Note: - (not detected)*

Ref. code: 25676522040077WTA

2.4 Soil Stabilization

Soil stabilization encompasses a range of techniques and chemical treatments aimed at improving the strength and durability of naturally unstable soils, making them more suitable for supporting construction activities (Xu et al., 2021). The primary goal is to address poor soil engineering properties, such as low bearing capacity, susceptibility to erosion, and volumetric changes caused by moisture variations. Stabilization methods include traditional practices like mechanical compaction and advanced techniques, such as jet grouting, deep soil mixing and electro-osmotic stabilizaton (Fondjo et al., 2021). Mechanical compaction reduces pore space and increases soil density through applied pressure. Additionally, stabilization procedures often involve compaction testing, pre-consolidation, and drainage measures, among other methods (Archibong et al., 2020).

Poor soil conditions can compromise the longevity and structural integrity of construction projects. Establishing a stable foundation is crucial for maintaining the durability and performance of buildings and pavements over time. Unstable soil can cause serious problems, such as differential settlement during seismic activity or shrink-swell behavior of expansive soils, which may result in pavement cracking (Negi et al., 2013). The utilization of soil stabilization methods can substantially enhance the strength and longevity of construction materials, leading to a reduction in overall project expenses. By improving the load-bearing capacity of the foundation, these methods enable the development of complex structures without necessitating expensive excavation or additional reinforcement measures (Zada et al., 2023). Furthermore, utilizing local materials as stabilizing agents can reduce transportation and material expenses, further lowering overall construction costs by minimizing the reliance on imported or expensive resources (Magnusson et al., 2015).

2.4.1 Chemical Stabilization

Chemical stabilization refers to the use of various additives, including lime, cement, fly ash, bottom ash, rice husk ash, polymers, and recycled construction materials, to enhance soil properties. Ongoing research continues to explore the use of these stabilizing agents in geotechnical engineering (Anupam et al., 2016; Barman & Dash, 2022), each presenting unique advantages and limitations. Studies have

Ref. code: 25676522040077WTA

demonstrated that these stabilizers can improve several geotechnical properties, including UCS, shear strength, CBR, hydraulic conductivity, and reduce soil shrinkage and swelling (Anupam et al., 2016; Barman & Dash, 2022; Bhurtel & Otaghsaraei, 2018).

Polymer compounds are typically manufactured through synthetic processes, resulting in challenges related to sourcing and high production costs. Commonly employed materials in soil stabilization include Fly Ash (FA), lime (L), and Rice Husk Ash (RHA), each offering distinct advantages such as cost-effectiveness, wide availability, and eco-friendliness (Domphoeun & Eisazadeh, 2024). In recent years, the focus on sustainable construction methods has intensified, leading to the exploration of alternative materials for soil stabilization. One promising approach involves utilizing demolition waste, particularly Recycled Concrete Aggregate (RCA), to enhance soil properties while concurrently addressing the issue of construction waste management (Kianimehr et al., 2019; Shourijeh et al., 2022).

2.4.2 Traditional Stabilizers

Lime is one of the most extensively utilized agents in soil stabilization, either by itself or in combination with other additives. This method is well-established in civil engineering for enhancing both the mechanical and chemical properties of soils (Al-Swaidani et al., 2016). Lime is commonly found in two variants: quicklime (CaO) and hydrated lime ($Ca(OH)_2$), both of which are utilized in soil stabilization to enhance strength, durability, and workability. This technique is particularly effective for stabilizing soils with high plasticity, expansive clays, or low bearing capacities (Ebailila et al., 2022; Negi et al., 2013; Obuzor et al., 2012). As an alternative to traditional cement stabilization, lime provides a cost-effective solution that can reduce both financial and environmental costs, often delivering results that are comparable or even superior to cement.

Cement is another traditional stabilizers that contains significant amounts of pozzolanic compounds, primarily silica and alumina, which enhance soil stabilization by improving its geotechnical characteristics, such as strength and durability (Pourakbar & Huat, 2017). However, cement use presents certain challenges. It is often costly, and its transportation and application can be difficult, particularly in remote

Ref. code: 25676522040077WTA

areas. Moreover, cement's high alkalinity may alter soil pH, negatively impacting plant growth (Consoli et al., 2021). The energy-intensive production of cement, which relies heavily on fossil fuels such as petroleum and natural gas, also leads to substantial CO_2 emissions. Additionally, improper application or inadequate curing of cement-stabilized soils can undermine long-term strength and durability, compromising structural integrity (Al-Mukhtar et al., 2012).

Lime-treated soil undergoes four key chemical processes: cation exchange, flocculation and agglomeration, carbonation, and pozzolanic reactions. Since the 1960s, significant advancements have been made in understanding these reactions and their effects on soil-lime mixtures (Thompson, 1967). Various forms of lime, particularly quicklime (CaO) and hydrated lime ($Ca(OH)_2$), have been widely used in geotechnical applications (Amadi & Okeiyi, 2017). Lime treatment is recognized as an economical method for modifying and stabilizing soils by improving their engineering properties. The term "lime modification" refers to the initial strength gains through cation exchange, while the pozzolanic reaction leads to further cementation effects. When lime reacts with water, it creates a cementing agent that enhances soil properties (Al-Mukhtar et al., 2012; Eisazadeh et al., 2011; Thompson, 1967).

The interaction between lime and pozzolanic materials generates calcium silicate hydrate (C-S-H) and calcium aluminate hydrate (C-A-H) compounds, which significantly enhance the properties of the soil. These reactions improve soil strength and reduce its density, making lime a highly efficient binder. Additionally, naturally occurring pozzolanic materials, such as clay minerals, fly ash, and blast furnace slag, can participate in these reactions, albeit to a lesser extent (Jha & Sivapullaiah, 2015). The breakdown of the $Ca(OH)_2$ complex produces Ca^{2+} and OH^- ions. The OH^- ions interact with the soil, attracting Ca^{2+} ions, which enhances cohesion and increases the soil's density and Strength combination of lime with pozzolanic materials forms calcium-silicate-hydrate (C-S-H) or calcium-alumina-hydrate (C-A-H) compounds, which further improve the soil's characteristics. The breakdown of the $Ca(OH)_2$ complex produces Ca^{2+} and OH^- ions. The OH^- ions interact with the soil, attracting Ca^{2+} ions, which enhances cohesion and increases the soil's density and strength (Muntohar & Hantoro, 2000).

Ref. code: 25676522040077WTA

These cementitious compounds are analogous to those produced in conventional Portland Cement (PC), although the mechanism of calcium silicate formation differs. In Portland cement, calcium silicate forms through the hydration of anhydrous calcium silicate, whereas in lime-treated soil, the silica originates from the soil minerals (Muntohar & Hantoro, 2000; Muntohar et al., 2013). When quicklime reacts with water, it produces $Ca(OH)_2$ and heat, a process known as lime slaking as represented by the following equations:

$$Ca(OH)_2 + SiO_2 = C - S - H \quad (2.1)$$
$$Ca(OH)_2 + AlO_3 = C - A - H$$

Where, C-S-H stands for Calcium Silica Hydrates and C-A-H stands for Calcium Alumina Hydrates.

The application of lime stabilization is extensively employed in geotechnical and environmental engineering, encompassing areas such as pollutant containment, stabilization of backfill materials (e.g., wet cohesive soils), highway subgrade capping, slope reinforcement, and foundation enhancement through lime piles or lime-treated soil columns (Afrin, 2017).

2.5 Construction and Demolition Waste

The management of waste is typically classified into two primary types: Municipal Solid Waste (MSW) and Construction and Demolition Waste (CDW). The US Environmental Protection Agency (2012) defines MSW as the waste generated from household activities, including organic waste such as food scraps and yard trimmings, along with paper, plastic, glass, and metal. This type of waste accounts for approximately 50% of the global MSW, while inorganic materials like paper and plastics contribute about 30%. Alternatively, construction, renovation, and demolition activities generate CDW, which includes materials like concrete, steel, wood, brick, and asphalt, accounting for 10–30% of the total waste volume in landfills worldwide (Hoornwerg & Bhada-Tata, 2012).

Over the past decade, the volume of CDW has grown significantly in many countries due to increased urbanization and infrastructure development (Arulrajah et

Ref. code: 25676522040077WTA

al., 2012; Huang et al., 2002). CDW presents a global challenge, with many countries experiencing increasing amounts of this waste due to urban growth and construction activities. For example, in 2014, the European Union generated approximately 13.3 million tons of CDW, while the United States produced 534 million tons. Myanmar contributed around 9.49 million tons, followed by Vietnam at 8.88 million tons (Huang et al., 2002; Thongkamsuk et al., 2017). In Thailand, CDW generation saw a sharp increase from an average of 1.1 million tons between 2002 and 2005 to 7.2 million tons by 2014 (Kofoworola & Gheewala, 2009; Thongkamsuk et al., 2017). Other Southeast Asian countries, such as Singapore, produced around 1.54 million tons since 2015, while Cambodia, Indonesia, and Laos continue to face challenges in CDW management, with limited data available on waste generation (Menegaki & Damigos, 2018; Wu et al., 2014).

In Thailand, rapid industrial and urban expansion has led to a rise in both MSW and CDW production. The country's construction industry is a major contributor to this increase. Figure 2.2 illustrated the composition of MSW and CDW in Thailand, the composition of these waste streams shows that organic waste, paper, and plastic are dominant components of MSW, while CDW is primarily composed of concrete, steel, sand, and wood, especially in areas with high-rise construction activities (Chinda et al., 2012; Kofoworola & Gheewala, 2009). Concrete and brick accounts for 46% of CDW by weight, followed by gypsum, insulation, metal and others, which together constitute 6%, 2%, 1% and 26%, respectively (Arisha et al., 2016).

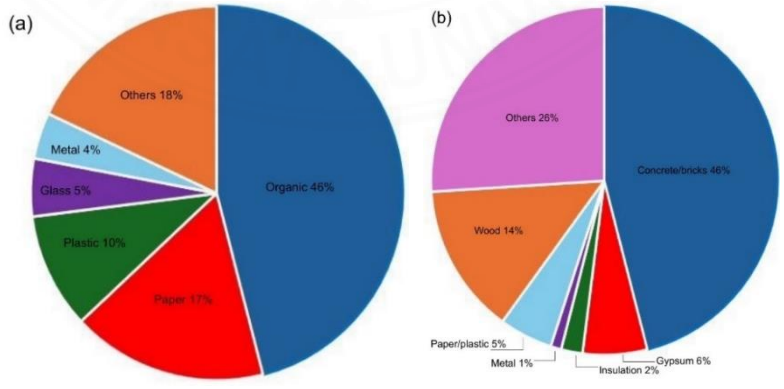

Figure 2.2 Waste management in Thailand (a) MSW and (b) CDW (Chinda et al., 2012).

Ref. code: 25676522040077WTA

Bangkok's waste management system relies on a network of transfer stations due to the lack of a permanent landfill within the city, as illustrated in Figure 2.3. Waste generated in Bangkok is transported to transfer stations such as Nong Kham, Sai Mai, and On-Nuch, where it is processed before being sent to landfills outside the city. For example, the Khampangsan landfill in Nakornpathom Province receives waste from the Nong Kham and Sai Mai stations, while the Phanomsarakham landfill in Chachoengsao Province processes waste from the On-Nuch station. The On-Nuch transfer station, which handles around 1,000 tons of waste per day, also operates as a composting facility, contributing to both waste reduction and resource recovery efforts (Arulrajah et al., 2012; Chinda et al., 2012; Kofoworola & Gheewala, 2009; Thongkamsuk et al., 2017).

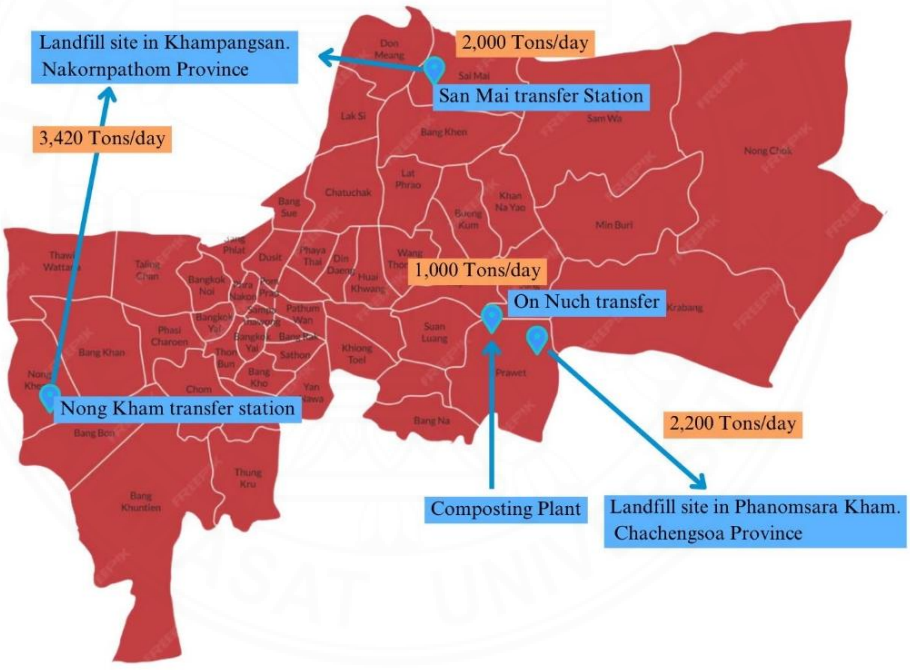

Figure 2.3 Transferred station in Bangkok(Modified by (Chinda et al., 2012).

An effective method for improving soil properties in geotechnical construction involves utilizing demolition waste materials, such as CB, RCA, and and RAP (Shourijeh et al., 2022). The reuse or recycling of demolition waste in construction not only mitigates pollution but also helps conserve natural aggregate resources. Among these materials, RCA constitutes a substantial fraction of the solid waste stream relative to CB and RAP, thereby making it a more widely utilized option in construction projects

Ref. code: 25676522040077WTA

(Kianimehr et al., 2019). Concrete waste is especially prevalent, accounting for 58% of the total weight, while brick, excavated rock, and asphalt contribute 16%, 15%, and 7%, respectively (Arulrajah et al., 2012; Victoria, 2010). The recycling of these materials, particularly through methods like converting concrete waste into crushed concrete aggregate, offers a more sustainable alternative to conventional soil stabilization techniques. Incorporating construction and demolition waste (CDW) into construction processes supports the circular economy framework by decreasing the reliance on virgin materials and mitigating the environmental impact associated with waste management (Villagrán-Zaccardi et al., 2022). Numerous studies have examined the sustainability of CDW for various technical applications, and many countries have successfully integrated recycled CDW as a key resource in geotechnical engineering.

2.5.1 Use of Recycled Concrete Aggregate as a Stabilizer

The rapid pace of urbanization and industrialization, driven by growing populations and economies, has led to significant exploitation of natural resources. Road construction, in particular, demands a large quantity of aggregate materials, constituting approximately 70 to 80 percent of the total road volume. The continuous extraction of these aggregates through quarrying not only depletes natural resources but also accelerates environmental degradation (Chiranjeevi et al., 2024). As a result, the need for sustainable alternative materials with performance comparable or superior to natural aggregates has become increasingly urgent. Recycled concrete aggregate (RCA) presents a viable alternative for use in the lower layers of pavement, offering a solution to both waste management challenges and resource conservation. The application of RCA in construction, especially for non-structural purposes, began over two decades ago and has since become a common practice (Bassani et al., 2019). However, RCA requires careful handling, which may involve mechanical or chemical stabilization to optimize its performance.

RCA, sourced from crushed concrete waste, not only reduces construction and demolition debris sent to landfills but also contributes to a more sustainable and environmentally friendly construction industry. Furthermore, RCA typically offers a more economical alternative to conventional aggregates, delivering significant cost advantages in soil stabilization applications. Incorporating RCA into soil stabilization

Ref. code: 25676522040077WTA

enhances the compressive strength, shear strength, and durability of treated soils, making them suitable for construction applications. By using RCA, the demand for virgin materials is diminished, thereby reducing environmental impact. The primary component of RCA is crushed concrete, although its composition can vary depending on the source material.

Compared to virgin aggregates, RCA typically exhibits lower density, higher water absorption capacity, and increased Los Angeles abrasion loss. While natural aggregates usually have water absorption rates below 3%, RCA can have absorption rates ranging from 3% to 10% (Arulrajah et al., 2013). Research has extensively investigated the use of RCA in enhancing the properties of clayey soils, particularly for road construction subbases and bases. Numerous studies have also explored the potential of RCA in improving fine-grained soils.

2.5.2 Properties of Recycled Concrete Aggregate

Evaluating RCA for various construction purposes depends on their physical properties. RCA, obtained from the crushing of demolished concrete structures, shows considerable variation in particle size, requiring proper gradation for effective pavement base and subbase layer design. Additionally, RCA generally has a lower density than natural aggregates due to the presence of residual mortar and potential low-density contaminants. The leftover mortar increases particle volume, leading to RCA's lower specific gravity relative to natural aggregates. Additionally, RCA generally demonstrates greater porosity and water absorption than natural aggregates due to the porous structure of the residual cement paste adhering to its surface. Table 2.4 summarizes the physical characteristics of RCA as reported in studies conducted in different countries.

Ref. code: 25676522040077WTA

Table 2.4 Physical properties of recycled concrete aggregate.

Properties of RCA	Authors									
	(Ma et al., 2022)	(Tran et al., 2022)	(Kumar et al., 2022a)	(Cabrera et al., 2021)	(Kianimehr et al., 2019)	(Mohammadinia et al., 2019)	(Bestgen et al., 2016)	(Haider et al., 2014)	(Azam & Cameron, 2013)	(Gabr & Cameron, 2012)
Location	Wuhan, China	Thailand	Delhi, India	Malaga, Spain	Shiraz, Iran	Victoria, Australia	United States	Maryland	Australia	South Australia
Max Particle Size (mm)	2	25	20	20	2.36	20	20	20	20	20
Compressive Strength (MPa)	30	24.7	35.6	ND	23 - 28	ND	ND	ND	ND	15-75
Specific Gravity (G_s)	2.26	2.57	2.24-2.45	ND	2.61	ND	2.29	2.29	2.55	2.55 - 2.6
Los Angeles Abrasion	ND	31	30.2-33.8	36	ND	31.1	55	55	43	37 - 39
Water absorption - coarse (%)	ND	3.2	4.23	8.31	ND	6.05	4.2	4.2	ND	5.5
Water absorption - fine (%)	ND	5.3	6.8	10.27	ND	13.6	9.23	9.23	ND	8.9
Water absorption - average (%)	21.42	4.25	5.52	9.29	ND	9.7	6.7	6.7	6.8	7.2

***Note: N.D (not detected)*

2.5.3 Chemical Composition of Recycled Concrete Aggregate

The chemical composition of RCA is a critical factor in evaluating its effectiveness for construction purposes, especially in soil stabilization and concrete production. Numerous studies (Bui et al., 2018; Martínez-Lage et al., 2020; Moreno-Pérez et al., 2018; Saravanakumar et al., 2016; Sohail et al., 2020; Yang & Lim, 2018) have investigated the chemical characteristics of RCA, highlighting a considerable variation in composition. This variability primarily results from differences in the original concrete source, including the types of cement and aggregate used and the properties of the adhered cement paste, which may be influenced by contaminants or degradation over time (Katz, 2003).

The major chemical components of RCA include silica (SiO_2), alumina (Al_2O_3), and ferric oxide (Fe_2O_3), similar to those found in natural aggregates. However, RCA also contains significant amounts of calcium oxide (CaO) and potassium oxide (K_2O). The high calcium content, predominantly originating from residual mortar and the absorbed cement binder within the recycled material, significantly affects the reactivity of RCA, particularly by contributing to pozzolanic reactions during cement hydration (Moreno-Pérez et al., 2018). The ratio of calcium to silica in RCA is a pivotal factor that influences pozzolanic activity and the material's performance in concrete mixes or stabilization processes (Angulo et al., 2009).

Structures from earlier construction periods often utilized traditional concrete with well-established properties. Upon demolition, the resulting concrete waste can be processed into RCA, thus addressing the issue of construction and demolition debris while promoting sustainability by reducing reliance on virgin resources (Mohammed, 2023). RCA typically shows a lower bulk specific gravity and higher water absorption capacity, consistent with previous research findings. Finer RCA particles exhibit even higher absorption rates, which can increase the moisture content within a mixture (Kianimehr et al., 2019; Mohammed, 2023; Mohammed & Najim, 2020). Research conducted by (Sanchez-Cotte et al., 2020) has demonstrated that, although RCA samples share similar chemical compounds, their concentrations can vary significantly. RCA tends to have elevated levels of silicon (Si) and aluminum (Al), likely due to the residual cement paste or mortar. A distinguishing feature between conventional

Ref. code: 25676522040077WTA

concrete and RCA is the higher concentrations of calcium (Ca) and sodium (Na) found in RCA. The residual cementitious properties of RCA can interact with water and soil minerals, forming additional cementitious bonds that enhance the strength of stabilized soil.

A comprehensive understanding of RCA's chemical composition is essential for optimizing its use in construction, as it directly affects the material's mechanical properties and behavior over time in various environmental settings. The following sections provide an in-depth examination of specific chemical oxides in RCA, summarized in Table 2.5, and discuss their implications for construction applications.

Table 2.5 Chemical composition of RCA.

Author	Chemical Composition RCA								
	SiO_2	Al_2O_3	Fe_2O_3	MgO	CaO	Na_2O	K_2O	MnO	TiO_2
(Martínez-Lage et al., 2020)	13.24	3.42	1.71	5.77	65.3	0.2	0.37	0.08	0.17
(Sohail et al., 2020)	53.9	1.7	18.2	12.5	10.8	1.1	0.2	0.2	-
(Moreno-Pérez et al., 2018)	56.64	14.68	5.18	1.23	14.03	4.69	1.91	0.94	0.7
(Yang & Lim, 2018)	54.67	8.58	3.21	2.1	17.38	1.32	2.08	0.07	0.33
(Bui et al., 2018)	62.56	12.52	5.82	1.83	12.01	2.69	1.3	0.12	0.62
(Saravanakumar et al., 2016)	53.44	11.9	5.9	0.94	18.84	2.19	3.89	-	0.1

2.6 Effect of Compaction on Lime and RCA as stabilized Soil

The Standard Proctor compaction test, a common method in geotechnical engineering, is pivotal in determining the optimal moisture content necessary to achieve maximum compaction and dry density for specific soil types. This procedure is essential for regulating soil behavior such as settlement, strength, and swelling, which are crucial for ensuring infrastructure stability. Research by Bell (Bell, 1996) and Ingles and (Ingles & Metcalf, 1972) highlights the importance of this test in understanding soil responses to varying moisture levels during construction. The correlation between moisture content and dry density is meticulously evaluated to forecast soil behavior, as achieving optimal compaction is crucial for ensuring the required strength and long-term durability.

Ref. code: 25676522040077WTA

Lime stabilization is a widely recognized method for enhancing soil properties, particularly suitable for clayey soils with elevated plasticity and liquid limits. The incorporation of lime modifies the soil's chemical composition and physical characteristics, resulting in increased strength, reduced plasticity, and improved workability. Studies by Sharma et al. (2008) and Al-Mukhtar et al. (2012) have demonstrated significant improvements in strength and stability in lime-treated soils due to pozzolanic reactions, which form C-S-H and C-A-H. Research indicates that the maximum dry density of lime-stabilized soils generally falls within a 4% to 8% range; however, higher lime content can lead to a reduction in dry density, as noted by Güllü and Fedakar (2017). This decreases results from the flocculation and agglomeration of clay particles, leading to larger voids and reduced compaction densities.

When RCA is used as a partial soil replacement, its compaction behavior differs from that of natural soils. Studies by Poon and Chan (2006) and Sasanipour and Aslani (2020) demonstrates that the reduced specific gravity and increased water absorption properties of RCA lead to a decrease in the maximum dry density of soil-RCA composites. This effect is largely attributed to the porous nature of RCA, which absorbs more water than natural aggregates, thereby increasing the optimal moisture content required for compaction. Furthermore, while RCA's rough surface texture promotes particle interlocking, its lightweight nature hinders it from achieving the same level of compaction as natural aggregates. As summarized in Table 2.7, these characteristics necessitate adjustments to compaction methods to optimize soil performance when RCA is incorporated in construction. Research by da Silva et al. (2023) underscores the environmental advantages of using RCA in soil stabilization, such as reducing the dependency on virgin materials and decreasing landfill waste.

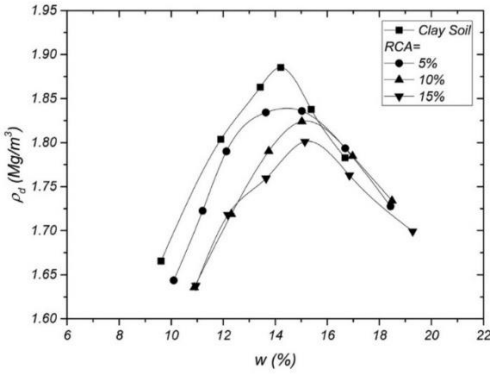

Figure 2.4 Compaction curve from (Kianimehr et al., 2019).

Ref. code: 25676522040077WTA

Table 2.6 Research done related to compaction test with lime as stabilized soil.

Author	Type of stabilizer	Type of soil	Stabilizer (%)	lime (%)	Results
Phai and Eisazadeh (2020)	Rice Husk Ash (RHA)	Bangkok Clay	4, 8, 12, 16	0, 4, 8 and 12	The addition of lime causes the MDD to fall dramatically, whereas the OMC of lime-RHA soil combinations increase.
Eisazadeh et al. (2019)	Bottom Ash (BA), Rice Husk Ash (RHA)	Bangkok Clay	10, 20, 30, and 50	4, 8, and 12	Increased amount of BA, RHA, and Lime results in increased OMC and decreased MDD due to the hydration impact and attraction for additional moisture during the chemical reaction processes.
Todingrara et al. (2017)	-	Laterite Soil	-	0, 2, 4, 6, 8 and 10	The ideal lime level is 6%, while the lime combinations tend to raise the OMC and decrease the MDD.
Dutta et al. (2017)	Fly Ash (FA) & Gypsum	-	0,5 to 4	2 to 10	The blend of 2% gypsum and 8% lime-FA yields the maximum MDD.
Muntohar et al. (2013)	Rice Husk Ash (RHA), Fibers	Laterite clay	12 and (0.1, 0.2, 0.4, 0.8 and 1.2)	12	The presence of lime in the combinations resulted in an increase in OMC.
Obuzor et al. (2012)	Ground Granulated Blast Furnace Slag	Clay soil	4, 8, 12 and 16	4, 8, 12 and 16	The presence of lime in the combinations results in increased OMC and decreased MDD.
Saeed et al. (2012)	Copper Nitrate Trihydrate and Zinc	Laterite clay	0.1, 5 and 10	5 and 10	The MDD reduced and the OMC increased as the lime content increased.
Muntohar and Hantoro (2000)	Rice Husk Ash (RHA)	Clay soil	7.5, 10 and 12.5	2, 4, 6, 8, 10 and 12	MDD reduces as the proportions of lime and RHA in the soil increase, while the OMC rises. The reduction in MDD indicates a decrease in compaction energy compared to the original soil, and the rise in OMC is a typical response to lime addition.

Ref. code: 25676522040077WTA

Table 2.7 Researchers done related to compaction test.

Author	Soil Type	Stabilizer Type	Stabilizer (%)	Result
Ma et al. (2022)	Clay soil	RCA	15, 30, 45	An increase in %RCA leads to a decrease both OMC and MDD.
Tran et al. (2022)	Laterite Soil	RCA	50, 70	An increase in %RCA leads to increased OMC and lower MDD.
Shourijeh et al. (2022)	Clay soil	RCA	5, 10, 15	An increase in %RCA leads to increased OMC and lower MDD.
Datta and Mofiz (2021)	Clay soil	RCA	30, 50, 70	A rise in the %RCA reduces the OMC and increases the MDD.
Tavakol et al. (2020)	Clay soil	RCA	50, 100	A rise in %RCA decreases the OMC and increases the MDD.
Mohammed and Najim (2020)	Clay soil	RCA	15, 25	An increase in %RCA leads to increased OMC and lower MDD.
Olufikayo and Benjamin (2019)	Laterite Soil	RCA	2, 4, 6, 10, 12	An increase in %RCA leads to increased OMC and MDD.
Kianimehr et al. (2019)	Clay soil	RCA	5, 10, 15	An increase in %RCA leads to increased OMC and lower MDD.
Kashoborozi et al. (2017)	Laterite Soil	RCA	30, 40, 50	An increase in %RCA leads to a drop in OMC and an increase in MDD.

Ref. code: 25676522040077WTA

2.7 Effect of UCS on Lime and RCA as Stabilized Soil

2.7.1 UCS Under Normal Conditions

The UCS test evaluates the compressive strength of materials, particularly for stabilizing soils without lateral confinement. This test is commonly applied to evaluate the improvement in soil strength after stabilization using various additives. The influence of lime on UCS has been extensively investigated, as lime is recognized for its ability to substantially improve the strength properties of soils, especially those with clay or lateritic compositions. The addition of lime to soil triggers pozzolanic reactions, resulting in the generation of cementitious materials that enhance the mechanical performance of the soil. Studies show that lime content between 2% and 14% of the dry soil mass results in substantial increases in UCS values (Muntohar et al., 2013), with optimal performance typically observed around 6% lime content (Todingrara et al., 2017). Additionally, the curing period plays a vital role, as extended curing durations from 1 day to 56 days allow for more complete pozzolanic reactions, leading to even greater improvements in UCS over time (Al-Mukhtar et al., 2012; Obuzor et al., 2012). These findings highlight lime's effectiveness in soil stabilization, with increased lime content and longer curing times consistently yielding higher UCS values.

The effect of RCA on UCS has also been the subject of considerable research, particularly in the context of replacing natural aggregates in soil stabilization projects. Studies investigating the impact of RCA on UCS indicate that as the proportion of RCA increases, so does the UCS value. For instance, research findings summarized in Table 2.9 reveal a consistent trend of higher UCS values as RCA content increases from 5% to 100%. In particular, Ma et al. (2022) and Kianimehr et al. (2019) observed that stabilizing soils with RCA in proportions between 5% and 30% led to notable enhancements in compressive strength, as depicted in Figure 2.5. The findings indicate that the inclusion of RCA improves soil strength and satisfies the standards for subbase and subgrade applications, particularly at a 15% RCA content, with further strength gains achieved over extended curing periods (Kianimehr et al., 2019; Ma et al., 2022; Tran et al., 2022)

Ref. code: 25676522040077WTA

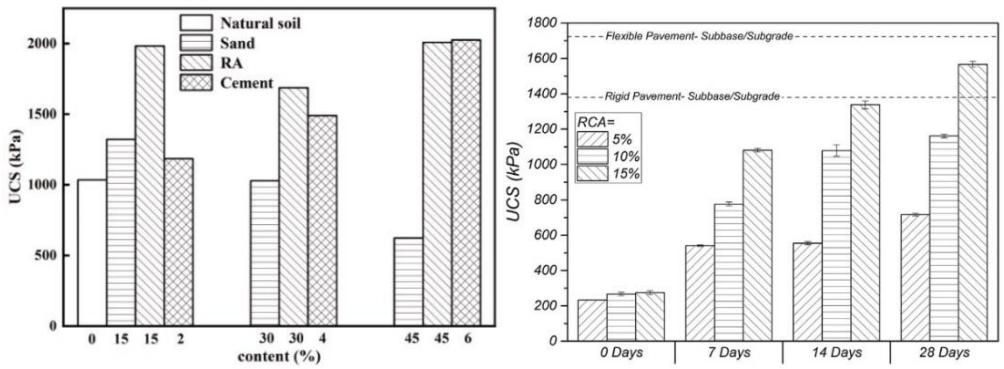

Figure 2.5 UCS value, left side by (Ma et al., 2022) and right side by (Kianimehr et al., 2019).

Table 2.8 UCS test of lime stabilized soil.

Author	Type of stabilizer	Type of soil	Curing period (day)	Results
Domphoeun and Eisazadeh (2024)	RHA, Lime and CF	Laterite Soil	28 days	20%RHA8L and 30%RHA8L the strength of UCS increased by 7.8 and 7.4-fold compared to untreated laterite soil.
Todingrara et al. (2017)	Lime	Laterite Soil	7 and 14	Increasing the lime content can enhance the UCS until it reaches the optimal 6%.
Dutta et al. (2017)	Fly Ash (FA) & Gypsum	-	7, 28, 56 and 90	Increase the UCS value up to 300-fold with an increase in the curing time.
Muntohar et al. (2013)	(RHA), Fibers	Laterite clay	1, 7, 14, 28and 56	Lime-stabilized soil increases UCS strength, while the amount of RHA in soil lime combinations increases UCS marginally.
Saeed et al. (2012)	Copper Nitrate Trihydrate and Zinc	Laterite clay	7 and 14	The strength of lime-treated laterite clay soil polluted with metal will be more problematic as the heavy metal content increases and cure times increase.
Al-Mukhtar et al. (2012)	-	Clay soil	7 and 90	Increasing the curing time additionally raises the UCS value.
Obuzor et al. (2012)	GGBFS	Clay soil	7, 14, 28, 56 and 90	Increasing curing time increases the UCS value.

Ref. code: 25676522040077WTA

Table 2.9 UCS test utilizing RCA in soil.

Author	Soil Type	Stabilizer Type	Stabilizer (%)	Curing (day)	Results
Shourijeh et al. (2022)	Clay soil	RCA	5, 10, 15	14, 28	An increase in %RCA results in increased UCS strength 61 times compared to clay soil which have value 141 kPa.
Tran et al. (2022)	Laterite Soil	RCA	50, 70	7, 28	Increased %RCA leads to increased UCS strength, 12% higher than LS-SS mixtures and 16 times different from untreated soil.
Tavakol et al. (2020)	Clay soil	RCA	50, 100	7 and 28	50%RCA and 50%clay have UCS value 335 psi compared to untreated soil is 106 psi, however the required strength of 1,725 kPa was not met.
Kianimehr et al. (2019)	Clay soil	RCA	5, 10, 15	7, 14, 28	With 15% RCA, the UCS value is increase 67% compared to UCS of untreated clay soil.
Olufikayo and Benjamin (2019)	Laterite Soil	RCA	2, 4, 6, 10, 12	0 and 7	The UCS increases as the amount of RCA increases to 10%, then decreases at 12% of RCA.
Karkush and Yassin (2019)	Clay soil	RCA	5, 10, 15	1	Increased %RCA leads to increased UCS strength.
Gabr and Cameron (2012)	Clay soil	RCA	60, 80, 90	7 and 28	Increased %RCA leads to increased UCS strength, the UCS value after 28 days range from 0.69 to 0.88 MPa.

Ref. code: 25676522040077WTA

2.7.2 UCS under Wetting-Drying Conditions

In geotechnical engineering, UCS testing under wetting-drying cycles is a critical method for evaluating the durability of soil and stabilization materials under varying environmental conditions, such as changes in moisture content and temperature fluctuations. This test is particularly relevant in tropical climates like Thailand, where high humidity, extreme heat, and heavy rainfall pose significant challenges to soil stability. The ability of stabilized soil to withstand these cycles without significant loss of strength is essential for ensuring the longevity and performance of construction materials in infrastructure projects (Consoli et al., 2021; Horpibulsuk et al., 2016; Neramitkornburi et al., 2015; Wahab et al., 2021).

The use of lime as a stabilizing agent in soils has been extensively studied, particularly in environments subjected to repeated wetting and drying. Lime improves soil strength and durability by inducing pozzolanic reactions that bind soil particles together, resulting in a more cohesive and resilient structure. Several studies have demonstrated that lime-stabilized soils exhibit higher UCS values, which are crucial for enhancing their resistance to the detrimental effects of wetting-drying cycles. Research by Kampala and Horpibulsuk (2013) on silty clay stabilized with calcium carbide residue and fly ash in Thailand highlights the importance of initial UCS in determining the soil's long-term performance under such conditions. Higher UCS values, achieved through lime stabilization, significantly improve the material's ability to endure repeated moisture and temperature variations, preventing excessive degradation.

Another study by Bhurtel and Eisazadeh (2020) focused on stabilizing high-plasticity Bangkok clay for road construction using a mixture of lime and bottom ash. Their results indicated that the inclusion of lime, particularly in combination with bottom ash, enhanced the clay's durability under wetting-drying conditions. The optimal mix of 12% lime and 50% bottom ash exhibited superior resistance to moisture-related degradation, as reflected by the high UCS values recorded during the durability tests. This suggests that lime plays a pivotal role in strengthening soils subjected to extreme environmental conditions, especially in tropical regions.

Studies have shown that RCA-stabilized soils can achieve UCS values comparable to, or even exceeding, those of traditional stabilization methods. However,

Ref. code: 25676522040077WTA

the durability of RCA under wetting-drying cycles depends on several factors, including the calcium-to-silica ratio and the presence of adhered mortar. Research has demonstrated that RCA's lower density and higher water absorption capacity make it more susceptible to moisture-induced strength loss compared to lime-stabilized soils. Nevertheless, when properly processed and combined with other stabilizing agents, RCA can provide adequate resilience under wetting-drying conditions. For instance, when RCA is incorporated into soil stabilization projects, it enhances not only the UCS but also reduces reliance on virgin materials, promoting more sustainable construction practices.

In summary, while both lime and RCA improve UCS and soil durability, lime tends to provide more consistent performance under extreme wetting-drying cycles due to its pozzolanic reactivity. RCA, on the other hand, offers an environmentally friendly alternative that, when combined with other stabilization techniques, can effectively enhance soil strength and durability in tropical environments. Table 2.10 presents an overview of numerous studies examining the durability of lime and RCA-stabilized soils when subjected to wetting-drying cycles.

Ref. code: 25676522040077WTA

Table 2.10 Wetting-drying tests performed by different researchers.

Author	Materials	Curing period (day)	Type of soaking	Soaking period	Test Done
Domphoeun and Eisazadeh (2024)	LS, CF, RHA, and Lime	56	Complete	5 hours	UCS Test (3 and 6 cycles).
Chiranjeevi et al. (2024)	RCA, NA & cement	28	Complete	5 hours	UCS and Weight Loss (12 cycles).
Wahab et al. (2021)	LS, Cement & Lime	7	Complete	5 hours	UCS (1, 2, 4,7, 12 and 15 cycles).
Tiwari et al. (2021)	Expansive Soil, Coir Fiber & Bottom Ash	28	Complete	12 hours	UCS Test (every 2, 4, 6, 8 and 10 of freeze and thaw test).
Bhurtel and Eisazadeh (2020)	Bangkok Clay, BA & Lime	28	Capillary soaked and Complete	24 hours	UCS and Permeability Test.
Biswal et al. (2020)	LS & Cement	7 and 28	Complete	5 hours	UCS, Mass loss and Volume changes test (12 cycles).
Donrak et al. (2016)	LS, Melamine Debris & Cement	28	Complete	5 hours	UCS and Mass loss Test (3, 7 and 12 cycles).

Ref. code: 25676522040077WTA

Table 2.11 Wetting-drying test related to RCA performed by different researchers.

Author	Materials	Curing period	Type of soaking	Soaking period	Results
Hoy et al. (2023)	RCA, cement & Steel slag	28 days	Complete	5 hours	The UCSw-d increased with the number of w-d cycles up to the third cycle, and gradually decreased thereafter.
Li and Hu (2020)	RCA, NA, cement	7 and 28 days	Complete	5 hours	The UCS tests showed a decrease in strength compared to traditional materials, but the increase in cement content and curing time helped improve the performance.
Rangel et al. (2020)	RCA, NA, cement	28 days	Complete	24 hours	RCA's performance was tested for its resistance to moisture variation, demonstrating its potential under w-d conditions.
Tam et al. (2018)	RCA & FA	28 days	Complete	12 hours	Nothing significant impacts on both UCS and durability under environmental conditions such as wetting-drying cycles.
Arulrajah et al. (2016)	RCA, FA & Lime	7, 28, and 56 days	Complete	12 hours	Their study focused on UCS and found that lime-stabilized RCA performed well under wetting-drying cycles.
Ismail and Ramli (2013)	RCA, Cement & FA	7, 28, and 56 days	Complete	12 hours	The treated RCA exhibited improved UCS and durability under prolonged wet-dry cycles, particularly with lime stabilization.
Kou and Poon (2012)	RCA & Cement	28 days	Complete	5 hours	RCA mixed with cement has a significant increase in UCS. However, after several w-d cycles, the strength decreases gradually due to the increase in material porosity.
Etxeberria et al. (2007)	RCA & Cement	28 days	Complete	5 hours	Found that up to 25% RCA replacement did not significantly affect compressive strength.
Poon and Chan (2006)	RCA, Cement & Lime	7 and 28 days	Complete	5 hours	Demonstrated improved performance of RCA when treated with lime, resulting in enhanced UCS and resilience under cyclic wetting and drying conditions.

2.8 Effect of Direct Shear on Lime and RCA as Stabilized Soil

The direct shear test serves as a fundamental method for analyzing soil shear strength, both in controlled laboratory conditions and real-world applications, yielding critical insights into soil stability and its mechanical performance under shear loading. The effects of soil stabilization using lime and RCA on shear strength have been extensively studied, with varying outcomes depending on factors such as soil type, stabilizer properties, and curing conditions. This section discusses the influence of lime and RCA on soil behavior during direct shear testing, beginning with lime treatment followed by the use of RCA as a replacement.

Lime has long been utilized as a soil stabilizer due to its ability to improve soil stability through pozzolanic reactions, which enhance the material's strength and stiffness. The inclusion of lime enhances the cohesion and internal friction angle of soils, leading to notable improvements in their shear strength. Research indicates that the efficiency of lime stabilization depends on factors such as lime dosage, curing duration, and the properties of the soil being treated. For instance, studies by Pushpakumara et al. (2023) highlighted that varying lime concentrations lead to different degrees of strength enhancement, with curing time being a critical factor in the development of soil strength. Longer curing periods facilitate the ongoing pozzolanic reactions, further improving the mechanical properties of lime-treated soils.

Direct shear tests have consistently demonstrated that incorporating RCA into soils enhances peak shear strength by modifying both cohesion and the internal friction angle of the mixture. As outlined in Table 2.13, the degree of strength improvement varies across different soil types when RCA is introduced. The proportion of RCA in the soil mixture significantly affects changes in cohesion and peak internal friction angle, with higher RCA contents typically resulting in greater strength enhancements. Additionally, the stabilization performance is influenced by the quality of RCA, which is determined by the properties of the original concrete.

Ref. code: 25676522040077WTA

Table 2.12 Direct Shear test of lime stabilized soil.

Author	Type of soil	lime	Results
Domphoeun and Eisazadeh (2024)	Laterite soil	8	The addition of lime improves the cohesiveness of natural soil. The presence of a lime activator causes pozzolanic reactions, which explain this behavior.
Rosone et al. (2023)	Clay Soil	2, 4, and 6%	After 28 days of curing, the soil treated with 6% lime yielded the best mixes and shear strength.
Pushpakumara et al. (2023)	Clay Soil	0, 10, and 20%	The soil treated with 20% lime has the maximum friction angle, but the cohesiveness decreases.
Sani and Eisazadeh (2023)	Laterite soil	6	During 7 days of curing under normal stress of 100 kPa, the lime-treated samples exhibited brittle failure and the highest shear stress.
Eliaslankaran et al. (2021)	Coastal Soil	0, 2, 4, 6, 8, 10 and 12 %	Soil treated with 8% lime raised the friction angle to 38.5 and enhanced cohesiveness by 33% when compared to untreated soil.
Pongvithayapanu et al. (2021)	Silica Sand	Waste Tire (0, 5, 15 and 25%)	For silica-Tire20mm, the greatest amount of tire corresponding to reduce the friction angle of DS test compared to untreated silica sand, the waste tire showed reduction trend for friction angle.
Liu et al. (2019)	Expansive soil	90, 225, 270, and 360 grams	The sheer strength of stabilized soil increases dramatically during the curing time.

Ref. code: 25676522040077WTA

Table 2.13 Direct Shear test utilizing RCA in soil.

Author	Soil Type	Stabilizer type & percentage	Conditions	N load (kPa)	Results
Anda et al. (2023)	-	RCA (relative density 20, 70 %)	Dry test	50, 100, 150	At low relative density, the RCA attained the shear stress value without experiencing any noticeable reduction. The strength development curve of the RCA-Geogrid interface showed no noticeable peaks.
Ma et al. (2022)	Clay soil	RCA (15, 30, 45 %)	Dry test	100, 200, 300, 400	An increase in %RCA will enhance total shear strength as well as cohesion (c) and peak internal friction angle.
Saberian et al. (2020)	-	RCA (100 %)	Dry Test	50, 100, 150	By increasing the duration of the shear stage, the shear stress grew to a maximum value and then stayed nearly constant.
Kianimehr et al. (2019)	Clay soil	RCA (5, 10, 15 %)	Dry test	25, 55, 105, 205	An increase in %RCA leads to increased strength, evidenced by increases in both cohesion (c) and peak internal friction angle.
Azam and Cameron (2013)	Clay Masonry	RCA (80 %)	-	25, 50, 75	Moisture content level affects shear strength.
McKelvey et al. (2002)	Clay slurry soil	RCA (100, 90, 80 %)	Dry and Wet	60, 120, 240, 300	Most of the samples examined reached their maximal shear stresses.

2.9 Effect of CBR on Lime and RCA as Stabilized Soil

The CBR test is a widely used penetration-based method to assess the strength and suitability of pavement and road subgrade materials. The CBR values are crucial in determining the appropriate design of pavement layers, including base and sub-base courses. This section discusses the effect of lime and RCA on CBR values, highlighting findings from various studies on soil stabilization. The addition of lime can significantly improve the CBR values as illustrated in Table 2.14, particularly in clay or lateritic soils. For instance, research by Phai and Eisazadeh (2020) demonstrated that the highest CBR values under unsoaked conditions were achieved by combining 10% rice husk ash (RHA) with 12% lime, with the maximum improvement observed after seven days of curing. Additionally, the optimal CBR under soaked conditions was attained by using 30% RHA and 12% lime, with testing conducted after 28 days of curing. These findings indicate that lime, when used in conjunction with other stabilizers like RHA, can substantially improve the bearing capacity of soils. Further studies Muntohar and Hantoro (2000); Muntohar et al. (2013) on lateritic soils stabilized with lime and RHA revealed an increase in CBR from 6.2% for untreated soil to 22.5% for a lime-RHA-treated mixture, demonstrating the significant enhancement in soil strength. These results suggest that lime stabilization not only improves soil performance under soaked and unsoaked conditions but also enhances the durability and load-bearing capacity of the treated soils.

The effect of RCA on CBR values is presented in Table 2.15. Research by Poon and Chan (2006) revealed that the use of RCA did not significantly alter the CBR values under both soaked and unsoaked conditions, whereas NA demonstrated a slight improvement, with an approximate 2% increase in CBR under unsoaked conditions. This suggests that RCA may not always provide the same performance enhancement as natural aggregates. However, other studies have shown more promising results with RCA. For instance, Haider et al. (2014) observed that RCA with varying gradations improved CBR by 114–131% and 148–167% after 7 days of curing. This demonstrates RCA's potential to enhance road subgrades, though its performance depends on factors like gradation and curing time, warranting further study to optimize its use in soil stabilization.

Ref. code: 25676522040077WTA

Table 2.14 CBR test of lime stabilized soil.

Author	Type of stabilizer	Type of soil	Curing period (days)	Conditions	Results
Muntohar et al. (2013)	Rice Husk Ash (RHA), Fibers	Laterite clay	3 days for soaked and 0 days for unsoaked	Soaked and Unsoaked	The lime/RHA mixture enhanced the bearing of soil in which the CBR increased from 6.2 to 22.5 and met the requirement to use as subgrade and subbase. The CBR value increased with an increase in the amount of fiber up to 0.8% and thereafter decreased.
Todingrara et al. (2017)	-	Laterite soil	-	Soaked and Unsoaked	During soaked conditions, increasing the lime content can raise the CBR value, with 6% being the ideal lime. Similar tendencies can be seen during saturated conditions.
Muntohar and Hantoro (2000)	Rice Husk Ash (RHA)	Clay soil	7	Unsoaked	Lime and RHA can improve engineering characteristics, with the optimal CBR value at 6% lime combinations. Practically, the effective lime content should be blended between 6-10%.
Ghorbani and Hasanzadehshooiili (2018)	-	Clay soil	7	Unsoaked	The CBR value increased by increasing lime concentration up to 8%, however the CBR value was reduced by 10% of lime.
Phai and Eisazadeh (2020)	Rice Husk Ash (RHA)	Bangkok Clay	7 and 28	Soaked and Unsoaked	Increased percentage of lime/RHA results in CBR value-soaked conditions at 28 days (12% lime and 30% RHA) exhibit the best CBR value, whereas 12% lime and 10% RHA show the maximum CBR value for unsoaked conditions.
Sharma et al. (2008)	Calcium Chloride and Rice Husk Ash	Clay soil	28	Soaked	Increased lime/RHA content leads to an increase in CBR value; 4% lime and 12% RHA has the highest CBR value.

Ref. code: 25676522040077WTA

Table 2.15 CBR test utilizing RCA in soil.

Author	Stabilizer type	Condition	Uses	Result
Beja et al. (2020)	RCA	Soaked	Sub-base	The strength CBR increases over time due to the pozzolanic processes generated by the mixing of water and non-hydrated cement from the mortar or concrete aggregate, and the soaked CBR has value 51% after 4 days of soaking.
Arisha et al. (2016)	RCA with clay masonry	Soaked	Sub-base	The soaked CBR values ranged from 70% to 153%, with the 100%RCA showing the highest CBR value.
Haider et al. (2014)	RCA	Unsoaked	Base	The CBR value on the first day of curing is 114% and 148% for two types of RCA, and it increases to 131% and 167% after 7 days of curing.
Gabr and Cameron (2012)	RCA	Soaked	Base	The CBR value for RCA class 1 is much greater than that of combinations with virgin aggregate. The increase in CBR value is due to the residual cement in RCA material.
Aatheesan et al. (2009)	RCA with clay masonry	Soaked	Sub-base	The soaked CBR values were at least 80%, meeting the requirements of Victoria's road specification.
Poon and Chan (2006)	NA & RCA	Soaked & Unsoaked	Sub-base	The CBR values of NA and RCA are 83% and 66%, respectively, during the soaked period, and 85% and 66% during the unsoaked period.
Blankenagel and Guthrie (2006)	RCM (Recycled concrete masonry)	Soaked	Base	The Soaked CBR value with a 7-day curing period is 55%.

Ref. code: 25676522040077WTA

2.10 Effect of Permeability on Lime and RCA as Stabilized Soil

Permeability is a key factor in assessing the ability of materials, including soil and pavement base layers, to allow water to pass through. Understanding the permeability characteristics of materials is essential for designing effective drainage systems in road construction. Efficient water drainage is crucial for prolonging the lifespan of pavement structures, as poor drainage can lead to significant structural deterioration over time. Permeability tests, commonly conducted using the constant head or falling head methods, provide valuable data on how well materials manage water flow, which is critical for preventing issues such as water accumulation and frost damage in pavement systems (Xue et al., 2013). Table 2.16 summarizes the differences in drainage efficiency between RCA and natural aggregate-based systems, highlighting the time required to remove water from pavement structures.

Table 2.16 Research done related to Permeability test.

Authors	Stabilizer Type	Stabilizer (%)	Method	Result
Sani and Eisazadeh (2023)	Bottom Ash, Coir Fiber and Lime	BA 30%, CF 0.5, 1 and 1.5%, L 6%	Constan Flow Method	The addition of 30% BA increased 20 times the k value to 7.9E-08 compared to untreated soil which is 3.7E-09.
Ye Htun et al. (2022)	Bottom Ash	0, 20, 40, and 60	Constan Flow Method	At 20% BA the k value rises 10 times higher compared to laterite soil grade B. whereas at 40% BA the k value reduces to 4.9E-9 and for Laterite soil grade D the highest k value is 4.14E10-8.
Agarwal et al. (2021)	RCA	RCA only	Constant Head	The permeability of RCA comparison to Sand result in similar value range of 1.E-05 and 1.E-04 respectively.
Azam and Cameron (2013)	RCA (Resource Co & Adelaide Resource Recovery)	Resource Co 80% and Adelaide Resource Recovery 80%	Falling Head	RCA from Adelaide Resource Recovery was significantly more permeable than RCA from ResourceCo, because the material was coarser and although it had much of the same fines content. The k value for RCO is 1.8E-08 and ARR is 2.00E-07.

Ref. code: 25676522040077WTA

Lime, commonly used as a stabilizing agent in soil, has a pronounced effect on the permeability with different soil types (Al-Mukhtar et al., 2012). Its effectiveness depends largely on the mineral composition of the soil being treated. Research by Cardoso et al. (2016) has demonstrated that when lime is incorporated into fine-grained, highly plastic soils, it enhances permeability by inducing flocculation of clay particles, which increases soil porosity. This process facilitates the movement of water through the soil, improving drainage. However, the opposite effect is observed when lime is used in coarse-grained soils, such as lateritic soils. In these cases, the addition of lime reduces permeability by filling soil voids and altering the flow paths of water through the material (Amadi & Okeiyi, 2017). This dual effect of lime on different soil types highlights the importance of understanding the specific soil characteristics before selecting lime as a stabilizing agent in construction projects.

In the context of road pavement construction, permeability is a critical property for securing the long-term performance and durability of the pavement structure. Proper drainage prevents water accumulation and the associated issues of pressure build-up and cracking, which can compromise the pavement's integrity. (RCA has gained popularity as an alternative to natural aggregates in both flexible and rigid pavement applications, not only for its structural support but also for its permeability characteristics, which are essential for managing drainage. Studies have shown that the permeability of RCA can match or even exceed that of natural aggregates, depending on its composition and processing. For instance, Bennert and Maher (2008) found that pavement mixtures containing up to 75% RCA achieved permeability coefficients comparable to those of natural aggregates, indicating that RCA can provide adequate drainage in pavement applications.

Further research Poon and Chan (2006) into the self-cementing properties of fine RCA in unbound subbase layers has also revealed promising results. When comparing subbase layers made from RCA and natural aggregates (NA), RCA samples consistently exhibited higher permeability. This suggests that RCA not only serves as a structural substitute but also enhances the drainage properties of the pavement system. These findings underscore the potential of RCA as a sustainable alternative to NA particularly in implementations where efficient water drainage is essential for pavement

Ref. code: 25676522040077WTA

longevity. Roadway drainage systems must be carefully designed to accommodate the specific permeability characteristics of the materials used, ensuring effective water removal and preventing structural issues.

2.11 Stabilization Mechanism of Recycled Concrete Aggregate

RCA generally exhibits a lower specific gravity, largely due to the presence of lightweight residual cement paste (mortar) that remains attached to the aggregate after the concrete waste is crushed. RCA is produced by crushing waste concrete, which is then repurposed as aggregate material for road construction (Fanijo et al., 2023). According to Verian et al. (2018), RCA consists of approximately 60–75% aggregate (both coarse and fine) and 25–35% residual mortar from the crushed concrete. During the production of RCA, some of the original mortar remains adhered to the aggregate. The higher the proportion of adhered mortar, the lighter the RCA, as the mortar is highly porous and has a lower density. This results in a substantial interface between the aggregate and paste, commonly referred to as the interfacial transition zone. The residual mortar plays a significant role in determining the physical properties and strength performance of RCA. The durability of RCA is typically assessed using crushing and Los Angeles (LA) abrasion tests. LA abrasion tests often show that RCA particles undergo mass loss ranging from 10 to 60%, as interaction with steel balls generates finer particles from the aggregate. This elevated mass loss is attributed to the presence of the residual mortar and fractured particles resulting from the crushing process (Fanijo et al., 2023; Verian et al., 2018).

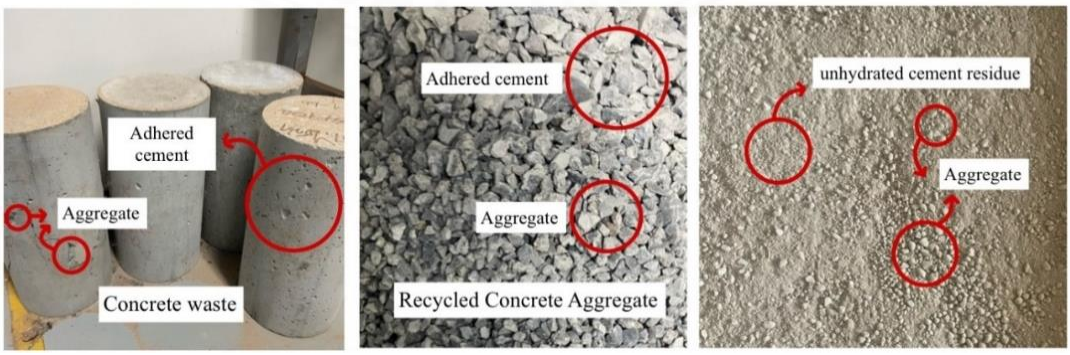

Figure 2.6 Process creates recycled concrete aggregate from crushing concrete waste.

Ref. code: 25676522040077WTA

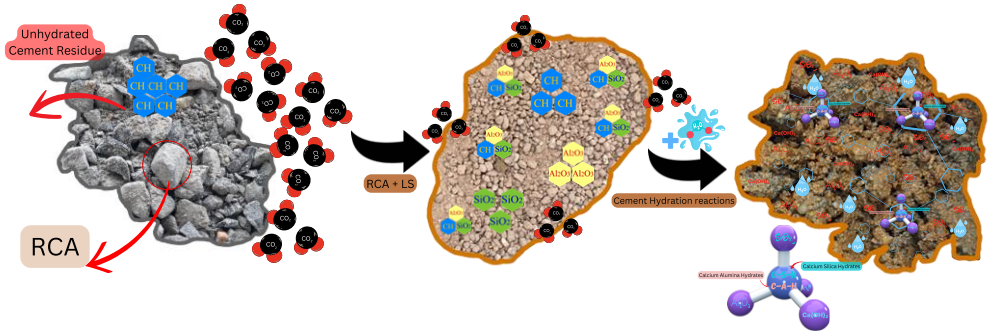

Figure 2.7 Chemical composition inside laterite soil and RCA.

RCA, which consists of crushed concrete, serves as an alternative to traditional aggregates, contributing to improved structural stability and interlocking of soil particles during compaction. This interlocking effect reduces soil deformation, enhances load-bearing capacity, and mitigates the expansion that frequently occurs in weak lateritic soils. The stabilization mechanism of RCA encompasses both physical and chemical processes (Shamsi Susahab et al., 2024). From a chemical perspective, the hydration of the residual cement paste within the RCA is essential. Upon contact with water, the residual cement undergoes a slow hydration process, producing calcium silicate hydrate (C-S-H) and calcium hydroxide ($Ca(OH)_2$). These compounds fill the voids and cracks within the soil, enhancing its cohesion and structural integrity (Fanijo et al., 2023; Shamsi Susahab et al., 2024). C-S-H, in particular, serves as a binding agent, strengthening the soil matrix. This process unfolds over several hours or days, depending on the availability of anhydrous cement and water. Increased temperature and humidity can accelerate the reaction. Meanwhile, the hydration of cement also leads to the formation of calcium hydroxide, which subsequently initiates a slower pozzolanic reaction, occurring over weeks to months (Gaboreau et al., 2020). RCA fosters this pozzolanic reaction by interacting with calcium hydroxide, silicon dioxide, and aluminum oxide in the soil to form calcium silicate hydrate (C-S-H) and calcium aluminate hydrate (C-A-H). These newly formed compounds bond soil particles together, reducing porosity and enhancing resistance to water infiltration and volume changes caused by moisture fluctuations (Shamsi Susahab et al., 2024; Zhao & Khoshnazar, 2021).

Ref. code: 25676522040077WTA

$$Ca(OH)_2 + SiO_2 = C - S - H \quad (2.2)$$
$$Ca(OH)_2 + AlO_3 = C - A - H$$

Where, C-S-H is Calcium Silica Hydrates, C-A-H is Calcium Alumina Hydrates.

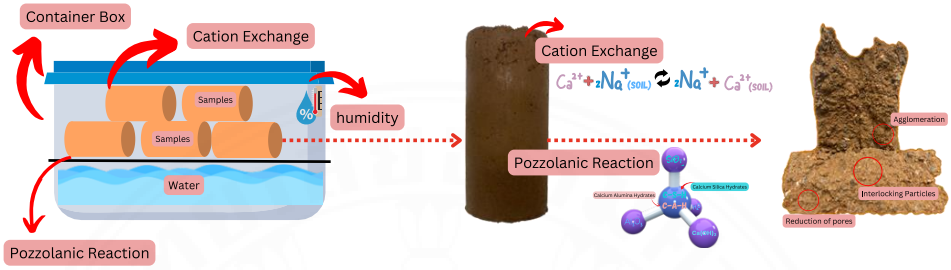

Figure 2.8 Cation exchange and pozzolanic reaction process.

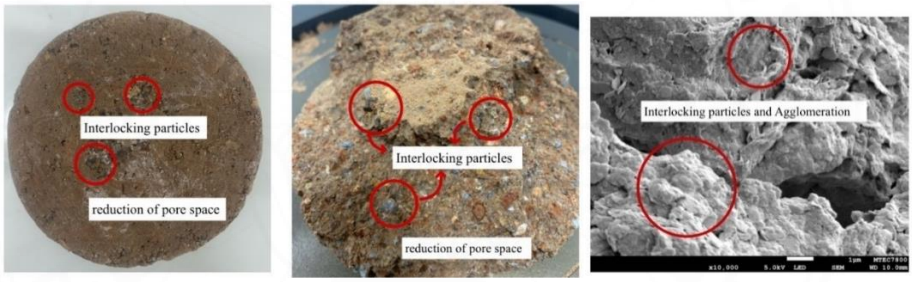

Figure 2.9 Interlocking particles of LS with RCA.

2.12 Requirements for Road Construction

In Thailand, road pavements are typically divided into two categories: flexible and rigid, both of which require stable soil foundations to ensure successful construction. In some instances, chemical stabilization techniques are employed to enhance the mechanical properties of weak soil foundations before road construction, enabling faster strength development (Obuzor et al., 2012; Sarhosis et al., 2016). The base and sub-base layers critical components of the pavement structure located beneath the surface layer are usually composed of natural aggregates, such as granular materials. Occasionally, soil stabilization methods are integrated into road construction projects to improve the performance of these layers (Tran et al., 2022).

Table 2.17 outlines the standards established by the Thai Department of Highways (DOH) for the direct use of lateritic soil in road construction. If the lateritic

Ref. code: 25676522040077WTA

soil does not meet the required standards set by the DOH, additional stabilization with materials such as demolition waste and lime is necessary to render it suitable for use in road construction. This process not only enhances the soil's suitability for infrastructural applications but also helps reduce transportation costs (Donrak et al., 2016; Meepon et al., 2019; Phummiphan et al., 2017). Table 2.18 provides a classification system for road aggregates according to the Unified Soil Classification System (USCS) and the American Association of State Highway and Transportation Officials (AASHTO), offering a general rating for various uses based on CBR values. The system categorizes materials as excellent, good, fair, poor to fair, and very poor, depending on their suitability for base, subbase, or subgrade layers in road construction.

Table 2.17 The specifications for engineering properties necessary for the utilization of subbase and base materials are outlined by the Department of Highways in Thailand (DOH-206/2532', 1989; DOH 201/2544, 2001; DOH 205/2559, 2016).

Properties	Department of Highways (DOH), Thailand	
	Subbase material (DOH 205/2559, 2016)	Base materials (DOH 201/2544, 2001)
California Bearing ratio, (%)	≥ 25	≥ 80
Liquid Limit, (%)	≤ 35	≤ 25
Plastic Limit, (%)	≤ 11	≤ 6
Plasticity Index, (%)	≤ 11	≤ 6
Los Angeles Abrasion loss, (%)	≤ 60	≤ 40
Passing No. 200 (%)	≤ 40	≤ 50

Table 2.18 Classification system to be used as road aggregate based on USCS and AASHTO (Chantruthai et al., 2017).

CBR (%)	General rating	Uses	Classification system	
			USCS	AASHTO
> 50	Excellent	Base	GM, GW	A-1-A, A-2-4, A-3
20 - 50	Good	Base	SM, SP, GP, GC, GM, SW	A-1-B, A-2-5, A-2-6, A3
7 - 20	Fair	Subbase	SC, CL, ML, OL	A2, A4, A6, A7
3 - 7	Poor to Fair	Subbase	CH, MH, OH, OL	A4, A5, A6, A7
0 - 3	Very poor	Subgrade	CH, CL, MH, OH	A5, A6, A7

Ref. code: 25676522040077WTA

In alignment with the standards presented in Table 2.17, the engineering properties for subbase and base materials are derived from the DOH standards DH-S205/2532 and DH-S201/2544. Table 2.19 details the requirements for cement-stabilized materials used in road pavements according to the Department of Highways, while Table 2.20 outlines the specifications for unbound base and subbase materials. These tables present the key parameters necessary for ensuring the durability and performance of road pavements in Thailand (DOH-206/2532', 1989). such as unconfined compressive strength, Los Angeles Abrasion loss, liquid limit, plastic index, and CBR.

Table 2.19 Requirements of cemented materials for road pavement based on Department of Highways Thailand standard (Teerawattanasuk et al., 2015).

Materials	Standard	Unconfined Compressive Strength (UCS) [kPa]
Soil cement base	DH-S 204/2556	1724
Soil cement subbase	DH-S 205/2532	689
Selected material "A"	DH-S 208/2532	407
Selected material "B"	DH-S 209/2532	332
Subgrade	DH-S 102/2532	294

Table 2.20 Requirements of Unbound Base and Subbase Materials (Department of Highways Thailand) (DOH-206/2532', 1989).

Properties	Standard	Requirements	
		Base course	Subbase course
Los Angeles Abrasion (%)	AASHTO T-89	≤ 40	≤ 60
Liquid Limit (%)	AASHTO T-89	≤ 25	≤ 35
Plastic Index (%)	AASHTO T-90	≤ 6	≤ 6
CBR (%)	AASHTO T-193	≥ 80	≥ 25

Ref. code: 25676522040077WTA

CHAPTER 3
MATERIALS AND RESEARCH METHODOLOGY

3.1 General Layout

Figure 3.1 presents a flowchart that illustrates the research methodology, which includes a comprehensive literature review, material acquisition, experimental procedures, and the final derivation of conclusions. This review was conducted meticulously to ensure a solid grasp of both laboratory techniques and previous research findings. Concurrently, laboratory experiments were conducted, involving basic tests for material classification according to established standards, as well as key tests to evaluate the feasibility of the proposed solutions. Following the completion of the experimental work, conclusions were drawn and are documented in the subsequent section. Aside from the literature review and conclusion sections, each phase of the research process is supported by its corresponding flowchart, as depicted below.

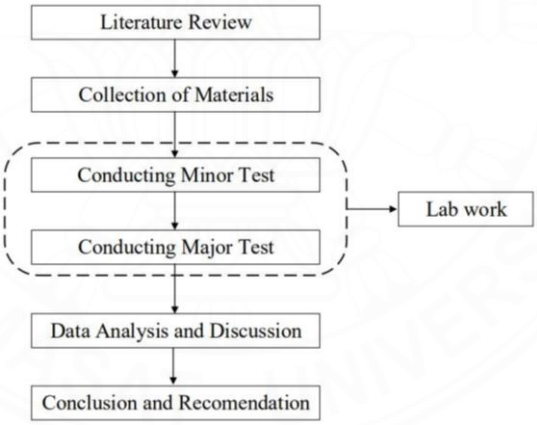

Figure 3.1 General outline for methodology.

The materials collected were subjected to basic tests, including Atterberg limits, particle size distribution, and specific gravity, for classification. Advanced analytical techniques, such as X-Ray Fluorescence (XRF) and Field Emission Scanning Electron Microscopy (FESEM), were utilized to determine the chemical compositions and microstructural characteristics of the raw materials. Mechanical tests were conducted on mixed designs to assess their geotechnical properties and the degree of improvement. The selected mixtures were subsequently examined using FESEM and Energy

Ref. code: 25676522040077WTA

Dispersive Spectroscopy (EDS) to understand the stabilizing mechanisms in comparison to untreated laterite soil. The findings were compared with existing studies in the literature and the standards set by the Department of Highways, Thailand, leading to conclusions and recommendations for future research.

3.2 Material Collection

The study identified laterite soil, recycled concrete aggregate, and lime as the primary materials. Subsequently, the sourcing and acquisition of these materials for experimentation was carried out as shown in Figure 3.2.

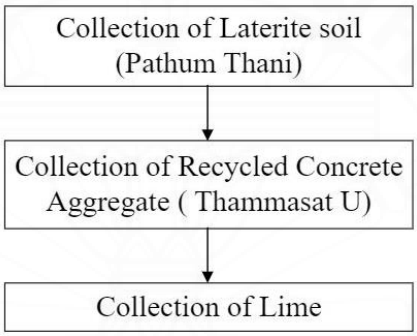

Figure 3.2 Collection of material.

3.3 Material Properties

3.3.1 Laterite Soil

Laterite soil, a mixture of soil and rock, is rich in silica, iron, and alumina, and is primarily found in tropical and subtropical areas. Its characteristic reddish color is due to the high content of iron oxide. The laterite soil used in this study, characterized by its red color, was sourced from Ban Mai, Pathum Thani, Thailand. The red laterite soil and texture of the laterite soil during our investigation are depicted in Figure 3.3, while its chemical composition is provided in Table 3.1. The primary oxides present in the sample include Silica (69.65%), Alumina (16.85%), and Iron (III) Oxide (7%).

Ref. code: 25676522040077WTA

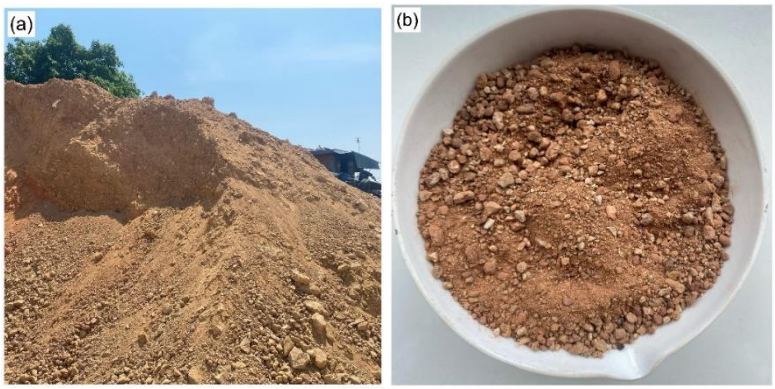

Figure 3.3 Texture of (a) Laterite Soil at the field and (b) Laterite soil sample.

Table 3.1 Chemical composition of materials as per XRF.

Oxides (%)	Laterite soil	RCA
SiO_2	69.65	24.20
CaO	0.41	62.82
Al_2O_3	16.85	3.74
Fe_2O_3	7.00	3.77
SO_3	0.03	2.07
MgO	1.08	1.06
K_2O	3.47	1.35
TiO_2	1.01	0.36
MnO	0.12	0.01
CuO	0.01	0.01

3.3.2 Recycled Concrete Aggregate

Concrete waste was sourced from the concrete laboratory at Thammasat University in the form of large cubes and cylinders, which were unsuitable for direct use in geotechnical experiments. To generate recycled concrete aggregates (RCA), the concrete waste was manually broken down into smaller pieces using a sledgehammer. The texture of the recycled concrete aggregates employed in this study is depicted in Figure 3.4.

Ref. code: 25676522040077WTA

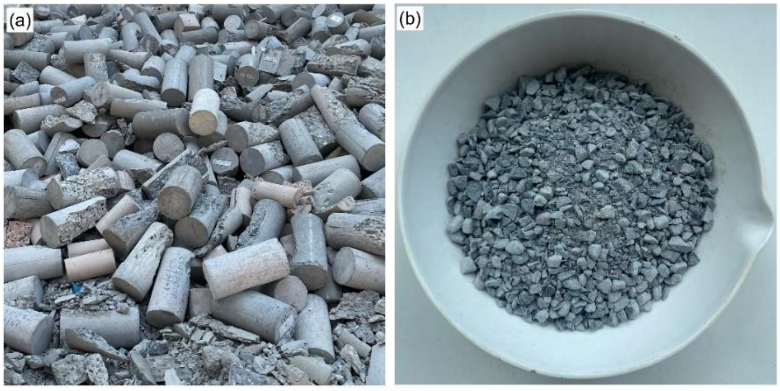

Figure 3.4 Texture of RCA (a) concrete waste and (b) recycled concrete aggregate.

3.3.3 Lime

Lime has become popular as a soil stabilizer because of its potential to improve soil engineering properties. Quicklime for the present study was obtained from Mega Home Public Company, a well-known provider in Pathum Thani, Thailand. The texture of the lime used for our work could be seen in Figure 3.5.

Figure 3.5 Texture of lime (a) package of lime and (b) texture of lime.

3.4 Methods and Experimental Setup

Figure 3.6 and Table 3.2 display the systematic experimental setup used in the study, along with additional details on the testing procedures. The geotechnical tests are categorized into two phases: preliminary (minor) and advanced (major) tests. The preliminary phase includes sieve analysis and specific gravity tests for both materials (lateritic soil and RCA), Atterberg limit tests (with RCA exhibiting no plasticity), and the Los Angeles abrasion test for RCA only. Upon completing the minor tests, the major phase involves several key tests, including standard compaction, Unconfined

Ref. code: 25676522040077WTA

Compressive Strength (UCS), California Bearing Ratio (CBR), Direct Shear (DS), and permeability tests.

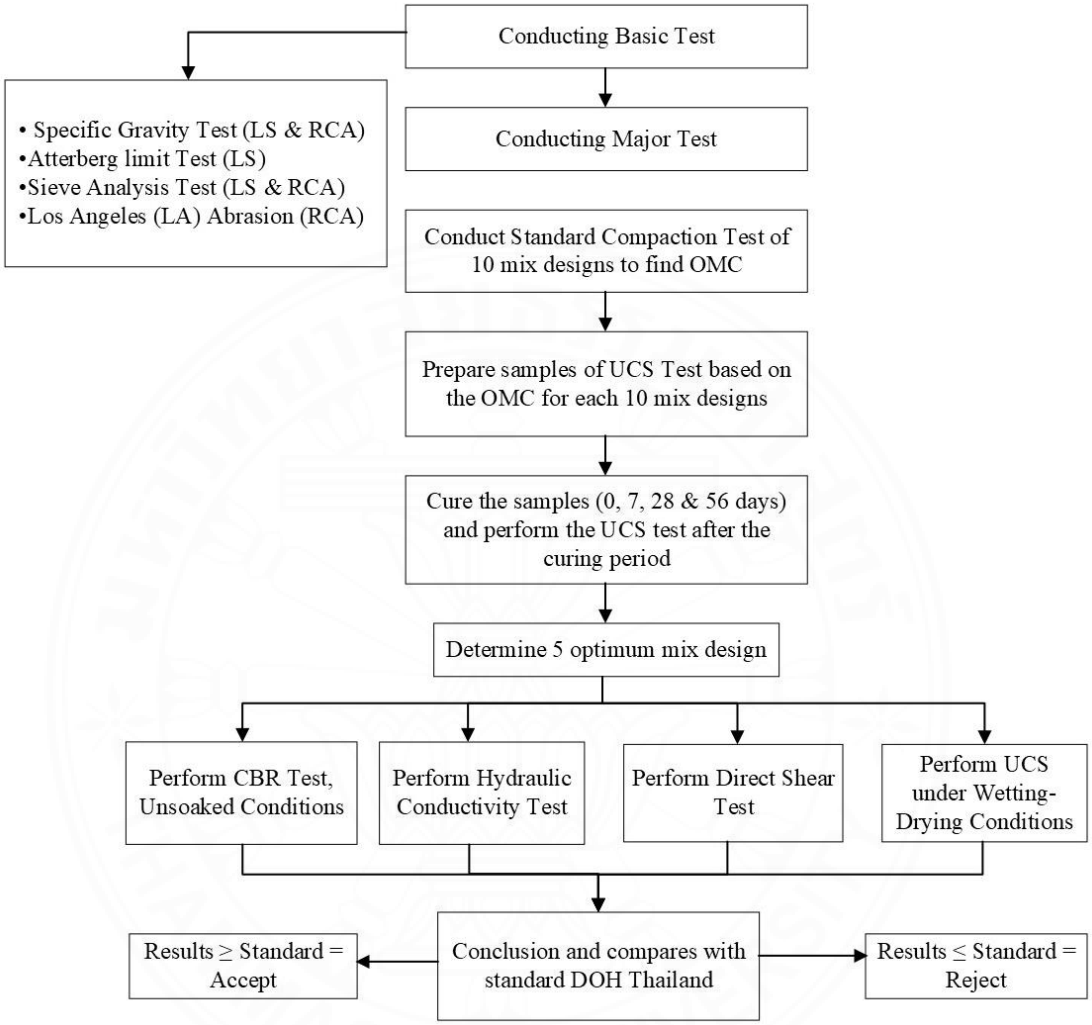

Figure 3.6 Experimental tests flowchart.

Since this study involved mixing soil with recycled concrete aggregate, all experimental work was conducted in a controlled laboratory setting with subsequent data analysis. Table 3.2 outlines the components and proportions used in the mix design. Soil testing is critical for evaluating the performance of RCA and lime stabilized LS, providing insights into their suitability for road applications. Table 3.3 presents the proportion of raw materials used in various mix designs based on the dry weight of the soil.

Ref. code: 25676522040077WTA

Table 3.2 Summary of the testing scheme.

Purpose	Test	Moisture	RCA (% by weight of soil)	L (% by weigh of sample)	Curing Period
Moisture - Density relationship	Standard Proctor Compaction	Various moisture contents to find OMC	0, 5, 15, 30, 45	0, 6	-
compressive strength development	Unconfined Compressive Strength	OMC	0, 5, 15, 30, 45	0, 6	0, 7, 28, and 56 days
evaluate the strength of soil subgrades or base	California Bearing Ratio	OMC	0, 5, 15, 30, 45	0, 6	0 and 7 days
Shear Strength development	Direct Shear	OMC	0, 30, 45	0, 6	0, 28, and 56 days
Microstructural Analysis	FESEM/EDS	Specimens collected after 56 days from Direct shear test			
Permeability Characteristics	Hydraulic Conductivity	OMC	0, 30, 45	0, 6	28 and 56 days

Table 3.3 Proportion of mixtures.

No	Mix Designation	LS (%)	RCA (% by weight of soil)	L (% by weight of sample)
1	100LS	100	0	0
2	95LS 5RCA	95	5	0
3	85LS 15RCA	85	15	0
4	70LS 30RCA	70	30	0
5	55LS 45RCA	55	45	0
6	100LS 6L	100	0	6
7	95LS 5RCA 6L	95	5	6
8	85LS 15RCA 6L	85	15	6
9	70LS 30RCA 6L	70	30	6
10	55LS 45RCA 6L	55	45	6

3.4.1 Particle Size Distribution

In this test, the soil samples were subjected to sieve analysis using a range of sieves to assess the particle size distribution of both laterite soil and RCA. Prior to the

Ref. code: 25676522040077WTA

analysis, both materials were oven-dried at 60°C. The sieve analysis for laterite soil followed the ASTM D422 standard, as shown in Figure 3.7.

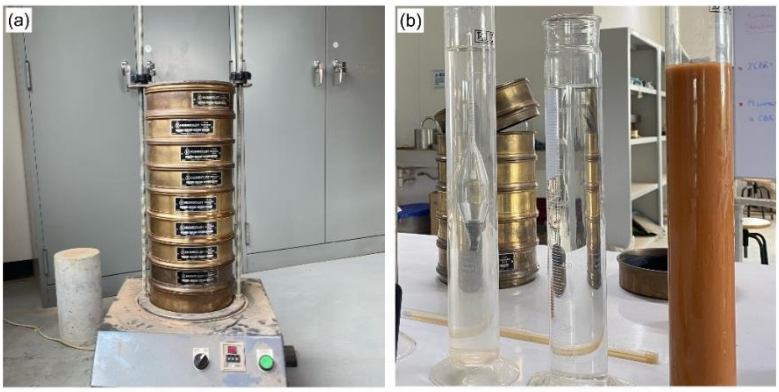

Figure 3.7 Particle size analysis of soils (a) sieve analysis and (b) hydrometer analysis.

3.4.2 Specific Gravity Test

Figure 3.8 presents the specific gravity values for both materials. The specific gravity test is employed to evaluate the density of soil particles by comparing the mass of a specific volume of soil to the mass of an equivalent volume of water. The specific gravity (Gs) of the lateritic soil was determined according to the ASTM D854-2014 standard, while the specific gravity of recycled concrete aggregate (RCA) was measured following the ASTM C128-2015 standard.

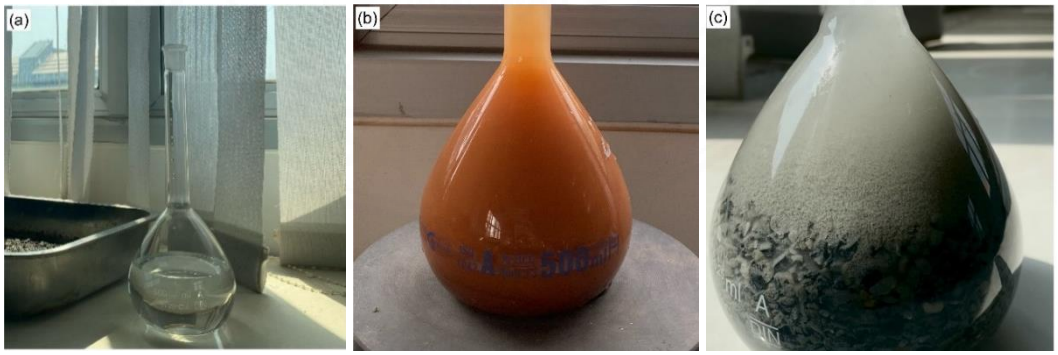

Figure 3.8 Specific gravity tests: (a) Pycnometer 500 ml, (b) Specific gravity test of soil, and (c) Specific gravity test of RCA.

3.4.3 Atterberg Limits Test

The Atterberg limit test assesses the plasticity and consistency properties of soil and is composed of two primary tests: the liquid limit test and the plastic limit test. The determination of the Liquid Limit (LL) and Plastic Limit (PL) for laterite soil was

Ref. code: 25676522040077WTA

conducted in accordance with ASTM D4318-2020 standards. In contrast, the recycled concrete aggregate exhibited a non-plastic behavior.

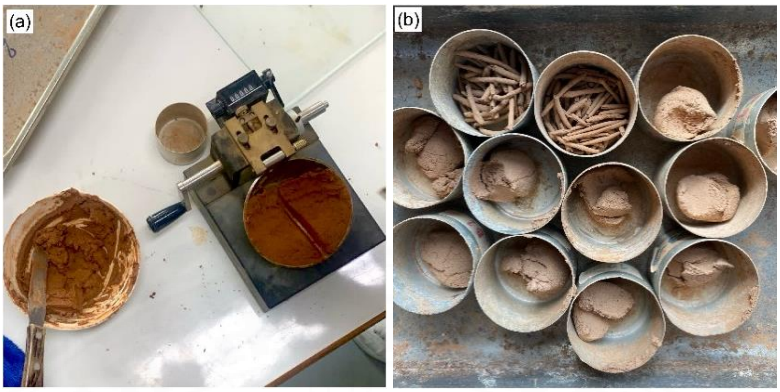

Figure 3.9 Atterberg limit equipment: (a) Casagrande device for liquid limit determination and (b) soil samples after oven drying.

3.4.4 Initial Consumption of Lime (ICL) Test

The ICL test quantifies the lime necessary to attain a specified pH level in acidic soil. In this procedure, soil samples are combined with lime, and the pH level is measured after a predefined duration. The ICL test serves as an efficient method for determining the lime quantity needed to elevate the pH of soil-lime mixtures to 12.4 within a one-hour timeframe. The ICL test was performed based on the Eades and Grim method prescribed in ASTM D6276 (1999).

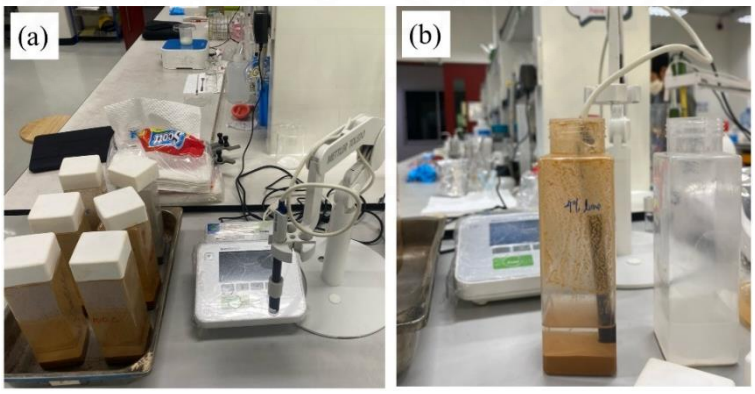

Figure 3.10 ICL test: (a) pH indicator and (b) conduct ICL test.

Ref. code: 25676522040077WTA

3.4.5 Standard Compaction Test

The moisture and density of 10 mix designs were determined in accordance with ASTM D698-2012 using standard proctor method. The standard was chosen to prepare the samples in lowest compaction effort. Initially, the materials were manually mixed in a dry state before water addition. Laterite soil was air-dried and sieved through No. 4 sieve. Subsequently, the laterite soil, RCA, and lime were mixed in varying proportions while still in a dry state. Moisture content was calculated after each compaction using three samples (top, middle, and bottom layers). For mixtures of laterite soil, RCA, and lime, compaction was delayed by 1 hour in accordance with ASTM D1557-2021.

Figure 3.11 Compaction test: (a) leveling the surface of the soil sample and (b) soil samples after oven drying to determine water content.

3.4.6 Unconfined Compressive Strength (UCS) Test

3.4.6.1 UCS Under Normal Conditions

The UCS test is a laboratory procedure used to measure the axial compressive strength of a soil specimen without any lateral confinement. The compaction energy was calculated utilizing the equation 3.1. The specimens needed for the UCS test were prepared using the same method as the compaction test. However, their dimensions were adjusted to a diameter of 70 mm and a height of 140 mm (twice the diameter). For this experiment, PVC pipes were utilized as shown in Figure 3.12. First, the raw material was mixed in dry conditions and then water was added in accordance with the OMC for each mix design and blend gently and evenly manually. After mixing, the samples were stored in zipped plastic for 1 hour to allow for mellowing and even moisture distribution. Gravel was utilized for filling the gap between the proctor mold

Ref. code: 25676522040077WTA

and the pipe, allowing it to be positioned properly. The samples were compacted in three layers similar to the standard proctor test and subsequently extruded. Then the samples were wrapped in plastic film, and subjected to 100% humidity at room temperature in a water bath conditions for 7, 28 and 56 days of curing. UCS tests were conducted in accordance with ASTM D5102-2009. The UCS test was carried out in accordance with ASTM 2166, employing a strain rate of 1 mm/min.

$$Compaction\ energy = \frac{(no\ of\ layers * no\ of\ blows * weight\ of\ hammer * height\ of\ fall)}{volume\ of\ mold} \quad (3.1)$$

Figure 3.12 UCS test: (a) compaction of soil in a PVC mold, (b) extrusion of the sample, (c) wrapping the samples for curing, and (d) conducting the UCS test.

3.4.6.2 UCS Under Wetting-Drying Conditions

The UCS method was utilized with soil material passing through sieve No. 4 (4.75 mm) as per ASTM 559. ASTM D 559-2003 outlines the standard procedures for wetting and drying compacted soil-cement mixes. Upon finishing the designated curing

Ref. code: 25676522040077WTA

duration for each specimen, they were completely submerged in potable water at room temperature for 5 hours. Subsequently, the specimens were dried in an oven at 71°C (160°F) for 2 days (48 hours), thereby completing one cycle of wetting and drying. The process was repeated, immersing the samples in water repeatedly to achieve 3 and 6 cycles. According to the standard, the specimens should be submerged in water for an additional two hours before conducting the UCS test. Figure 3.13 shows the UCS samples for wetting-drying conditions fully submerged in water to simulate heavy rainfall-induced flooding.

Figure 3.13 UCS under wetting and drying: (a) samples under wetting conditions, (b) samples after soaking for 5 hours, (c) samples during drying conditions, and (d) samples after oven drying for 2 days.

3.4.7 California Bearing Ratio (CBR) Test

The CBR test is a widely accepted method used in road construction to evaluate the strength and load-bearing capacity of soil. It is also employed to assess the potential strength of materials used in the subgrade, subbase, and base courses. In this research, the soil mixture is compacted to its optimum moisture content, determined by the

Ref. code: 25676522040077WTA

compaction test, and is arranged in three layers, each compacted with 56 blows. Two load plates, each applying a force of 50 N, are placed on the surface of the sample before it is inserted into the CBR machine. The test is performed at a loading rate of 1 mm/min, utilizing a cylindrical piston with a 49 mm diameter. Testing is carried out on both the top and bottom surfaces of the sample. The CBR test is performed following ASTM D1883 standards, focusing on samples that have been cured for 7 days to replicate the short-term behavior of road materials, in accordance with the Department of Highways (DOH) standards.

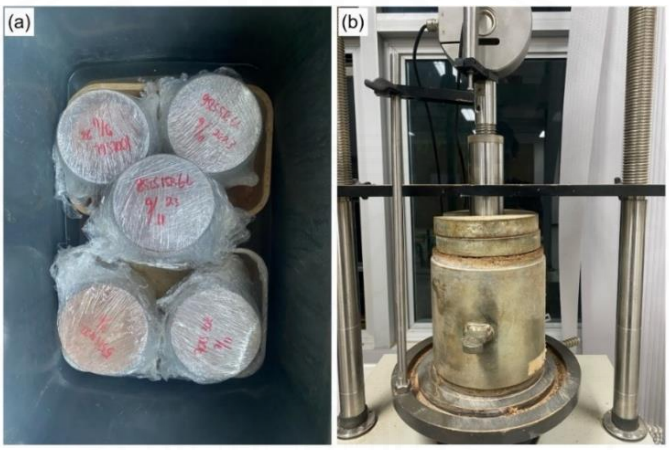

Figure 3.14 California Bearing Ratio: (a) Curing conditions of unsoaked CBR samples and (b) set up for performing the CBR test.

3.4.8 Direct Shear Test

The direct shear test is a commonly employed technique for determining the shear strength characteristics of materials, which is essential for evaluating the stability of slopes, retaining walls, and foundations that rely on soil shear strength for support. This test was conducted in accordance with ASTM D3080-2011 standards. For sample preparation, material mixtures were compacted into cylinder molds at the OMC for each mix design using the standard Proctor compaction method, with mold dimensions of 101 mm in diameter and 117 mm in height. The compacted samples were then extruded and cut into three specimens, each with average dimensions of 99 mm in diameter and 30 mm in height, and stored in plastic bags until testing, taking into account the curing time for samples without lime mixtures. In contrast, lime mixtures were left in the same shape for 5-7 days to prevent trimming difficulties caused by strong cementation bonds

Ref. code: 25676522040077WTA

during extended curing times. Researchers noted that cutting the samples into three specimens immediately after extrusion was impractical due to the weak characteristics of lime-treated mixes at that stage. To prevent moisture loss, the trimmed direct shear specimens were placed back into plastic containers until testing. Normal loads of 25, 50, and 100 kPa were applied to the soil specimens to simulate field pressures. The loading rate was maintained at 0.2 mm/min until failure occurred or the strain reached the maximum accepted value of 15% for drained test conditions. Figure 3.15 illustrates the stages of direct shear sample preparation and testing.

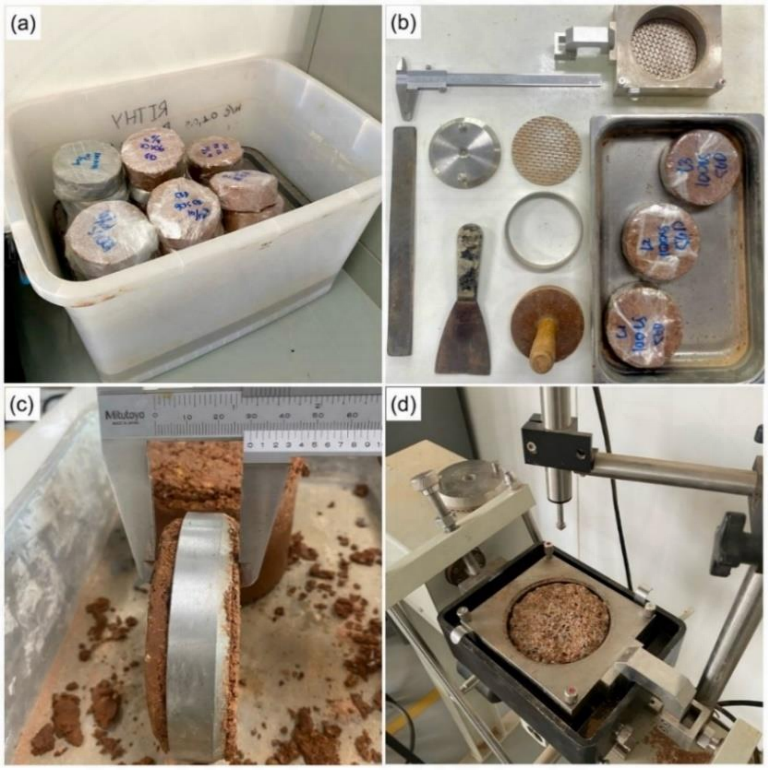

Figure 3.15 Direct shears: (a) curing conditions (b) sample preparation, (c) sample measurement, and (d) shear box set up.

3.4.9 Permeability Test

The constant-flow procedure, typically commonly used to determine the hydraulic conductivity of concrete specimens, was applied in this work to assess the permeability of soil mixtures. This technique provides a benefit over the standard falling-head methodology by allowing for the consistent application of pressure, which speeds up testing time. Sani and Eisazadeh (2023); Ye Htun et al. (2022) showed that this procedure is also successful in evaluating soil mixtures. Once a steady flow had

Ref. code: 25676522040077WTA

been achieved, hydraulic conductivity was measured. The permeability coefficient was derived using an equation 3.2 and Figure 3.16 illustrates the permeability equipment used to conduct the test.

$$k = \frac{QL\rho g}{PA} \tag{3.2}$$

where in this equation, *k* represents the coefficient of permeability (m/s), Q stands for the velocity of water movement (m^3/s), L denotes the longitudinal dimension of the sample (m), p indicates the density of water (kg/m^3), g represents the acceleration due to gravity (m/s^2), P signifies the applied water pressure (Pa), and A represents the cross-sectional area of the specimen (m^2).

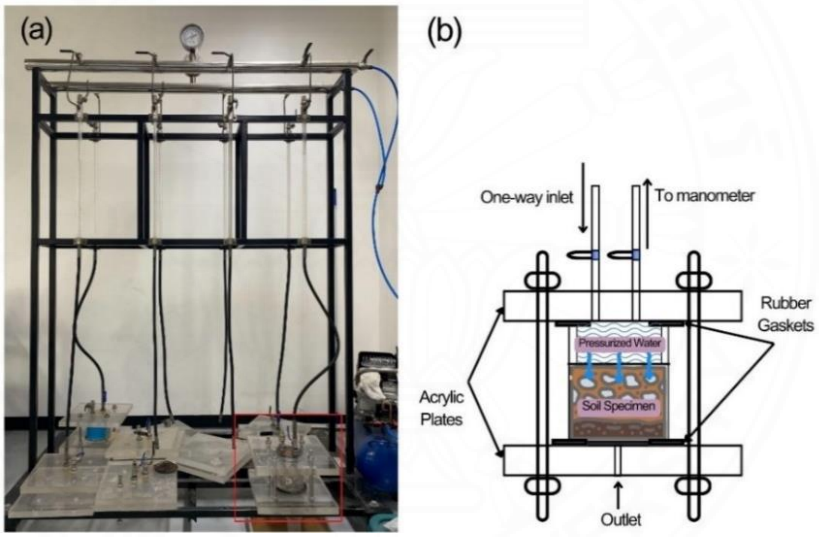

Figure 3.16 Permeability: (a) Entire permeability test assembled and (b) schematic diagram.

3.4.10 FESEM & EDS Analysis

FESEM stands for Field Emission Scanning Electron Microscopy, while EDS refers to Energy-Dispersive Spectroscopy. These analytical techniques play a vital role in examining the morphology and chemical composition of materials. FESEM enables researchers to examine the microstructure of samples at elevated magnification, offering valuable insights into the spatial distribution and organization of soil particles, as well as any changes resulting from the application of stabilization agents. Similarly, EDS analysis provides information about the elemental composition of samples. Figure

Ref. code: 25676522040077WTA

3.17 depicts the instrument model JSM-7800F Prime, manufactured by JEOL Asia Pte. Ltd., which was utilized for conducting FESEM and EDS tests.

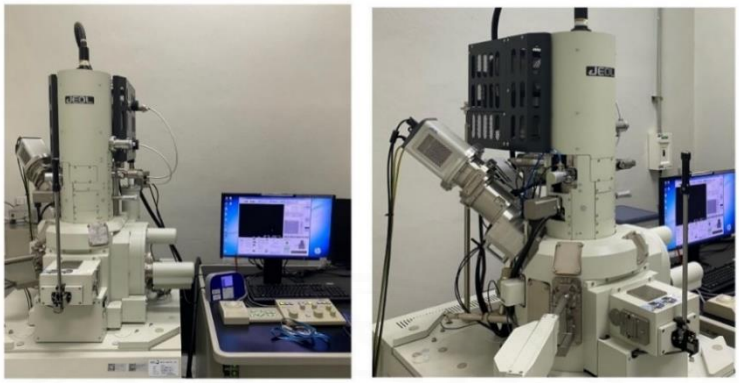

Figure 3.17 FESEM (left) & EDS machine (right).

Prior to conducting FESEM and EDS analyses, it is essential to coat samples to enhance conductivity. This precaution is necessary because the primary electrons used in SEM imaging can induce charging effects on non-conductive surfaces, resulting in blurred or distorted images and inaccurate EDS spectra. Gold coating is commonly employed for this purpose. The coating process typically requires only a few moments, depending on the coating method and specimen size. Generally, samples are coated with a thin layer of gold using techniques such as spray coating or thermal evaporation. This method involves depositing a thin layer of gold atoms onto the sample surface within a high-vacuum chamber, as shown in Figure 3.18.

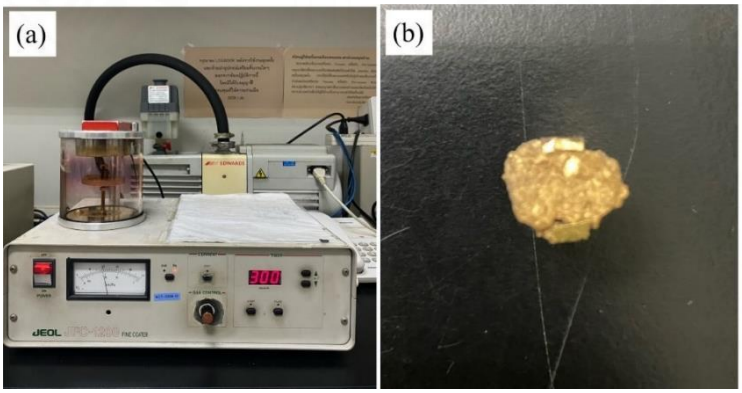

Figure 3.18 (a) Sputter Coater and (b) sample coated with Gold.

Ref. code: 25676522040077WTA

CHAPTER 4
RESULTS AND DISCUSSION

4.1 Basic Engineering Properties

The engineering properties of LS and RCA are detailed in Table 4.1. The red LS used in this study was obtained from Ban Mai, Pathum Thani, Thailand. This location was chosen due to its representative soil conditions. The specific gravity (G_s) values for the LS and RCA were 2.67 and 2.43, respectively. Initial assessments indicated that the RCA had a compressive strength of 30.4 MPa. Based on the USCS and AASHTO classification system, LS is classified as lean clay (CL) and A-6, while RCA is classified as Poorly Graded Sand (SP) and A-3.

Table 4.1 Geotechnical properties of laterite soil and RCA.

Properties	Laterite Soil	RCA
Sieve Analysis		
Gravel (%) [D>4.75 mm]	0.00	0.00
Sand (%) [0.075 mm<D<4.75 mm]	42.1	68.7
Fines Content (%) [D<0.075 mm]	57.9	31.3
Specific gravity	2.67	2.43
Proctor Compaction		
Optimum Moisture Content (OMC) (%)	11	11.8
Maximum Dry Unit Weight (MDUW) (kN/m³)	19.9	18.8
USCS Classification	CL	SP
AASHTO Classification	A-6	A-3
Los Angeles Abrasion	-	30.1
Color	Brown to red	Grey

***Note (-) Not possible*

4.2 Atterberg Limit

Atterberg limits test was performed to assess the liquid limit (LL), plastic limit (PL), and plasticity index (PI) of the soil mixtures, with the results provided in Table 4.2. The outcomes of the Atterberg limit tests show that an increase in the proportion of RCA in the laterite soil mixture leads to a decrease in the PI, suggesting that RCA contributes to reducing the plasticity of the natural soil. In mixtures containing a high proportion of RCA and lime, non-plastic (NP) behavior was observed, indicating that

Ref. code: 25676522040077WTA

the combination of lime and a high RCA content further reduces the plasticity of the material. Interestingly, pure RCA also exhibited non-plastic behavior.

Table 4.2 Atterberg limit properties.

Mix Design	LL (%)	PL (%)	PI
100LS	31.6	15.3	16.2
95LS5RCA	31.5	15.8	15.7
85LS15RCA	31.0	18.4	12.6
70LS30RCA	30.2	22.8	7.3
55LS45RCA	28.9	23.5	5.4
100LS6L	32.8	24.9	7.9
95LS5RCA6L	32.6	25.5	7.1
85LS15RCA6L	33.3	28.4	4.8
70LS30RCA6L	-	-	NP
55LS45RCA6L	-	-	NP
100RCA	-	-	NP

***Note (-) Not possible*

4.3 Particle Size Distribution

The particle size distribution of the LS and RCA materials was analyzed. The gradation curves are presented in Figure 4.1, with additional details regarding their size distributions provided in Table 4.1. The LS material contains approximately 42.1% sand particles and 57.9% fines, whereas the RCA is primarily composed of sand-sized particles, accounting for 68.7% of the total.

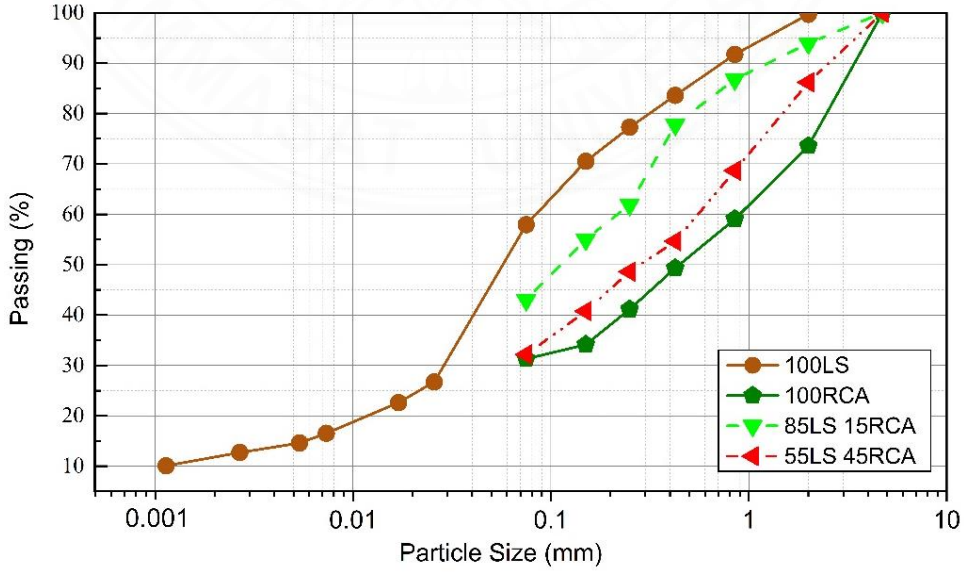

Figure 4.1 Particle size distribution of laterite soil and RCA.

Ref. code: 25676522040077WTA

4.4 ICL Test

Reactive components in RCA, such as silica and alumina, participate in pozzolanic reactions with soil particles (Disfani et al., 2014; Donrak et al., 2016), which require an alkaline environment with a pH around 12.5 (Garber et al., 2011; Prusinski & Bhattacharja, 1999). Different from Portland cement, RCA has already undergone cement hydration, leading to lower concentrations of calcium ions being released (Al-Mukhtar et al., 2012; Halsted et al., 2008). The pH values shown in Table 4.3 confirm that incorporating RCA produces a highly alkaline environment, favorable for chemical soil stabilization.

The ICL test is commonly used to determine the minimum amount of lime required for soil stabilization. This test was conducted on soil slurries composed of 100% lateritic soil, with varying lime contents from 2% to 6%. To initiate the pozzolanic reaction, the minimum lime requirement corresponds to a pH of 12.4, which is equivalent to the pH of a fully saturated lime solution. After one hour of curing, a lime content of 6% mixed with 100% lateritic soil was selected for further study. This selection was based on the rapid consumption of lime during the first hour of curing, followed by more gradual changes, likely due to the absence of ion-exchange minerals. According to Al-Mukhtar et al. (2012), this lime content is considered optimal for achieving effective soil stabilization.

Table 4.3 pH values for the materials.

Category	Value
Laterite soil	7.87
RCA	12.38
Laterite soil + 6% lime	12.40
Laterite soil + 5% lime	12.37
Laterite soil + 4% lime	12.35
Laterite soil + 3% lime	12.32
Laterite soil + 2% lime	12.27

Note: 1) The ICL was measured in accordance with ASTM D 6279 (ASTM D 6276, 1999) and 2) the pH was determined using ASTM D 4972 (ASTM D 4972, 2019).

Ref. code: 25676522040077WTA

4.5 Compaction Test

Figure 4.2 illustrates the compaction characteristics of various mix designs incorporating LS, RCA, and lime. The peak observed in the compaction curve of LS around the OMC is indicative of its moisture-sensitive nature, a characteristic typical of residual soils, where slight changes in moisture content significantly affect their compaction properties (Sani & Eisazadeh, 2023). Figure 4.3 demonstrates the impact of RCA and lime on the optimum moisture content (OMC) and maximum dry unit weight (MDUW) of laterite soil. It is evident that an increase in RCA content led to a rise in OMC and a decrease in MDUW, a trend that aligns with the results observed in previous studies (Kianimehr et al., 2019; Mohammed & Najim, 2020; Olufikayo & Benjamin, 2019; Shourijeh et al., 2022; Tran et al., 2022). The increase in OMC with RCA addition can be attributed to the porous and water absorptive nature of RCA particles. RCA has a relatively lower specific gravity (G_s=2.43) compared to the LS (G_s=2.67) and has sand-sized particles with rough surface, which reduces the particles rearrangement within the soil matrix, therefore reducing the overall unit weight. The flocculation of soil particles due to addition of lime also contributed to this reduction (Beja et al., 2020; Gangu & Shankar, 2024). Furthermore, adding lime increased the OMC while lowering the MDUW. The increase in OMC is due to the hydration reaction in lime treated soils, where calcium ions react with water and require more moisture for optimal compaction (Al-Mukhtar et al., 2012; Bell, 1996). The reduction in MDUW resulted from the agglomeration and flocculation of soil particles (Muntohar et al., 2013; Sani & Eisazadeh, 2024). The combination of RCA and lime may alter the particle size distribution and compaction behavior, as the relatively larger and rough-surfaced RCA particles create additional voids and lime causes fine particle aggregation, creating pore spaces that reduce the unit weight of the compaction samples (Aldaood et al., 2014; Koohmishi & Palassi, 2022).

Ref. code: 25676522040077WTA

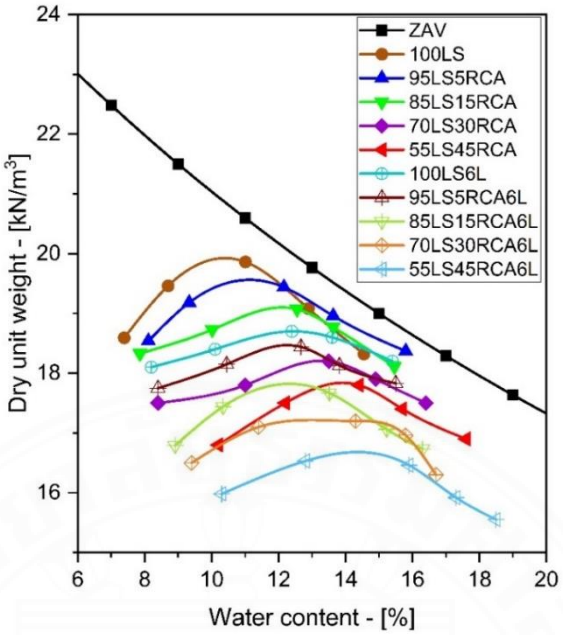

Figure 4.2 Compaction curve for all mix designs.

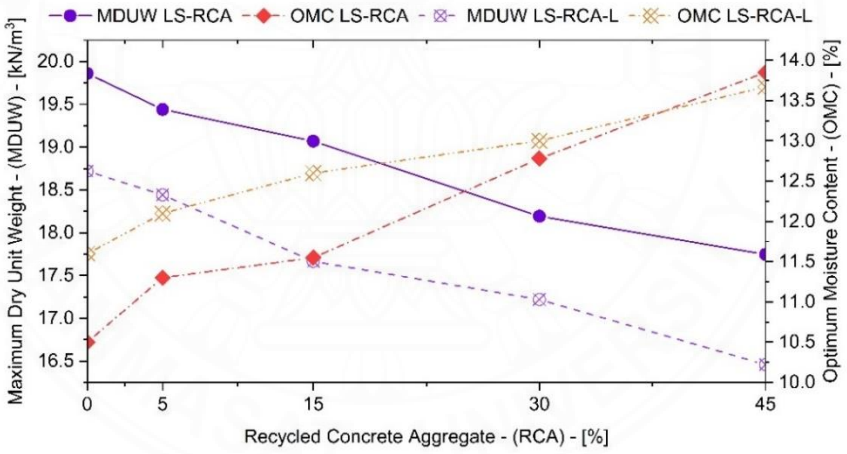

Figure 4.3 Variation of OMC and MDUW.

4.6 UCS Test

4.6.1 Axial Stress-strain Curve

Figure 4.4 illustrates the stress-strain curves obtained from UCS tests for various mix designs over curing periods ranging from 0 to 56 days, capturing both early and long-term mechanical properties. The findings reveal that replacing LS with RCA and adding lime improved the mechanical properties of the soil. The UCS values of LS-RCA mixtures progressively increased with higher RCA content, showing a 3.5-fold

Ref. code: 25676522040077WTA

improvement over untreated soil at 45% RCA content in uncured conditions (Figure 4.4a). The inclusion of lime had a significant impact on strength behavior, RCA alone exhibited more ductile characteristics, with higher strain but lower strength. In contrast, the addition of lime resulted in brittle failure at higher axial stresses, indicating a higher compressive strength. The calcium-based additives from both RCA and lime contribute to the formation of a stiffer and more brittle soil matrix (Mohammadinia et al., 2020; Sosahab et al., 2023). This improvement can be attributed to the chemical composition of RCA, which includes residual anhydrous cement. Although the cementation provided by RCA is weaker than that of traditional cement, its presence, derived from concrete debris, contributes to strength improvement.

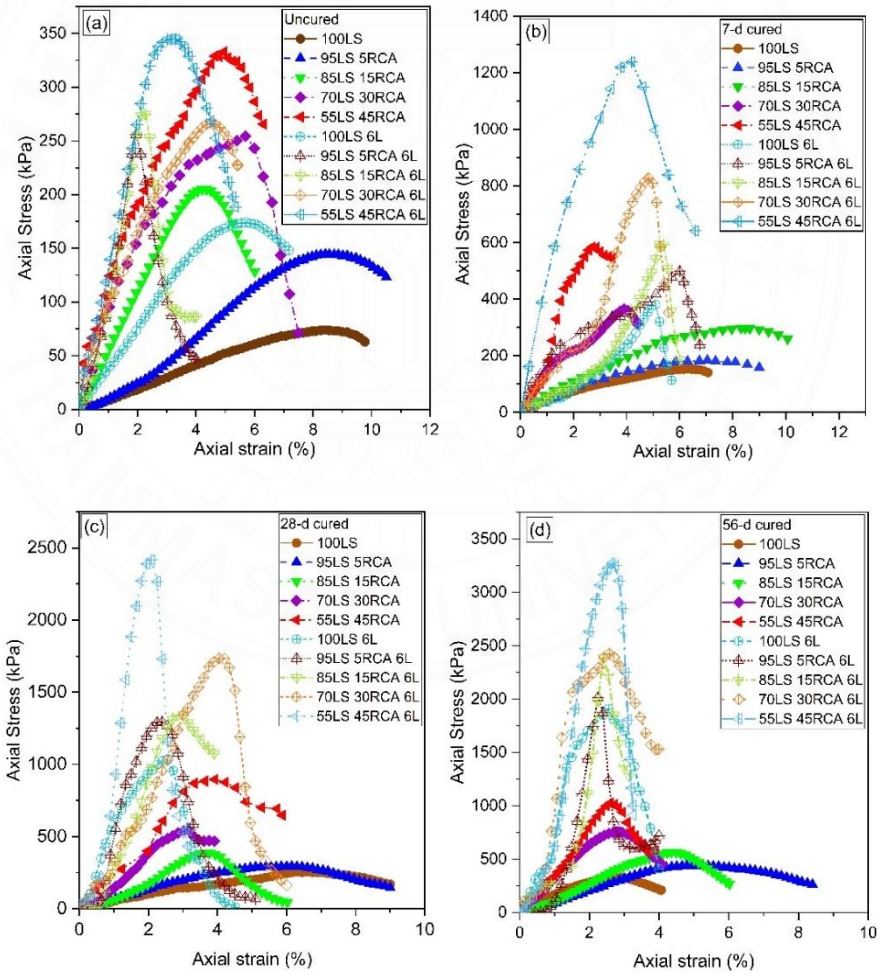

Figure 4.4 Stress-strain curve (a) uncured, (b) 7 days, (c) 28 days and (d) 56 days curing.

Ref. code: 25676522040077WTA

4.6.2 Maximum compressive strength (q_u)

The UCS test results presented in Figure 4.5 indicate a significant improvement in compressive strength (q_u) as the curing progresses from 0 to 56 days, emphasizing the influence of RCA and lime on the strength of LS. The uncured samples showed relatively low q_u values across all mixtures, indicating limited strength due to the insufficient time for hydration and pozzolanic reactions between the RCA and lime. After 7 days of curing, a steady increase in q_u values was observed, signifying the initiation of bonding and early strength development as a result of ion exchange and hydration. Mixtures incorporating lime showed a continuous increase in strength with extended curing time, which is attributed to enhanced bonding and stiffness from ongoing hydration and pozzolanic reactions, consistent with previous research findings (Bassani et al., 2019; Beja et al., 2020; Blankenagel & Guthrie, 2006; Cardoso et al., 2016; Haider et al., 2014).

The LS-RCA-L mixtures demonstrated higher q_u values at the early curing stages than the free-lime mixtures. This phenomenon can be attributed to the porosity of RCA, which hinders the effective filling of larger pores by soil particles, thereby compromising compactness and strength relative to lime-based mixtures. However, as curing duration extended, the formation of additional reaction products occurred, which effectively occupied voids and contributed to an increase in compressive strength. It is essential to recognize that both cementitious hydration and pozzolanic reactions require sufficient time to develop and should not be regarded unfavorably (Skibsted & Snellings, 2019; Verian et al., 2018). Notably, the majority of mixtures achieved the minimum UCS threshold determined by the DOH Thailand for subgrade or subbase-cemented soil materials within 7 days.

A significant increase in the UCS values was observed after 28 days of curing across all the mixed designs. This improvement can primarily be attributed to the sustained pozzolanic reaction between lime and RCA, coupled with ongoing hydration, which secure particle bonding and improves the stability of the soil structure. The elevated UCS values observed in mixtures with higher RCA content (e.g., 30% and 45%) at this point indicate that RCA contributes positively to stabilization, particularly when used in combination with lime. The prolonged curing period facilitates the

Ref. code: 25676522040077WTA

complete development of the pozzolanic reaction, resulting in materials that are stronger and more rigid.

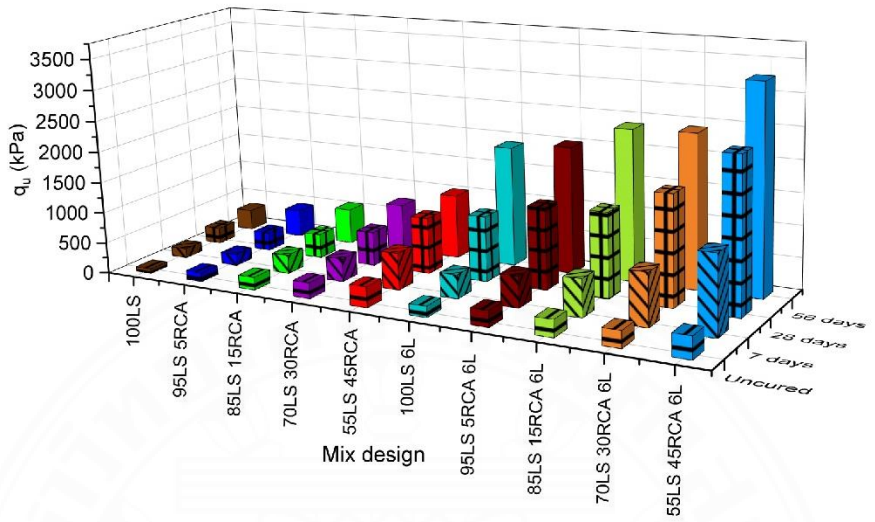

Figure 4.5 UCS test – Maximum compressive strength (qu) for all mix designs.

The combination of RCA, lime, and extended curing resulted in substantial UCS gains. The cementitious reaction triggered by RCA upon interaction with water and LS, alongside lime-induced pozzolanic reactions, supported continuous hardening of the soil matrix. Table 4.4 shows significant UCS improvements for RCA and lime-treated mixtures compared to untreated soil, with untreated soil showing a UCS of 328.1 kPa, below the DOH Thailand minimum for subbase materials after 56 days (Arulrajah et al., 2014; DOH 205/2559, 2016; Phummiphan et al., 2017). According to DOH standards, cement-stabilized UCS must reach a minimum of 689 kPa for subbase and 1724 kPa for base materials after 7 days. The 45% RCA and 6% lime mixture yielded a 7.1-fold increase due to lime-initiated pozzolanic reactions and unhydrated RCA cement particles (Li, 2020; Tavakol et al., 2019). The strength development index (SDI) was calculated as follows:

$$SDI = \frac{q_u(mix\ design) - q_u(LS)}{q_u(LS)} \tag{4.1}$$

where q_u represents the UCS values of the specific mix design and LS denotes the laterite soil.

Ref. code: 25676522040077WTA

Table 4.4 Strength Development Index (SDI).

Mix Design	Maximum stress (q_u) - [kPa]				SDI			
	0 Day	7 Days	28 Days	56 Days	0 Day	7 Days	28 Days	56 Days
100LS	74.0	153.3	257.3	328.2	0.0	0.0	0.0	0.0
95LS 5RCA	144.5	184.0	294.2	439.0	1.0	0.2	0.1	0.3
85LS 15RCA	204.9	297.4	389.2	565.5	1.8	0.9	0.5	0.7
70LS 30RCA	254.5	366.0	549.1	755.1	2.4	1.4	1.1	1.3
55LS 45RCA	333.0	584.6	896.2	1024.4	3.5	2.8	2.5	2.1
100LS 6L	174.1	380.3	1037.1	1910.4	1.4	1.5	3.0	4.8
95LS 5RCA 6L	255.9	498.5	1294.7	2015.5	2.5	2.3	4.0	5.1
85LS 15RCA 6L	274.7	593.4	1341.1	2390.9	2.7	2.9	4.2	6.3
70LS 30RCA 6L	266.6	827.6	1734.6	2423.3	2.6	4.4	5.7	6.4
55LS 45RCA 6L	344.7	1238.1	2416.7	3272.3	3.7	7.1	8.4	9.0

4.6.3 Secant elastic modulus (E_{50})

While the q_u values of the soil reflect its capacity to bear loads and resist external forces, the elastic modulus (E_{50}) represents the stiffness and deformation resistance under similar conditions. Figure 4.6 presents the E_{50} values for all mixtures at different curing ages. Similar to the q_u results, the mixtures treated with lime consistently exhibited higher E_{50} values than those without lime across all curing periods. The highest E_{50} values were recorded at 56 days, highlighting the role of the curing duration in enhancing the stiffness of the material. The 55LS45RCA6L mix exhibited the most significant increase in E_{50}, indicating the effectiveness of RCA as a high-strength aggregate and the beneficial effect of lime as a binder. The results revealed a steady increase in E_{50} with an increase in RCA content from 5% to 45%, suggesting that RCA improves the structural integrity and load-bearing capacity of the mixture, which is consistent with findings from previous studies (Hoy et al., 2023; Karkush & Yassin, 2019; Kianimehr et al., 2019).

Ref. code: 25676522040077WTA

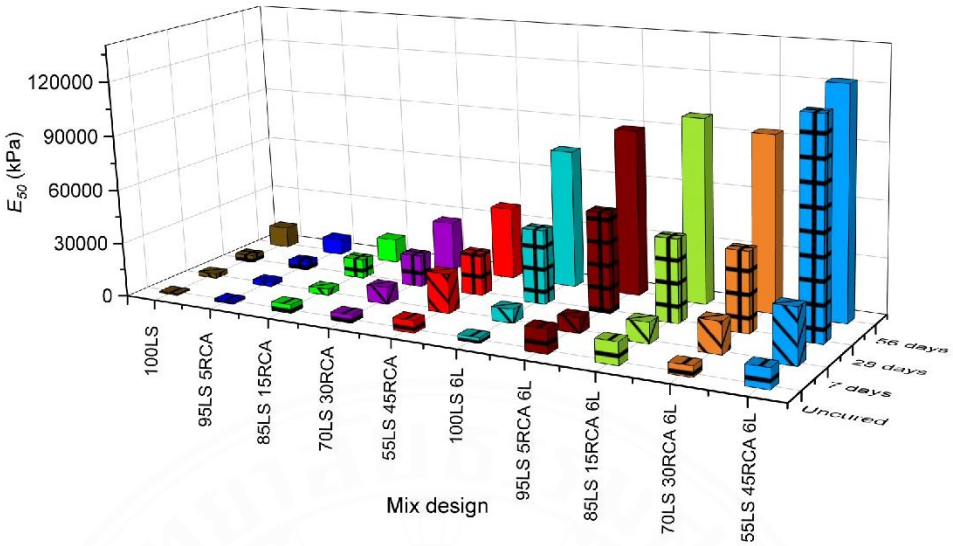

Figure 4.6 UCS test – Secant Elastic Modulus (E50) for all mix designs.

4.6.4 Relationship between q_u and E_{50}

Figure 4.7 illustrates the relationship between q_u and E_{50} values for both the treated and untreated mixtures at various curing ages. Notably, the correlation followed a linear trend, with a determination coefficient (R^2) of 0.95. This strong correlation suggests that q_u and E_{50} values are closely interconnected, regardless of the RCA content and curing time. Furthermore, this suggests that the changes in the stiffness of the soil matrix are closely correlated with its load-bearing capacity. Similar trend were observed for RCA-soil mixtures (Shamsi Susahab et al., 2024).

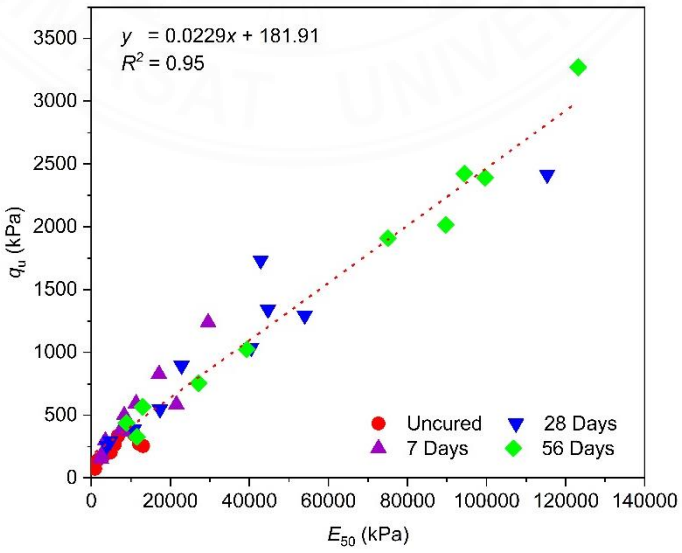

Figure 4.7 Relation between *qu* and E_{50} values of mixtures at all curing age.

Ref. code: 25676522040077WTA

4.6.5 Effect of wetting and drying cycles on UCS

The UCS of subbase materials is crucial for assessing their ability to withstand compressive loads in pavement engineering applications (Arulrajah et al., 2012). The UCS can vary widely depending on the material type (Azam & Cameron, 2013; Bui et al., 2018). Figure 4.8 illustrates the correlation between the UCS after wetting-drying (w-d) cycles and the number of cycles for the studied mixtures at 28- and 56- days of curing. The untreated soil failed during the first cycle, while the UCS(w-d) of treated mixtures increased through the 3rd cycle and then decreased after the 6th cycle. This initial increase is attributed to the accelerated formation of cementitious compounds, which enhance strength development and improve bond stability. The strength gain observed up to the third cycle suggest that the formation of new cementitious compounds reinforces UCS(w-d) without deterioration. However, the subsequent decrease in the sixth cycles is likely caused by volumetric changes that induce internal stresses within the soil samples, weakening bond integrity. Additionally, the dissolution of cementitious compounds may contribute to surface degradation and microcracking, further reducing strength. These results were consistent with those reported (Hoy et al., 2023; Neramitkornburi et al., 2015; Tran et al., 2022).

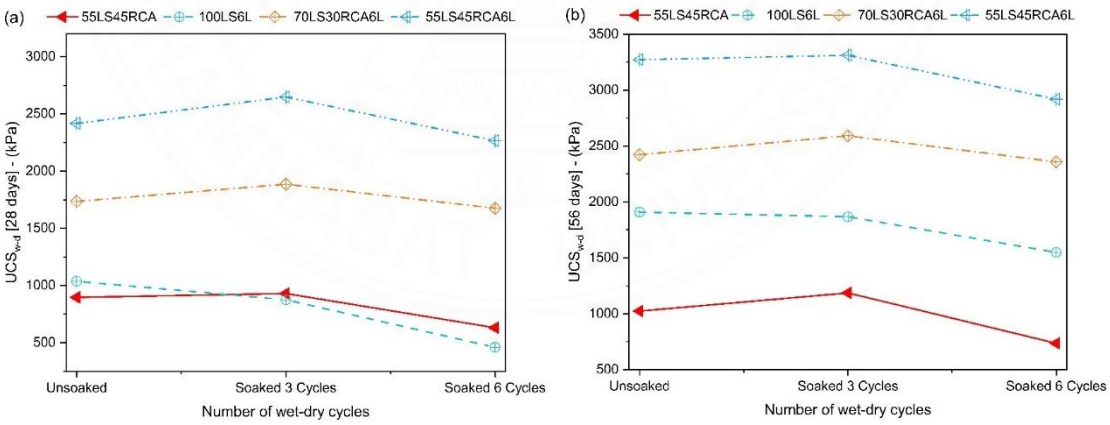

Figure 4.8 UCS under wetting drying conditions (a) 28 days and (b) 56 days curing period.

4.6.6 Effect of wetting and drying cycles on water absorption

The wetting and drying cycles have a significant influence on the water absorption of the mixtures. As illustrated in Figure 4.9, water absorption is observed after 28 and 56 days of curing. The water absorption shows the progressive increase

Ref. code: 25676522040077WTA

with each cycle. This is primarily due to structural deterioration, which raises the porosity and facilitates water penetration. For samples cured for 56 days, lime played a vital role in mitigating water absorption by enhancing the bond between RCA and soil particles and forming cementitious compounds, which reduced porosity and water ingress. These observations align with previous research on water absorption under wetting and drying conditions involving lime treatments (Aldaood et al., 2014; Muntohar, 2019; Razali et al., 2023).

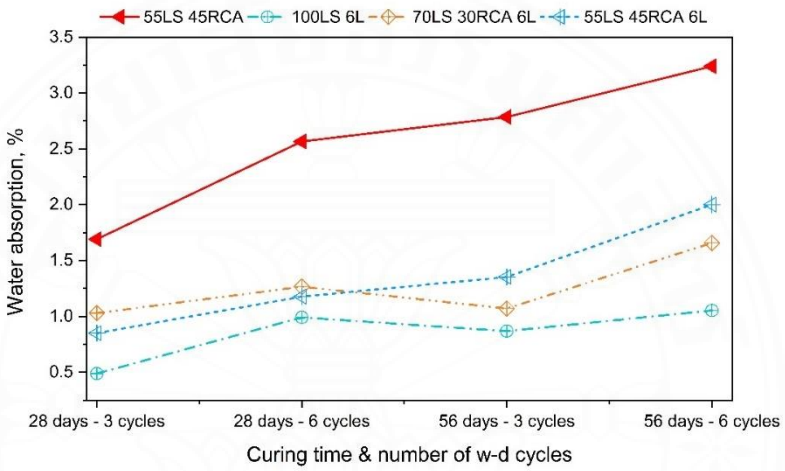

Figure 4.9 Effect of wetting-drying conditions water absorption.

4.7 Direct Shear Test

The shear stress-horizontal displacement curve of all mix designs cured for 28 and 56 days under a normal stress of 100 kPa are presented in Figure 4.10. The natural soil demonstrated a better ductility compared to the treated samples. The RCA lime-stabilized mixtures exhibited a significant increase in the peak shear stresses especially after 56 days of curing with a brittle failure characteristic. This improvement is due to the formation of new cementitious materials (calcium silicate hydrate (C-S-H) gel) that bonded the particles together and resulted in improved cohesion. The irregular shape and rough surface of RCA particles also increased the interlocking and friction between particles, as reported in previous studies (Azam & Cameron, 2013; McKelvey et al., 2002; Saberian et al., 2020). In Table 4.5, the effect of RCA on the shear strength parameters, i.e., cohesion (c') and friction angle (ϕ'), were listed. The results suggested that increasing the RCA content and curing duration could enhance both the cohesion and friction angle of the treated soil. The untreated soil displayed relatively small

Ref. code: 25676522040077WTA

changes in the cohesion and friction angle values over time, which aligns with the absence of chemical reactions in the natural soil.

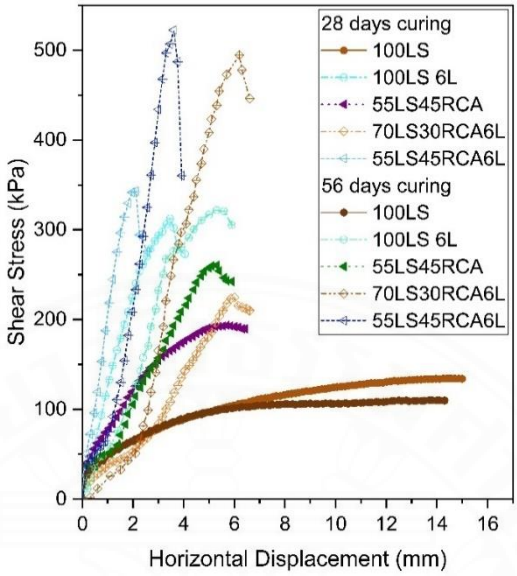

Figure 4.10 Shear stress-displacement behavior of all mixes under 100 kPa normal stress.

Table 4. 5 Shear strength parameters.

Mix Designs	Uncured		28 days		56 days	
	c’ (kPa)	ϕ’ (°)	c’ (kPa)	ϕ’ (°)	c’ (kPa)	ϕ’ (°)
100 LS	22.7	44.3	24.8	41.0	30.1	39.4
100 RCA	34.9	56.4	325.8	67.3	414.3	61.3
55 LS 45 RCA	28.3	48.8	107.6	40.6	258.9	34.3
100 LS 6 L	25.6	41.9	177.5	57.4	319.8	55.4
70 LS 30 RCA 6 L	33.9	48.9	182.8	58.3	265.5	50.4
55 LS 45 RCA 6 L	64.6	39.8	237.3	45.8	394.1	55.1

4.8 California Bearing Ratio Test

The influence of incorporating RCA into soil stabilization processes on the CBR test results can vary depending on the properties and condition of the RCA used. RCA has shown potential to increase the strength and load-bearing capacity of stabilized soil, thereby improving the CBR (Ma et al., 2022). The CBR results presented in Table 4.6 demonstrate a significant improvement in the soil-bearing capacity when treated with RCA and lime. The untreated LS, with a CBR value of 6.7%, reached a CBR value of 32.7% with the addition of 45% RCA after seven days of curing. This value exceeds the minimum threshold of 25% specified by DOH Thailand for subbase pavement. The

Ref. code: 25676522040077WTA

improvement in the CBR value was due to the unhydrated cement within the RCA, which promoted self-cementing properties when mixed with soil. The results align with previous studies that have highlighted the role of unhydrated cement in crushed concrete in improving soil strength during curing (Blankenagel & Guthrie, 2006; Haider et al., 2014; Thai et al., 2022). The addition of lime further boosted the CBR values by ion-exchange reactions and flocculation of clay particles.

Table 4.6 California Bearing Ratio with different curing time.

Mix design	Uncured	7 Days	DOH Standard for subbase
100 LS	2.8	6.7	*NP*
95 LS 5 RCA	4.1	13.0	*NP*
85 LS 15 RCA	7.6	15.8	*NP*
70 LS 30 RCA	12.3	17.8	*NP*
55 LS 45 RCA	16.7	32.7	*P*
100 LS 6L	4.0	17.3	*NP*
95 LS 5 RCA 6L	5.8	29.7	*P*
85 LS 15 RCA 6L	10.5	33.7	*P*
70 LS 30 RCA 6 L	14.1	37.2	*P*
55 LS 45 RCA 6L	19.7	46.6	*P*

Note: *P = Passed, NP = Not Passed*

4.9 Hydraulic Conductivity Results

Figure 4.11 demonstrated the changes in hydraulic conductivity when RCA and lime were incorporated into the soil. The hydraulic conductivity (k) of natural laterite soil was determined to be 2.6×10^{-8} m/s and 3.8×10^{-8} m/s after 28 and 56 days of curing, respectively. Similar low permeability coefficients have been reported for tropical laterite soils by (Sani & Eisazadeh, 2023; Ye Htun et al., 2022). The addition of 45% RCA increased the k value to 3.01×10^{-7} m/s after 56 days of curing. This indicated an increase of more than seven times compared to the natural soil. This increase was due to the porous and coarse-grained nature of RCA and enhanced water absorption capacity (Islam et al., 2023; Rahman et al., 2015). Nonetheless, the addition of lime significantly reduced the permeability coefficient. This reduction is likely due to the void-filling effect of cementitious materials formed during the pozzolanic reaction. This behavior is further supported by the microstructural changes observed through FESEM images which revealed the development of a denser matrix.

Ref. code: 25676522040077WTA

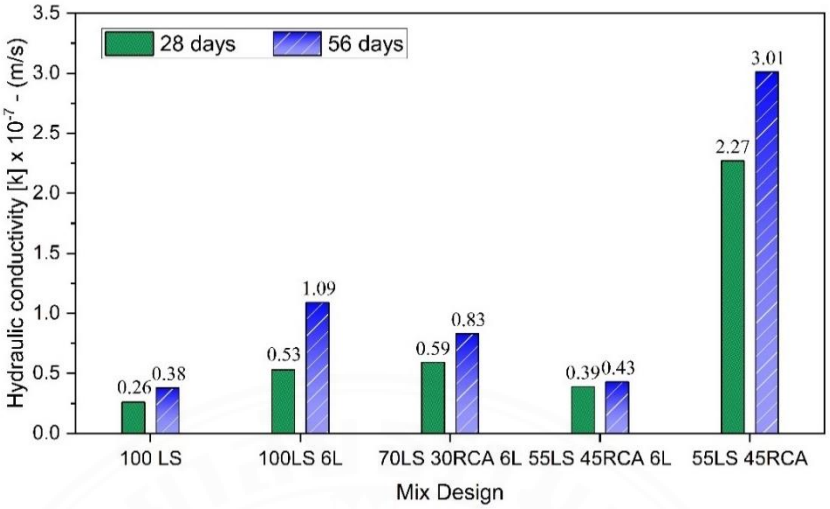

Figure 4.11 Effect of RCA content on the k values with different mixed designs.

4.10 FESEM and EDS analysis

Field Emission Scanning Electron Microscopy (FESEM) is a powerful tool for studying the changes in morphology of the soil and detecting the formation of cementitious materials. Figure 4.12 showed the FESEM images for various mix designs cured for 56 days. As seen in Figure 4.12(b), in pure laterite soil, the flaky soil structure is relatively dense and less porous. However, in mixes containing 45% RCA (Figure 4.12(c)), larger agglomerates with rougher surface are clearly visible. In samples containing lime (Figure 4.12(d)), white lumps were observed indicating the formation of cementitious materials on the soil surface (Domphoeun & Eisazadeh, 2024; Sani & Eisazadeh, 2023; Suksiripattanapong et al., 2022). Figure 4.13 shows the EDS spectra of the natural and RCA-lime treated soil after 56 days of curing. The rectangular selection area was chosen to include the white lumps (Figure 4.13(b)). The findings indicated that in RCA-lime stabilized soil, substantially higher Ca peaks were evident. Furthermore, the reduction in Si and Al peaks clearly indicated the consumption of these chemicals in the pozzolanic reaction and the formation of cementitious materials, which is consistent with the high strength and low permeability values (Danso & Manu, 2020; Domphoeun & Eisazadeh, 2024; Jha & Sivapullaiah, 2015; Sani & Eisazadeh, 2023).

Ref. code: 25676522040077WTA

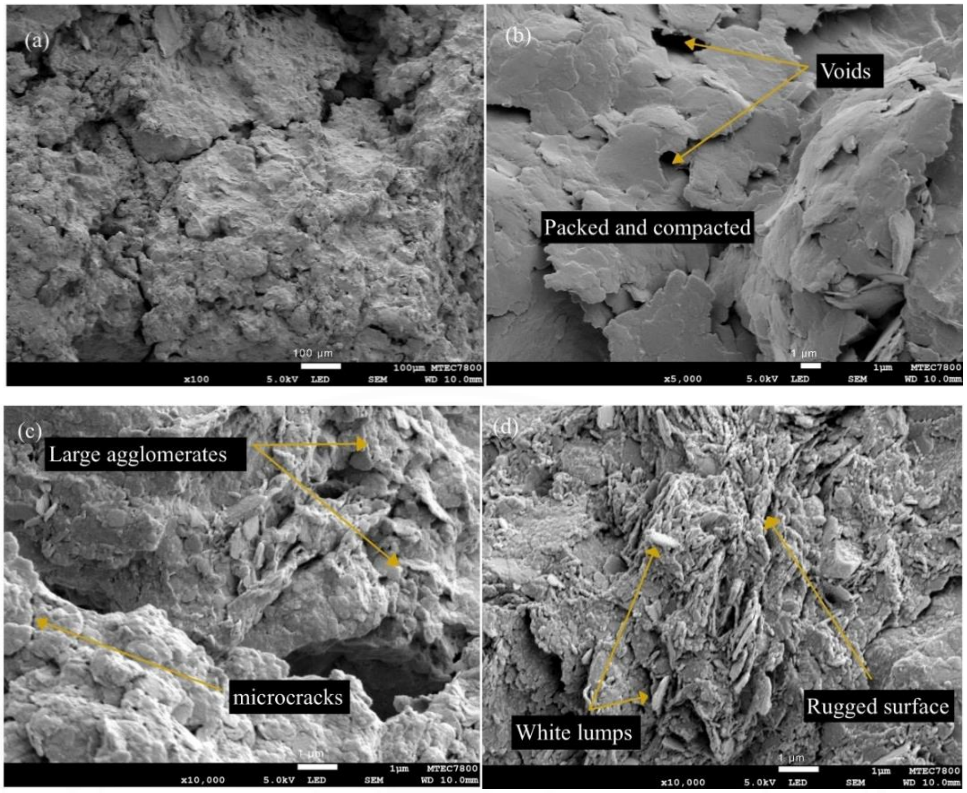

Figure 4.12 FESEM images (a) 100LS (x100), (b) 100LS (x5K), (c) 45%RCA, and (d) 45%RCA 6%L.

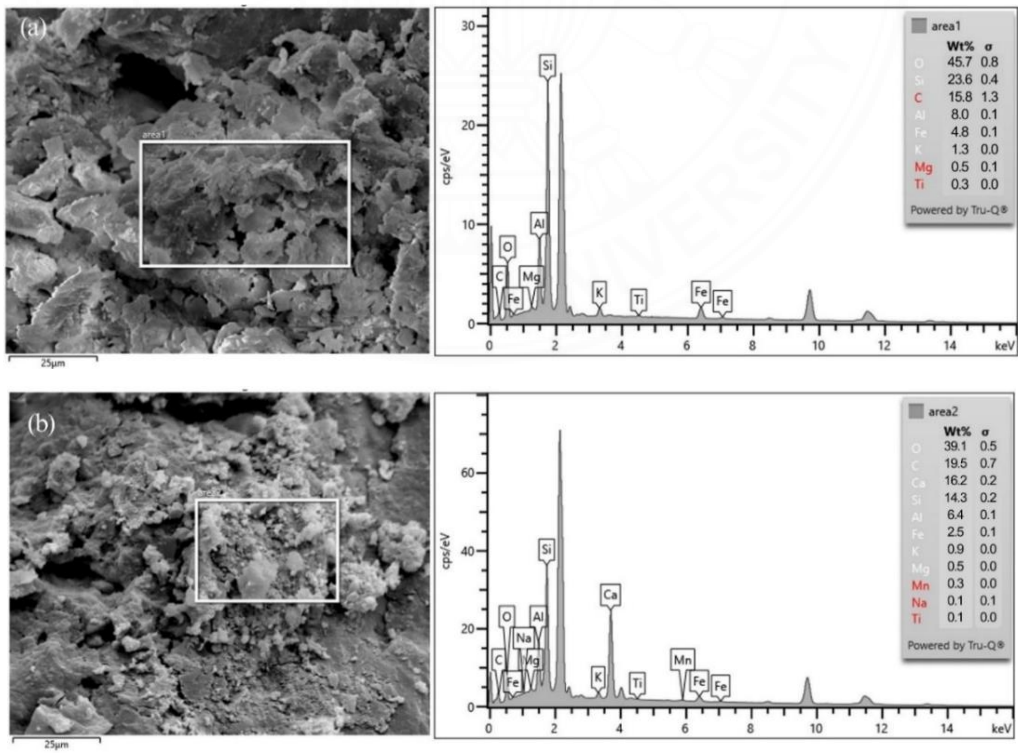

Figure 4.13 EDS spectra of specimens (a) 100LS and (b) 55LS45RCA6L.

Ref. code: 25676522040077WTA

CHAPTER 5
CONCLUSION

5.1 Conclusion

This study evaluated the compaction characteristics, compressive strength development, shear strength, CBR and permeability of tropical laterite soil stabilized using RCA and lime as a subbase material. The findings indicate that the inclusion of RCA and lime significantly improves the strength, resulting in notable improvements in the engineering properties of the laterite soil. The principal outcomes are as follows:

1) The addition of RCA to LS increased the OMC and reduced the MDUW. The decrease in MDUW was consistent with the lower G_s of RCA and rougher irregular shaped particles. The addition of lime further increased the OMC and decreased the MDUW of the LS and LS-RCA mixed. The former was attributed to the water demand of lime hydration reaction whereas the latter was linked to the increased interparticle porosity due to agglomeration and flocculation in lime-treated mixes.
2) Utilizing RCA and incorporating lime into LS improved the UCS values, with longer curing durations resulting in higher q_u values. The use of RCA only exhibited ductile behavior, while the addition of lime resulted in brittle failure under higher axial stress. The calcium-based components from both RCA and lime contributed to a stiffer and more brittle soil matrix. The mix designs containing 30% and 45% RCA along with 6% lime attained the highest UCS values after a 7-day curing period, meeting the DOH standards for subbase materials in Thailand. After 28 days, other mixed designs also conformed to these standards. This performance is due to the involvement of RCA in cementitious and pozzolanic reactions facilitated by the addition of lime, resulting in the formation of calcium silicate hydrate gels.
3) The UCS(w-d) behavior of RCA-stabilized LS demonstrated progressive improvement over time, in contrast to untreated soil, which failed during the initial cycle. Stabilized mixtures showed an increase in UCS(w-d) values up until the third cycle, after which a reduction was observed at the sixth cycle. This initial strength increase can be attributed to the accelerated formation of cementitious compounds that enhance bonding stability and strength development. The observed decrease in

Ref. code: 25676522040077WTA

UCS(w-d) after the sixth cycle likely stems from volumetric changes that introduce internal stresses within the soil samples, weakening the bond strength. Additionally, the dissolution of cementitious compounds may lead to surface degradation and the formation of microcracks, further reducing the UCS(w-d). Despite this reduction, UCS(w-d) values remained above the DOH Thailand minimum strength requirement (UCS > 689 kPa) even after the sixth cycle.

4) The repeated wetting-drying cycles significantly influenced water absorption. Structural deterioration of RCA increased porosity, enabling greater water penetration. However, for samples cured over 56 days, the addition of 6% lime mitigated these effects. The lime enhanced the bond between RCA and soil particles, generating additional cementitious compounds that reduced porosity and filled voids, thereby limiting water ingress.
5) Treating the soil with RCA and lime improved both cohesion (c') and friction angle (ϕ) parameters. This improvement is due to the formation of new cementitious materials (calcium silicate hydrate (C-S-H) gel) that bonded the particles together and resulted in improved cohesion. The irregular shape and rough surface of RCA particles also increased the interlocking and friction between particles.
6) The inclusion of RCA and lime increased the bearing capacity of the soil, meeting the subbase CBR value requirements set by the DOH, Thailand. The improvement in the CBR value was due to the unhydrated cement within the RCA which promoted self-cementing properties when mixed with soil and pozzolanic reactions of lime. The results align with UCS values that have highlighted the role of unhydrated cement in crushed concrete in enhancing soil strength during curing.
7) For road applications requiring higher load-carrying capacity and lower permeability, the use of lime in RCA treated laterite soil is advisable. The presence of lime could minimize the water infiltration, which can weaken the cementation bond and degrade durability of the subbase layer over time.

5.2 Recommendation for Future Works

Drawing from the conclusions presented above, it is evident that further research is essential to address several key areas, the further studies should be done as the follows:

Ref. code: 25676522040077WTA

1) To enhance the understanding of the suitability of RCA and lime in road pavement design, it is recommended to perform California Bearing Ratio (CBR) tests across a broader range of particle sizes under both soaked and unsoaked conditions.
2) To thoroughly evaluate UCS under wetting and drying conditions, it is essential to increase both the variety of mix designs and the number of wetting-drying cycles. This method is vital for obtaining a more comprehensive understanding of material performance under diverse environmental and loading scenarios. Furthermore, the inclusion of durability assessments is crucial.
3) RCA-lime stabilized laterite soil has shown promising potential for use in subbase pavement applications. While the economic feasibility of using recycled concrete aggregate as a soil replacement material varies by region, its advantages include reducing landfill waste and lowering carbon emissions. Future research should focus on field investigations to better assess its practical applications.

Ref. code: 25676522040077WTA

REFERENCES

Aatheesan, T., Arulrajah, A., Newman, G., Bo, M. W., & Wilson, J. (2009). Crushed brick blends with crushed concrete for pavement sub-base and drainage applications. *Australian Geomechanics*, *44*(2), 65.

Abd Rashid, M. F., Alias, N., Ahmad, K., Ramli, M. Z., & Ibrahim, Z. (2019). Vibration impact towards deformable laterite soil with different moisture content. IOP Conference Series: Earth and Environmental Science,

Afrin, H. (2017). A review on different types soil stabilization techniques. *International Journal of Transportation Engineering and Technology*, *3*(2), 19-24.

Agarwal, A., Datta, M., Ramana, G., Soni, N., & Satyakam, R. (2021). Geotechnical characterization of recycled aggregates (RA) comprising of mixed waste from construction & demolition (C&D) plants. Proceedings of the Indian Geotechnical Conference 2019: IGC-2019 Volume II,

Al-Mukhtar, M., Khattab, S., & Alcover, J.-F. (2012). Microstructure and geotechnical properties of lime-treated expansive clayey soil. *Engineering Geology*, *139*, 17-27.

Al-Swaidani, A., Hammoud, I., & Meziab, A. (2016). Effect of adding natural pozzolana on geotechnical properties of lime-stabilized clayey soil. *Journal of Rock Mechanics and Geotechnical Engineering*, *8*(5), 714-725.

Aldaood, A., Bouasker, M., & Al-Mukhtar, M. (2014). Impact of wetting–drying cycles on the microstructure and mechanical properties of lime-stabilized gypseous soils. *Engineering geology*, *174*, 11-21.

Amadi, A., & Okeiyi, A. (2017). Use of quick and hydrated lime in stabilization of lateritic soil: comparative analysis of laboratory data. *International Journal of Geo-Engineering*, *8*, 1-13.

Anda, R., Wang, L., Ying, M.-j., & Huang, Y.-t. (2023). Analysis of Shear Characteristics of Recycled Concrete Aggregate–Geogrid Interface. *Journal of Materials in Civil Engineering*, *35*(7), 04023169.

Angulo, S. C., Ulsen, C., John, V. M., Kahn, H., & Cincotto, M. A. (2009). Chemical–mineralogical characterization of C&D waste recycled aggregates from São Paulo, Brazil. *Waste management*, *29*(2), 721-730.

Anupam, A. K., Kumar, P., & Ransinchung, R. (2016). Effect of fly ash and rice husk ash on permanent deformation behaviour of subgrade soil under cyclic triaxial loading. *Transportation Research Procedia*, *17*, 596-606.

Archibong, G., Sunday, E., Akudike, J., Okeke, O., & Amadi, C. (2020). A review of the principles and methods of soil stabilization. *International Journal of Advanced Academic Research| Sciences*, *6*(3), 2488-9849.

Archwichai, L., Youngme, W., Somphadung, S., Changsuwan, S., Wannakao, P., Hokjaroen, S., & Wannakao, L. (1993). Engineering properties of lateritic soils from Khon Kaen and its vicinity, Thailand. *Journal of Southeast Asian Earth Sciences*, *8*(1-4), 549-556.

Arisha, A., Gabr, A., El-Badawy, S., & Shwally, S. (2016). Using blends of construction & demolition waste materials and recycled clay masonry brick in pavement. *Procedia engineering*, *143*, 1317-1324.

Arulrajah, A., Disfani, M. M., Horpibulsuk, S., Suksiripattanapong, C., & Prongmanee, N. (2014). Physical properties and shear strength responses of recycled

Ref. code: 25676522040077WTA

construction and demolition materials in unbound pavement base/subbase applications. *Construction and Building Materials*, *58*, 245-257.

Arulrajah, A., Mohammadinia, A., Phummiphan, I., Horpibulsuk, S., & Samingthong, W. (2016). Stabilization of recycled demolition aggregates by geopolymers comprising calcium carbide residue, fly ash and slag precursors. *Construction and Building Materials*, *114*, 864-873.

Arulrajah, A., Piratheepan, J., Ali, M., & Bo, M. (2012). Geotechnical properties of recycled concrete aggregate in pavement sub-base applications. *Geotechnical Testing Journal*, *35*(5), 743-751.

Arulrajah, A., Piratheepan, J., Disfani, M. M., & Bo, M. (2013). Resilient moduli response of recycled construction and demolition materials in pavement subbase applications. *Journal of materials in civil engineering*, *25*(12), 1920-1928.

ASTM D 4972. (2019). Standard Test Method for pH of Soils. In (Vol. 19428 - 2959). West Conshocken: PA.

ASTM D 6276. (1999). Standard Test Methods for Using pH to Estimate the Soil-Lime Proportion Requirement for Soil Stabilization. In (Vol. 19428 - 2959). West Conshohocken: PA.

Azam, A., & Cameron, D. (2013). Geotechnical properties of blends of recycled clay masonry and recycled concrete aggregates in unbound pavement construction. *Journal of materials in civil engineering*, *25*(6), 788-798.

Barman, D., & Dash, S. K. (2022). Stabilization of expansive soils using chemical additives: A review. *Journal of Rock Mechanics and Geotechnical Engineering*, *14*(4), 1319-1342.

Bassani, M., Tefa, L., Russo, A., & Palmero, P. (2019). Alkali-activation of recycled construction and demolition waste aggregate with no added binder. *Construction and Building Materials*, *205*, 398-413.

Beja, I. A., Motta, R., & Bernucci, L. B. (2020). Application of recycled aggregates from construction and demolition waste with Portland cement and hydrated lime as pavement subbase in Brazil. *Construction and Building Materials*, *258*, 119520.

Bell, F. (1996). Lime stabilization of clay minerals and soils. *Engineering Geology*, *42*(4), 223-237.

Bennert, T., & Maher, A. (2008). *The use of recycled concrete aggregate in a dense graded aggregate base course*.

Bestgen, J. O., Hatipoglu, M., Cetin, B., & Aydilek, A. H. (2016). Mechanical and environmental suitability of recycled concrete aggregate as a highway base material. *Journal of Materials in Civil Engineering*, *28*(9), 04016067.

Bhurtel, A., & Eisazadeh, A. (2020). Strength and durability of bottom ash and lime stabilized Bangkok clay. *KSCE Journal of Civil Engineering*, *24*, 404-411.

Bhurtel, A., & Otaghsaraei, A. E. (2018). *STRENGTH AND DURABILITY ASSESSMENT OF BOTTOM ASH AND LIME STABILIZED CLAYEY SOIL AS SUSTAINABLE ROAD MATERIAL IN THAILAND* Thammasat University].

Biswal, D. R., Sahoo, U. C., & Dash, S. R. (2020). Fatigue characteristics of cement-stabilized granular lateritic soils. *Journal of Transportation Engineering, Part B: Pavements*, *146*(1), 04019038.

Ref. code: 25676522040077WTA

Blankenagel, B. J., & Guthrie, W. S. (2006). Laboratory characterization of recycled concrete for use as pavement base material. *Transportation research record*, *1952*(1), 21-27.

Buchanan, F. H. (1807). *A Journey from Madras Through the Countries of Mysore, Canara, and Malabar, Performed Under the Orders of the Most Noble the Marquis Wellesley, Governor General of India* (Vol. 1). Cadell.

Bui, N. K., Satomi, T., & Takahashi, H. (2018). Mechanical properties of concrete containing 100% treated coarse recycled concrete aggregate. *Construction and Building Materials*, *163*, 496-507.

Cabrera, M., Martinez-Echevarria, M., López-Alonso, M., Agrela, F., & Rosales, J. (2021). Self-compacting recycled concrete using biomass bottom ash. *Materials*, *14*(20), 6084.

Cardoso, R., Silva, R. V., de Brito, J., & Dhir, R. (2016). Use of recycled aggregates from construction and demolition waste in geotechnical applications: A literature review. *Waste Management*, *49*, 131-145.

Chan, C.-M., & Low, L.-P. (2010). Development of a Strength Prediction Model for" Green" Compressed Stabilised Earthbricks. *Journal of Sustainable Development*, *3*(3), 140.

Chantruthai, P., Areepong, T., Issaro, S., & Jaritngam, S. (2017). Investigating lateritic soil properties and impacts from quarrying activity on communities in Southern Thailand: A Case Study. *Engineering Journal*, *21*(1), 265-278.

Chinda, T., Leewattana, N., & Leeamnuayjaroen, N. (2012). The study of landfill situations in Thailand. Mae Fah Luang University International Conference, Mae Fah Luang University,

Chindaprasirt, P., Jitsangiam, P., & Horpibulsuk, S. (2020). Performance and evaluation of calcium carbide residue stabilized lateritic soil for construction materials. *Case Studies in Construction Materials*, *13*, e00389.

Chindaprasirt, P., Jitsangiam, P., Sakdinakorn, R., Daprom, P., & Kroehong, W. (2023). Effects of sulfate attack under wet and dry cycles on strength and durability of Cement-Stablized laterite. *Construction and Building Materials*, *365*, 129968.

Chiranjeevi, K., Yatish, R., Kumar, D. H., Mulangi, R. H., & Shankar, A. R. (2024). Utilization of recycled concrete aggregates for pavement base courses–A detailed laboratory study. *Construction and Building Materials*, *411*, 134122.

Consoli, N. C., Párraga Morales, D., & Saldanha, R. B. (2021). A new approach for stabilization of lateritic soil with Portland cement and sand: strength and durability. *Acta Geotechnica*, *16*, 1473-1486.

da Silva, S. R., de Brito, J., & de Oliveira Andrade, J. J. (2023). Synergic effect of recycled aggregate, fly ash, and hydrated lime in concrete production. *Journal of Building Engineering*, *70*, 106370.

Danso, H., & Manu, D. (2020). Influence of coconut fibres and lime on the properties of soil-cement mortar. *Case Studies in Construction Materials*, *12*, e00316.

Datta, S., & Mofiz, S. (2021). Stabilization of Road Subgrade Soil Using Recycled Aggregates. *International journal on emerging technologies*, *12*(1), 87-93.

Disfani, M. M., Arulrajah, A., Haghighi, H., Mohammadinia, A., & Horpibulsuk, S. (2014). Flexural beam fatigue strength evaluation of crushed brick as a supplementary material in cement stabilized recycled concrete aggregates. *Construction and Building Materials*, *68*, 667-676.

Ref. code: 25676522040077WTA

DOH-206/2532'. (1989). Department of Highways Analysis and Research Division Soil Cement Subbase Standards. In.

DOH 201/2544. (2001). Department of Highways, Analysis and Research Division, Base Materials. In.

DOH 205/2559. (2016). Department of Highways, Analysis and research Division, Soil Cement Subbase Standard. In.

Domphoeun, R., & Eisazadeh, A. (2024). Flexural and Shear Strength Properties of Laterite Soil Stabilized with Rice Husk Ash, Coir Fiber, and Lime. *Transportation Infrastructure Geotechnology*, 1-20.

Donrak, J., Rachan, R., Horpibulsuk, S., Arulrajah, A., & Du, Y. J. (2016). Improvement of marginal lateritic soil using melamine debris replacement for sustainable engineering fill materials. *Journal of Cleaner Production*, *134*, 515-522.

Dutta, R. K., Khatri, V. N., & Panwar, V. (2017). Strength characteristics of fly ash stabilized with lime and modified with phosphogypsum. *Journal of Building Engineering*, *14*, 32-40.

Ebailila, M., Kinuthia, J., Oti, J., & Al-Waked, Q. (2022). Sulfate soil stabilisation with binary blends of lime–silica fume and lime–ground granulated blast furnace slag. *Transportation Geotechnics*, *37*, 100888.

Eisazadeh, A., Bhurtel, A., & Phai, H. (2019). Compaction characteristics of Bangkok clay stabilized using rice husk ash, bottom ash, and lime. IOP Conference Series: Materials Science and Engineering,

Eisazadeh, A., Kassim, K. A., & Nur, H. (2011). Characterization of phosphoric acid- and lime-stabilized tropical lateritic clay. *Environmental Earth Sciences*, *63*, 1057-1066.

Eliaslankaran, Z., Daud, N. N. N., Yusoff, Z. M., & Rostami, V. (2021). Evaluation of the effects of cement and lime with rice husk ash as an additive on strength behavior of coastal soil. *Materials*, *14*(5), 1140.

Etxeberria, M., Marí, A. R., & Vázquez, E. (2007). Recycled aggregate concrete as structural material. *Materials and structures*, *40*, 529-541.

Fanijo, E. O., Kolawole, J. T., Babafemi, A. J., & Liu, J. (2023). A comprehensive review on the use of recycled concrete aggregate for pavement construction: Properties, performance, and sustainability. *Cleaner Materials*, 100199.

Fondjo, A. A., Theron, E., & Ray, R. P. (2021). Stabilization of expansive soils using mechanical and chemical methods: a comprehensive review. *Civ Eng Archit*, *9*(5), 1295-1308.

Gaboreau, S., Grangeon, S., Claret, F., Ihiawakrim, D., Ersen, O., Montouillout, V., Maubec, N., Roosz, C., Henocq, P., & Carteret, C. (2020). Hydration properties and interlayer organization in synthetic CSH. *Langmuir*, *36*(32), 9449-9464.

Gabr, A., & Cameron, D. (2012). Properties of recycled concrete aggregate for unbound pavement construction. *Journal of Materials in Civil Engineering*, *24*(6), 754-764.

Gangu, S. K., & Shankar, S. (2024). Recycled Concrete Aggregate Stabilized with Lime-Fly Ash and Cement for Utilization as a Semirigid Base Course of Low-Volume Roads. *Journal of Materials in Civil Engineering*, *36*(4), 04024014.

Garber, S., Rasmussen, R. O., & Harrington, D. (2011). Guide to cement-based integrated pavement solutions.

Ref. code: 25676522040077WTA

Ghorbani, A., & Hasanzadehshooiili, H. (2018). Prediction of UCS and CBR of microsilica-lime stabilized sulfate silty sand using ANN and EPR models; application to the deep soil mixing. *Soils and foundations*, *58*(1), 34-49.

Güllü, H., & Fedakar, H. İ. (2017). Response surface methodology for optimization of stabilizer dosage rates of marginal sand stabilized with Sludge Ash and fiber based on UCS performances. *KSCE Journal of Civil Engineering*, *21*, 1717-1727.

Haider, I., Cetin, B., Kaya, Z., Hatipoglu, M., Cetin, A., & Ahmet, H. A. (2014). Evaluation of the mechanical performance of recycled concrete aggregates used in highway base layers. Geo-Congress 2014: Geo-Characterization and Modeling for Sustainability,

Halsted, G. E., Adaska, W. S., & McConnell, W. T. (2008). Guide to cement-modified soil (CMS).

Hoang, N. H., Ishigaki, T., Kubota, R., Yamada, M., & Kawamoto, K. (2020). A review of construction and demolition waste management in Southeast Asia. *Journal of Material Cycles and Waste Management*, *22*, 315-325.

Hoornwerg, D., & Bhada-Tata, P. (2012). A global review of solid waste management. *Washington, District of Columbia: Urban Development & Local Government Unit World Bank.*

Horpibulsuk, S., Suddeepong, A., Chamket, P., & Chinkulkijniwat, A. (2013). Compaction behavior of fine-grained soils, lateritic soils and crushed rocks. *Soils and Foundations*, *53*(1), 166-172.

Horpibulsuk, S., Suksiripattanapong, C., Samingthong, W., Rachan, R., & Arulrajah, A. (2016). Durability against wetting–drying cycles of water treatment sludge–fly ash geopolymer and water treatment sludge–cement and silty clay–cement systems. *Journal of Materials in Civil Engineering*, *28*(1), 04015078.

Hoy, M., Nhieu, D. V., Horpibulsuk, S., Suddeepong, A., Chinkulkijniwat, A., Buritatum, A., & Arulrajah, A. (2023). Effect of wetting and drying cycles on mechanical strength of cement-natural rubber latex stabilized recycled concrete aggregate. *Construction and Building Materials*, *394*, 132301.

Huang, W.-L., Lin, D.-H., Chang, N.-B., & Lin, K.-S. (2002). Recycling of construction and demolition waste via a mechanical sorting process. *Resources, Conservation and Recycling*, *37*(1), 23-37.

Ingles, O. G., & Metcalf, J. B. (1972). *Soil stabilization principles and practice*.

Islam, S., Islam, J., Hoque, N. M. R., & Hasan, K. (2023). Improving geotechnical properties of soil of hillock slope using crushed recycled concrete aggregates. *Journal of engineering research*, *11*(4), 293-300.

Ismail, S., & Ramli, M. (2013). Engineering properties of treated recycled concrete aggregate (RCA) for structural applications. *Construction and Building Materials*, *44*, 464-476.

Jain, A., Borongan, G., Kashyap, P., Thawn, N., Honda, S., & Memon, M. (2017). Summary report: waste management in ASEAN countries. *United Nations Environment Programme, Thailand*.

Jha, A. K., & Sivapullaiah, P. (2015). Mechanism of improvement in the strength and volume change behavior of lime stabilized soil. *Engineering Geology*, *198*, 53-64.

Ref. code: 25676522040077WTA

Jotisankasa, A., Mahannopkul, K., & Sawangsuriya, A. (2020). Evaluating slope stability with respect to pore-water pressure and suction variation with rainfall: A case study of fill granitic slope in northern Thailand. In *Unsaturated Soils: Research & Applications* (pp. 1235-1240). CRC Press.

Kampala, A., & Horpibulsuk, S. (2013). Engineering properties of silty clay stabilized with calcium carbide residue. *Journal of Materials in Civil Engineering*, *25*(5), 632-644.

Karkush, M. O., & Yassin, S. (2019). Improvement of geotechnical properties of cohesive soil using crushed concrete. *Civil Engineering Journal*, *5*(10), 2110-2119.

Kashoborozi, O., Aturinda, E., Jjuuko, S., & Kalumba, D. (2017). Use of Crushed Concrete Aggregate Waste in Stabilization of Clayey Soils for Sub Base Pavement Construction.

Katz, A. (2003). Properties of concrete made with recycled aggregate from partially hydrated old concrete. *Cement and concrete research*, *33*(5), 703-711.

Kheoruenromne, I. (1987). Red and yellow soils and laterite formation in the Northeast Plateau, Thailand. *Chemical Geology*, *60*(1-4), 319-326.

Kianimehr, M., Shourijeh, P. T., Binesh, S. M., Mohammadinia, A., & Arulrajah, A. (2019). Utilization of recycled concrete aggregates for light-stabilization of clay soils. *Construction and Building Materials*, *227*, 116792.

Kofoworola, O. F., & Gheewala, S. H. (2009). Estimation of construction waste generation and management in Thailand. *Waste Management*, *29*(2), 731-738.

Koohmishi, M., & Palassi, M. (2022). Mechanical properties of clayey soil reinforced with PET considering the influence of lime-stabilization. *Transportation Geotechnics*, *33*, 100726.

Kou, S., & Poon, C. S. (2012). Enhancing the durability properties of concrete prepared with coarse recycled aggregate. *Construction and building materials*, *35*, 69-76.

Kumar, G. S., Saini, P., Deoliya, R., Mishra, A. K., & Negi, S. (2022a). Characterization of laterite soil and its use in construction applications: A review. *Resources, Conservation & Recycling Advances*, 200120.

Kumar, G. S., Saini, P., Deoliya, R., Mishra, A. K., & Negi, S. (2022b). Characterization of laterite soil and its use in construction applications: a review. *Resources, Conservation & Recycling Advances*, *16*, 200120.

Li, C. (2020). Mechanical and transport properties of recycled aggregate concrete modified with limestone powder. *Composites Part B: Engineering*, *197*, 108189.

Li, Q., & Hu, J. (2020). Mechanical and durability properties of cement-stabilized recycled concrete aggregate. *Sustainability*, *12*(18), 7380.

Liu, Y., Wang, Q., Liu, S., ShangGuan, Y., Fu, H., Ma, B., Chen, H., & Yuan, X. (2019). Experimental investigation of the geotechnical properties and microstructure of lime-stabilized saline soils under freeze-thaw cycling. *Cold Regions Science and Technology*, *161*, 32-42.

Ma, Q., Hu, Z., Hu, Z., & Li, J. (2022). Strength characteristics and micro-scale mechanism of high liquid limit clay treated by recycled construction and demolition wastes (CDW) aggregates. *Construction and Building Materials*, *332*, 127367.

Ref. code: 25676522040077WTA

Magnusson, S., Lundberg, K., Svedberg, B., & Knutsson, S. (2015). Sustainable management of excavated soil and rock in urban areas–a literature review. *Journal of Cleaner Production*, *93*, 18-25.

Maignien, R. (1966). *Compte rendu de recherches sur les latérites*. Unesco.

Makul, N., Fediuk, R., Amran, M., Zeyad, A. M., de Azevedo, A. R. G., Klyuev, S., Vatin, N., & Karelina, M. (2021). Capacity to develop recycled aggregate concrete in South East Asia. *Buildings*, *11*(6), 234.

Martínez-Lage, I., Vázquez-Burgo, P., & Velay-Lizancos, M. (2020). Sustainability evaluation of concretes with mixed recycled aggregate based on holistic approach: Technical, economic and environmental analysis. *Waste Management*, *104*, 9-19.

McKelvey, D., Sivakumar, V., Bell, A., & McLaverty, G. (2002). Shear strength of recycled construction materials intended for use in vibro ground improvement. *Proceedings of the Institution of Civil Engineers-Ground Improvement*, *6*(2), 59-68.

Meepon, I., Voottipruex, P., & Teerawattanasuk, C. (2019). Marginal lateritic soil treated using ceramic waste for rural road application. *GEOMATE Journal*, *16*(53), 70-77.

Menegaki, M., & Damigos, D. (2018). A review on current situation and challenges of construction and demolition waste management. *Current opinion in green and sustainable chemistry*, *13*, 8-15.

Mohammadinia, A., Arulrajah, A., D'Amico, A., & Horpibulsuk, S. (2020). Alkali activation of lime kiln dust and fly ash blends for the stabilisation of demolition wastes. *Road Materials and Pavement Design*, *21*(6), 1514-1528.

Mohammadinia, A., Arulrajah, A., Horpibulsuk, S., & Shourijeh, P. T. (2019). Impact of potassium cations on the light chemical stabilization of construction and demolition wastes. *Construction and Building Materials*, *203*, 69-74.

Mohammed, S. (2023). Investigation of concrete properties using recycled waste concrete aggregate.

Mohammed, S. I., & Najim, K. B. (2020). Mechanical strength, flexural behavior and fracture energy of Recycled Concrete Aggregate self-compacting concrete. Structures,

Moreno-Pérez, E., Hernández-Ávila, J., Rangel-Martínez, Y., Cerecedo-Sáenz, E., Arenas-Flores, A., Reyes-Valderrama, M. I., & Salinas-Rodríguez, E. (2018). Chemical and mineralogical characterization of recycled aggregates from construction and demolition waste from Mexico City. *Minerals*, *8*(6), 237.

Muntohar, A. S. (2019). Effect of moisture on the strength of stabilized clay with lime-rice husk ash and fibre against wetting-drying cycle. *International Journal of Integrated Engineering*, *11*(9), 100-109.

Muntohar, A. S., & Hantoro, G. (2000). Influence of rice husk ash and lime on engineering properties of a clayey subgrade. *Electronic Journal of Geotechnical Engineering*, *5*(2000), 1-13.

Muntohar, A. S., Widianti, A., Hartono, E., & Diana, W. (2013). Engineering properties of silty soil stabilized with lime and rice husk ash and reinforced with waste plastic fiber. *Journal of materials in civil engineering*, *25*(9), 1260-1270.

Ref. code: 25676522040077WTA

Negi, A. S., Faizan, M., Siddharth, D. P., & Singh, R. (2013). Soil stabilization using lime. *International Journal of Innovative Research in Science, Engineering and Technology*, *2*(2), 448-453.

Neramitkornburi, A., Horpibulsuk, S., Shen, S. L., Chinkulkijniwat, A., Arulrajah, A., & Disfani, M. M. (2015). Durability against wetting–drying cycles of sustainable Lightweight Cellular Cemented construction material comprising clay and fly ash wastes. *Construction and Building Materials*, *77*, 41-49.

Nghiem, H. T., Phan, Q. M., Kawamoto, K., Ngo, K. T., Nguyen, H. G., Nguyen, T. D., Isobe, Y., & Kawasaki, M. (2020). An investigation of the generation and management of construction and demolition waste in Vietnam. *Detritus*, *12*(Apr), 135-149.

Obuzor, G., Kinuthia, J., & Robinson, R. (2012). Soil stabilisation with lime-activated-GGBS—A mitigation to flooding effects on road structural layers/embankments constructed on floodplains. *Engineering geology*, *151*, 112-119.

Ok, B., Sarici, T., Talaslioglu, T., & Yildiz, A. (2020). Geotechnical properties of recycled construction and demolition materials for filling applications. *Transportation Geotechnics*, *24*, 100380.

Olufikayo, A., & Benjamin, A. (2019). Strength Characteristics of Lateritic Soil Stabilized with Recycled Concrete.

Oyelami, C. A., & Van Rooy, J. L. (2016). A review of the use of lateritic soils in the construction/development of sustainable housing in Africa: A geological perspective. *Journal of African Earth Sciences*, *119*, 226-237.

Panoottikorn, L. (2018). Thailand Country Report 2018. *Asian Disaster Reduction Centre Visiting Researcher Program*.

Pereira-De-Oliveira, L., Macedo, L., Neto, J., Santos, D., & Silva, H. (2019). Viability of lateritic soil as alkaline activated precursor. MATEC Web of Conferences,

Phai, H., & Eisazadeh, A. (2020). Geotechnical properties of rice husk ash-lime-stabilised Bangkok clay. *Journal of Engineering Science and Technology*, *15*(1), 198-215.

Phummiphan, I., Horpibulsuk, S., Phoo-ngernkham, T., Arulrajah, A., & Shen, S.-L. (2017). Marginal lateritic soil stabilized with calcium carbide residue and fly ash geopolymers as a sustainable pavement base material. *Journal of Materials in Civil Engineering*, *29*(2), 04016195.

Pongsivasathit, S., Horpibulsuk, S., & Piyaphipat, S. (2019). Assessment of mechanical properties of cement stabilized soils. *Case Studies in Construction Materials*, *11*, e00301.

Pongvithayapanu, P., Pornpreedawan, U., & Phusing, D. (2021). การ ปรับ เทียบ ตัวแปร กำลัง และ สติ ฟ เน ส ใน แบบ จำลอง ดิน ของ ดิน ทราย ผสม เศษ ยาง รถยนต์ ด้วย วิธี ไฟ ไน ต์ อิ ลิ เมน ต์. *Engineering and Technology Horizons*, *38*(4), 99-114.

Poon, C. S., & Chan, D. (2006). Feasible use of recycled concrete aggregates and crushed clay brick as unbound road sub-base. *Construction and Building Materials*, *20*(8), 578-585.

Pourakbar, S., & Huat, B. K. (2017). A review of alternatives traditional cementitious binders for engineering improvement of soils. *International Journal of Geotechnical Engineering*, *11*(2), 206-216.

Prusinski, J. R., & Bhattacharja, S. (1999). Effectiveness of Portland cement and lime in stabilizing clay soils. *Transportation research record*, *1652*(1), 215-227.

Ref. code: 25676522040077WTA

Pushpakumara, B., Gunasekara, M., & Gannile, Y. (2023). Variation of mechanical and chemical properties of old and new clay bricks. *Journal of Construction Engineering and Management*, *149*(4), 04023006.

Rahman, M. A., Imteaz, M. A., Arulrajah, A., Piratheepan, J., & Disfani, M. M. (2015). Recycled construction and demolition materials in permeable pavement systems: geotechnical and hydraulic characteristics. *Journal of Cleaner Production*, *90*, 183-194.

Rangel, C. S., Amario, M., Pepe, M., Martinelli, E., & Toledo Filho, R. D. (2020). Influence of wetting and drying cycles on physical and mechanical behavior of recycled aggregate concrete. *Materials*, *13*(24), 5675.

Ratananikom, W., Yimsiri, S., & Likitlersuang, S. (2015). Undrained shear strength of very soft to medium stiff Bangkok clay from various laboratory tests. *Geotechnical Engineering, Journal of the SEAGS & AGSSEA*, *46*(1).

Razali, R., Rashid, A. S. A., Lat, D. C., Horpibulsuk, S., Roshan, M. J., Rahman, N. S. A., & Rizal, N. H. A. (2023). Shear strength and durability against wetting and drying cycles of lime-stabilised laterite soil as subgrade. *Physics and Chemistry of the Earth, Parts A/B/C*, *132*, 103479.

Reis, G. S. d., Quattrone, M., Ambrós, W. M., Grigore Cazacliu, B., & Hoffmann Sampaio, C. (2021). Current applications of recycled aggregates from construction and demolition: A review. *Materials*, *14*(7), 1700.

Rosone, M., Moscato, F., Celauro, C., & Ziccarelli, M. (2023). Evaluation of the In-Situ Behaviour of a Lime-Treated Clay in a Real-Scale Experimental Embankment. National Conference of the Researchers of Geotechnical Engineering,

Saberian, M., Li, J., Perera, S. T. A. M., Ren, G., Roychand, R., & Tokhi, H. (2020). An experimental study on the shear behaviour of recycled concrete aggregate incorporating recycled tyre waste. *Construction and Building Materials*, *264*, 120266.

Saeed, K. A., Eisazadeh, A., & Kassim, K. A. (2012). Lime stabilized Malaysian lateritic clay contaminated by heavy metals. *Electron. J. Geotech. Eng*, *17*, 1807-1816.

Sanchez-Cotte, E. H., Fuentes, L., Martinez-Arguelles, G., Quintana, H. A. R., Walubita, L. F., & Cantero-Durango, J. M. (2020). Influence of recycled concrete aggregates from different sources in hot mix asphalt design. *Construction and Building Materials*, *259*, 120427.

Sani, Y. H., & Eisazadeh, A. (2023). Influence of coir fiber on the strength and permeability characteristics of bottom ash-and lime-stabilized laterite soil. *International Journal of Geosynthetics and Ground Engineering*, *9*(5), 63.

Sani, Y. H., & Eisazadeh, A. (2024). Performance evaluation of laterite soil embankment stabilized with bottom ash, coir fiber, and lime. *Journal of Mountain Science*, *21*(7), 2334-2351.

Saravanakumar, P., Abhiram, K., & Manoj, B. (2016). Properties of treated recycled aggregates and its influence on concrete strength characteristics. *Construction and Building Materials*, *111*, 611-617.

Sarhosis, V., De Santis, S., & de Felice, G. (2016). A review of experimental investigations and assessment methods for masonry arch bridges. *Structure and Infrastructure Engineering*, *12*(11), 1439-1464.

Ref. code: 25676522040077WTA

Sasanipour, H., & Aslani, F. (2020). Durability properties evaluation of self-compacting concrete prepared with waste fine and coarse recycled concrete aggregates. *Construction and Building Materials*, *236*, 117540.

Shamsi Susahab, J., Ardakani, A., & Hassanlourad, M. (2024). Strength improvement of clay subgrade soil stabilised with recycled concrete aggregate and granulated blast furnace slag. *Road Materials and Pavement Design*, 1-16.

Sharma, R. S., Phanikumar, B., & Rao, B. V. (2008). Engineering behavior of a remolded expansive clay blended with lime, calcium chloride, and rice-husk ash. *Journal of materials in civil engineering*, *20*(8), 509-515.

Shourijeh, P. T., Rad, A. M., Bigloo, F. H. B., & Binesh, S. M. (2022). Application of recycled concrete aggregates for stabilization of clay reinforced with recycled tire polymer fibers and glass fibers. *Construction and Building Materials*, *355*, 129172.

Skibsted, J., & Snellings, R. (2019). Reactivity of supplementary cementitious materials (SCMs) in cement blends. *Cement and Concrete Research*, *124*, 105799.

Soe, M., Won-In, K., Takashima, I., & Charusiri, P. (2008). Lateritic soil mapping of the Phrae basin, northern Thailand using satellite data. *Science Asia*, *34*, 307-316.

Sohail, M. G., Alnahhal, W., Taha, A., & Abdelaal, K. (2020). Sustainable alternative aggregates: Characterization and influence on mechanical behavior of basalt fiber reinforced concrete. *Construction and Building Materials*, *255*, 119365.

Sosahab, J. S., Ardakani, A., & Hassanlourad, M. (2023). Resilient response and strength of highly expansive clay subgrade stabilized with recycled concrete aggregate and granulated blast furnace slag. *Construction and Building Materials*, *408*, 133816.

Suksiripattanapong, C., Sakdinakorn, R., Tiyasangthong, S., Wonglakorn, N., Phetchuay, C., & Tabyang, W. (2022). Properties of soft Bangkok clay stabilized with cement and fly ash geopolymer for deep mixing application. *Case Studies in Construction Materials*, *16*, e01081.

Tam, V. W., Soomro, M., & Evangelista, A. C. J. (2018). A review of recycled aggregate in concrete applications (2000–2017). *Construction and Building materials*, *172*, 272-292.

Tam, V. W., & Tam, C. M. (2006). A review on the viable technology for construction waste recycling. *Resources, Conservation and Recycling*, *47*(3), 209-221.

Tan, Y., Hu, M., & Li, D. (2016). Effects of agglomerate size on California bearing ratio of lime treated lateritic soils. *International Journal of Sustainable Built Environment*, *5*(1), 168-175.

Tanthanawiwat, K., Gheewala, S. H., Nilsalab, P., Schoch, M., & Silalertruksa, T. (2024). Environmental sustainability and cost performances of construction and demolition waste management scenarios: A case study of timber and concrete houses in Thailand. *Journal of Cleaner Production*, *436*, 140652.

Tavakol, M., Hossain, M., & Tucker-Kulesza, S. E. (2019). Subgrade soil stabilization using low-quality recycled concrete aggregate. Eighth International Conference on Case Histories in Geotechnical Engineering,

Ref. code: 25676522040077WTA

Tavakol, M., Kulesza, S., Jones, C., & Hossain, M. (2020). Effect of low-quality recycled concrete aggregate on stabilized clay properties. *Journal of Materials in Civil Engineering*, *32*(8), 04020196.

Teerachaikulpanich, N., & Phupat, V. (2003). Geological and geotechnical engineering properties of Bangkok clay. *proceedings of the Japan National Conference on Geotechnical Engineering*(0), 143-144. https://doi.org/10.11512/jiban.JGS38.0.143.0

Teerawattanasuk, C., Voottipruex, P., & Horpibulsuk, S. (2015). Mix design charts for lightweight cellular cemented Bangkok clay. *Applied Clay Science*, *104*, 318-323.

Thai, H. N., Nguyen, T. D., Nguyen, V. T., Nguyen, H. G., & Kawamoto, K. (2022). Characterization of compaction and CBR properties of recycled concrete aggregates for unbound road base and subbase materials in Vietnam. *Journal of Material Cycles and Waste Management*, 1-15.

Thompson, M. R. (1967). Factors influencing the plasticity and strength of lime-soil mixtures. *University of Illinois. Engineering Experiment Station. Bulletin; no. 492*.

Thongkamsuk, P., Sudasna, K., & Tondee, T. (2017). Waste generated in high-rise buildings construction: A current situation in Thailand. *Energy Procedia*, *138*, 411-416.

Tiwari, N., Satyam, N., & Puppala, A. J. (2021). Strength and durability assessment of expansive soil stabilized with recycled ash and natural fibers. *Transportation Geotechnics*, *29*, 100556.

Todingrara, Y. T., Tjaronge, M., Harianto, T., & Ramli, M. (2017). Performance of laterite soil stabilized with lime and cement as a road foundation. *International Journal of Applied Engineering Research*, *12*(14), 4699-4707.

Tran, N. Q., Hoy, M., Suddeepong, A., Horpibulsuk, S., Kantathum, K., & Arulrajah, A. (2022). Improved mechanical and microstructure of cement-stabilized lateritic soil using recycled materials replacement and natural rubber latex for pavement applications. *Construction and Building Materials*, *347*, 128547.

Udoeyo, F. F., Iron, U. H., & Odim, O. O. (2006). Strength performance of laterized concrete. *Construction and Building Materials*, *20*(10), 1057-1062.

Vallerga, B., & Van Til, C. (1970). Classification and engineering properties of lateritic materials. *Highway Research Record*, *310*, 52-67.

Vejchasarn, P., Shearman, J. R., Chaiprom, U., Phansenee, Y., Suthanthangjai, A., Jairin, J., Chamarerk, V., Tulyananda, T., & Amornbunchornvej, C. (2021). Population structure of nation-wide rice in Thailand. *Rice*, *14*(1), 1-10.

Verian, K. P., Ashraf, W., & Cao, Y. (2018). Properties of recycled concrete aggregate and their influence in new concrete production. *Resources, Conservation and Recycling*, *133*, 30-49.

Vichan, S., & Rachan, R. (2013). Chemical stabilization of soft Bangkok clay using the blend of calcium carbide residue and biomass ash. *Soils and Foundations*, *53*(2), 272-281.

Victoria, S. (2010). Victorian recycling industries annual report 2008–2009. *ISSN 1836*, *9902*.

Villagrán-Zaccardi, Y. A., Marsh, A. T., Sosa, M. E., Zega, C. J., De Belie, N., & Bernal, S. A. (2022). Complete re-utilization of waste concretes–Valorisation

Ref. code: 25676522040077WTA

pathways and research needs. *Resources, Conservation and Recycling*, *177*, 105955.

Wahab, N. A., Roshan, M. J., Rashid, A. S. A., Hezmi, M. A., Jusoh, S. N., Nik Norsyahariati, N. D., & Tamassoki, S. (2021). Strength and durability of cement-treated lateritic soil. *Sustainability*, *13*(11), 6430.

Wu, Z., Ann, T., Shen, L., & Liu, G. (2014). Quantifying construction and demolition waste: An analytical review. *Waste management*, *34*(9), 1683-1692.

Xu, D.-M., Fu, R.-B., Wang, J.-X., Shi, Y.-X., & Guo, X.-P. (2021). Chemical stabilization remediation for heavy metals in contaminated soils on the latest decade: Available stabilizing materials and associated evaluation methods-A critical review. *Journal of Cleaner Production*, *321*, 128730.

Xue, L., Li, H.-B., Brodsky, E. E., Xu, Z.-Q., Kano, Y., Wang, H., Mori, J. J., Si, J.-L., Pei, J.-L., & Zhang, W. (2013). Continuous permeability measurements record healing inside the Wenchuan earthquake fault zone. *Science*, *340*(6140), 1555-1559.

Yaghoubi, E., Yaghoubi, M., Guerrieri, M., & Sudarsanan, N. (2021). Improving expansive clay subgrades using recycled glass: Resilient modulus characteristics and pavement performance. *Construction and Building Materials*, *302*, 124384.

Yang, S., & Lim, Y. (2018). Mechanical strength and drying shrinkage properties of RCA concretes produced from old railway concrete sleepers using by a modified EMV method. *Construction and Building Materials*, *185*, 499-507.

Ye Htun, T. H., Julnipitawong, P., Chimoye, W., & Tangtermsirikul, S. (2022). Investigation of bottom ash as a partial replacement to conventional subbase soils. *Proceedings of the Institution of Civil Engineers-Ground Improvement*, *176*(4), 249-260.

Yukalang, N., Clarke, B., & Ross, K. (2017). Barriers to effective municipal solid waste management in a rapidly urbanizing area in Thailand. *International journal of environmental research and public health*, *14*(9), 1013.

Zada, U., Jamal, A., Iqbal, M., Eldin, S. M., Almoshaogeh, M., Bekkouche, S. R., & Almuaythir, S. (2023). Recent advances in expansive soil stabilization using admixtures: current challenges and opportunities. *Case Studies in Construction Materials*, e01985.

Zhang, H.-L., Tang, Y., Meng, T., & Zhan, L.-T. (2021). Evaluating the crushing characteristics of recycled construction and demolition waste for use in road bases. *Transportation Geotechnics*, *28*, 100543.

Zhao, D., & Khoshnazar, R. (2021). Hydration and microstructural development of calcined clay cement paste in the presence of calcium-silicate-hydrate (C–S–H) seed. *Cement and Concrete Composites*, *122*, 104162.

Ref. code: 25676522040077WTA

APPENDIX

Ref. code: 25676522040077WTA

APPENDIX A
DATA COLLECTED

1. Particle Size Distribution

Table A.1 Particle size distribution of Laterite soil.

Sieve No.	Sieve size (mm)	Mass of soil retained (g)	Percent of mass retained (%)	Cumulative percent remained (%)
4	4.740	0	0.00	100.00
10	2.000	0.18	0.30	99.70
20	0.850	4.78	7.97	91.73
40	0.425	4.88	8.13	83.60
60	0.250	3.8	6.33	77.27
100	0.150	4.05	6.75	70.52
200	0.075	7.55	12.58	57.93
pan	< 0,075	34.76	57.93	0.00
Mass < 0,075		34.76		
The amount of weight retained		60		

Table A.2 Particle size distribution of recycled concrete aggregate.

Sieve No.	Sieve size (mm)	Mass of soil retained (g)	Percent of mass retained (%)	Cumulative percent remained (%)
4	4.740	0	0.00	100.00
10	2.000	15.86	26.43	73.57
20	0.850	8.7	14.50	59.07
40	0.425	5.83	9.72	49.35
60	0.250	4.91	8.18	41.17
100	0.150	4.23	7.05	34.12
200	0.075	1.67	2.78	31.33
pan	< 0,075	18.8	31.33	0.00
Mass < 0,075		18.8		
The amount of weight retained		60		

Ref. code: 25676522040077WTA

Table A.3 Values of correction factor, a, for different specific gravities of soil particles.

Specific Gravity	Correction Factor[A]
2.95	0.94
2.90	0.95
2.85	0.96
2.80	0.97
2.75	0.98
2.70	0.99
2.65	1.00
2.60	1.01
2.55	1.02
2.50	1.03
2.45	1.05

[A]For use in equation for percentage of soil remaining in suspension when using Hydrometer 152H.

Table A.4 Values of Effective Depth Based on Hydrometer and values of K.

Hydrometer 151H		Hydrometer 152H			
Actual Hydrometer Reading	Effective Depth, *L*, cm	Actual Hydrometer Reading	Effective Depth, *L*, cm	Actual Hydrometer Reading	Effective Depth, *L*, cm
1.000	16.3	0	16.3	31	11.2
1.001	16.0	1	16.1	32	11.1
1.002	15.8	2	16.0	33	10.9
1.003	15.5	3	15.8	34	10.7
1.004	15.2	4	15.6	35	10.6
1.005	15.0	5	15.5		
1.006	14.7	6	15.3	36	10.4
1.007	14.4	7	15.2	37	10.2
1.008	14.2	8	15.0	38	10.1
1.009	13.9	9	14.8	39	9.9
1.010	13.7	10	14.7	40	9.7
1.011	13.4	11	14.5	41	9.6
1.012	13.1	12	14.3	42	9.4
1.013	12.9	13	14.2	43	9.2
1.014	12.6	14	14.0	44	9.1
1.015	12.3	15	13.8	45	8.9
1.016	12.1	16	13.7	46	8.8
1.017	11.8	17	13.5	47	8.6
1.018	11.5	18	13.3	48	8.4
1.019	11.3	19	13.2	49	8.3
1.020	11.0	20	13.0	50	8.1
1.021	10.7	21	12.9	51	7.9
1.022	10.5	22	12.7	52	7.8
1.023	10.2	23	12.5	53	7.6
1.024	10.0	24	12.4	54	7.4
1.025	9.7	25	12.2	55	7.3
1.026	9.4	26	12.0	56	7.1
1.027	9.2	27	11.9	57	7.0
1.028	8.9	28	11.7	58	6.8
1.029	8.6	29	11.5	59	6.6
1.030	8.4	30	11.4	60	6.5
1.031	8.1				
1.032	7.8				
1.033	7.6				
1.034	7.3				
1.035	7.0				
1.036	6.8				
1.037	6.5				
1.038	6.2				

Ref. code: 25676522040077WTA

Table A.5 Values of Temperature and Specific Gravity of soil particles.

Temperature,° C	Specific Gravity of Soil Particles								
	2.45	2.50	2.55	2.60	2.65	2.70	2.75	2.80	2.85
16	0.01510	0.01505	0.01481	0.01457	0.01435	0.01414	0.01394	0.01374	0.01356
17	0.01511	0.01486	0.01462	0.01439	0.01417	0.01396	0.01376	0.01356	0.01338
18	0.01492	0.01467	0.01443	0.01421	0.01399	0.01378	0.01359	0.01339	0.01321
19	0.01474	0.01449	0.01425	0.01403	0.01382	0.01361	0.01342	0.1323	0.01305
20	0.01456	0.01431	0.01408	0.01386	0.01365	0.01344	0.01325	0.01307	0.01289
21	0.01438	0.01414	0.01391	0.01369	0.01348	0.01328	0.01309	0.01291	0.01273
22	0.01421	0.01397	0.01374	0.01353	0.01332	0.01312	0.01294	0.01276	0.01258
23	0.01404	0.01381	0.01358	0.01337	0.01317	0.01297	0.01279	0.01261	0.01243
24	0.01388	0.01365	0.01342	0.01321	0.01301	0.01282	0.01264	0.01246	0.01229
25	0.01372	0.01349	0.01327	0.01306	0.01286	0.01267	0.01249	0.01232	0.01215
26	0.01357	0.01334	0.01312	0.01291	0.01272	0.01253	0.01235	0.01218	0.01201
27	0.01342	0.01319	0.01297	0.01277	0.01258	0.01239	0.01221	0.01204	0.01188
28	0.01327	0.01304	0.01283	0.01264	0.01244	0.01255	0.01208	0.01191	0.01175
29	0.01312	0.01290	0.01269	0.01249	0.01230	0.01212	0.01195	0.01178	0.01162
30	0.01298	0.01276	0.01256	0.01236	0.01217	0.01199	0.01182	0.01165	0.01149

Table A.6 Particle size distribution of Laterite soil according to hydrometer analysis.

t	Hydrometer scale		Temp (°C)	R'= R1+m	L1	L cm	Constant (K)	(D mm)	Interpolation Ct	R	A	Weight percent	PA (%)
	R1	R2											
2	43	20	30	44	3.22	9.05	0.012098	0.0257349	3.8	27.8	0.9951	0.4611	26.71
5	38	20	31	39	4.35	10.18	0.011884	0.0169571	4.6	23.57	0.9951	0.3909	22.64
30	31	20	32	32	5.93	11.76	0.011691	0.0073203	5.2	17.22	0.9951	0.2856	16.54
60	27	18	32	28	6.83	12.67	0.011691	0.0053715	5.2	15.22	0.9951	0.2524	14.62
250	25	18	32	26	7.28	13.12	0.011691	0.0026780	5.2	13.22	0.9951	0.2192	12.70
1440	21	18	33	22	8.19	14.02	0.011498	0.0011346	6.5	10.52	0.9951	0.1744	10.11

Ref. code: 25676522040077WTA

2. Specific Gravity

Table A.7 Specific Gravity of Laterite Soil.

Test No	A1	A2	A3
Mass of flask (g)	161.06	165.67	169.78
Method of air removal	Heat	Heat	Heat
WBWS = W flask + water + soil (g)	718.05	722.61	728.86
Temperature (T1)	31.5	31.25	31.25
Temperature (T2)	30.5	31.5	31
WBW = W flask + Water (g)	657.55	662.66	666.93
Ws = W dry soil (g)	95.63	95.96	99.26
Vp = (Wpw,c-Wp)/Pwc	498.85	499.35	499.51
Ww = Ws + WBW - WBWS (g)	35.13	36.01	37.33
Gs = Ws/Ww	2.72	2.66	2.66
Specific gravity, Gs	2.71	2.66	2.65
Average Gs	2.67		

Table A.8 Specific Gravity of Recycled Concrete Aggregate.

W of P + water, g (B)	W of SSD, g (S)	W of P + S + water, g (C)	W of oven-dry, g (A)	Bulk sp,gr	Bulk sp, gr (SSD)	Apparent sp, gr	Absorption (%)
657.65	502.7	949.24	468.53	2.219	2.381	2.648	7.293
658.16	504.07	958.49	470.27	2.308	2.474	2.767	7.187
Average				2.264	2.428	2.708	7.240

Note: *W is weight, P is pycnometer, S is sample, and SSD is Saturated surface dry.*

3. Atterberg Limit

Table A.9 Plastic limit of laterite soil.

Container No	A11	A12	A13
Wt. Cup, g (W1)	17.33	17.07	17.05
Wt. Cup + Wet soil, g (W2)	39.83	39.80	39.81
Wt. Cup + Dry soil, g (W3)	36.81	36.73	36.86
Wt. Water, g (Ww)	3.02	3.07	2.95
Wt. Dry soil (Ws)	19.48	19.66	19.81
Water Content, w	15.50	15.62	14.89
Average	15.34		

Ref. code: 25676522040077WTA

Table A.10 Liquid Limit of Laterite Soil.

No of trial	1		2		3		4		5	
Container No	A1	A2	A3	A4	A5	A6	A7	A8	A9	A10
No of blow count	35	33	30	26	24	22	20	18	13	11
Wt. Cup,g (W1)	16.55	16.40	16.17	17.16	17.14	17.16	15.73	16.37	16.36	14.96
Wt. Cup + Wet soil,g (W2)	41.86	41.76	41.76	43.37	43.12	43.83	40.98	42.51	43.44	39.02
Wt. Cup + Dry soil, g (W3)	36.31	36.17	35.74	37.32	36.80	37.48	34.54	35.78	36.66	32.16
Wt. Water, g (Ww)	5.55	5.59	6.02	6.05	6.32	6.35	6.44	6.73	6.78	6.86
Wt. Dry soil (Ws)	19.76	19.77	19.57	20.16	19.66	20.32	18.81	19.41	20.30	17.20
Water Content, w	28.09	28.28	30.76	30.01	32.15	31.25	34.24	34.67	33.40	39.88
Average	28.18		30.39		31.70		34.45		36.64	

4. Compaction Results

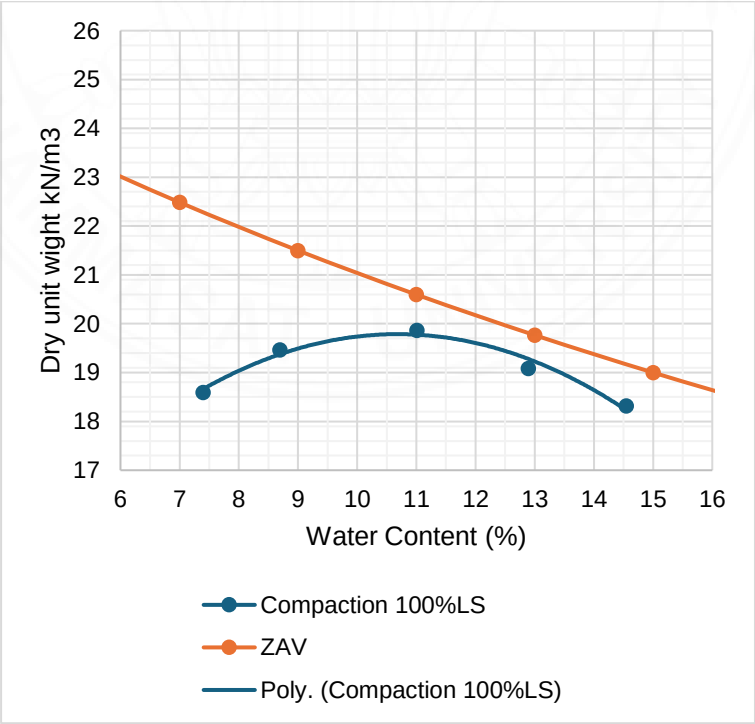

Figure A.1 Compaction of 100% laterite soil.

Ref. code: 256765220400 77WTA

Table A.11 Compaction results for all mix designs.

Mix Design	MDUW (kN/m^3)	OMC (%)
100%LS	19.86	10.500
95%LS 5%RCA	19.44	11.300
85%LS 15% RCA	19.07	11.550
70%LS 30%RCA	18.19	12.780
55%LS 45%RCA	17.75	13.850
100%LS + 6%Lime	18.72	11.600
95%LS 5%RCA + 6%Lime	18.44	12.100
85%LS 15% RCA + 6%Lime	17.67	12.600
70%LS 30%RCA + 6%Lime	17.22	13.000
55%LS 45%RCA + 6%Lime	16.46	13.670
100%RCA	18.8	11.8

5. Unconfined Compressive Strength

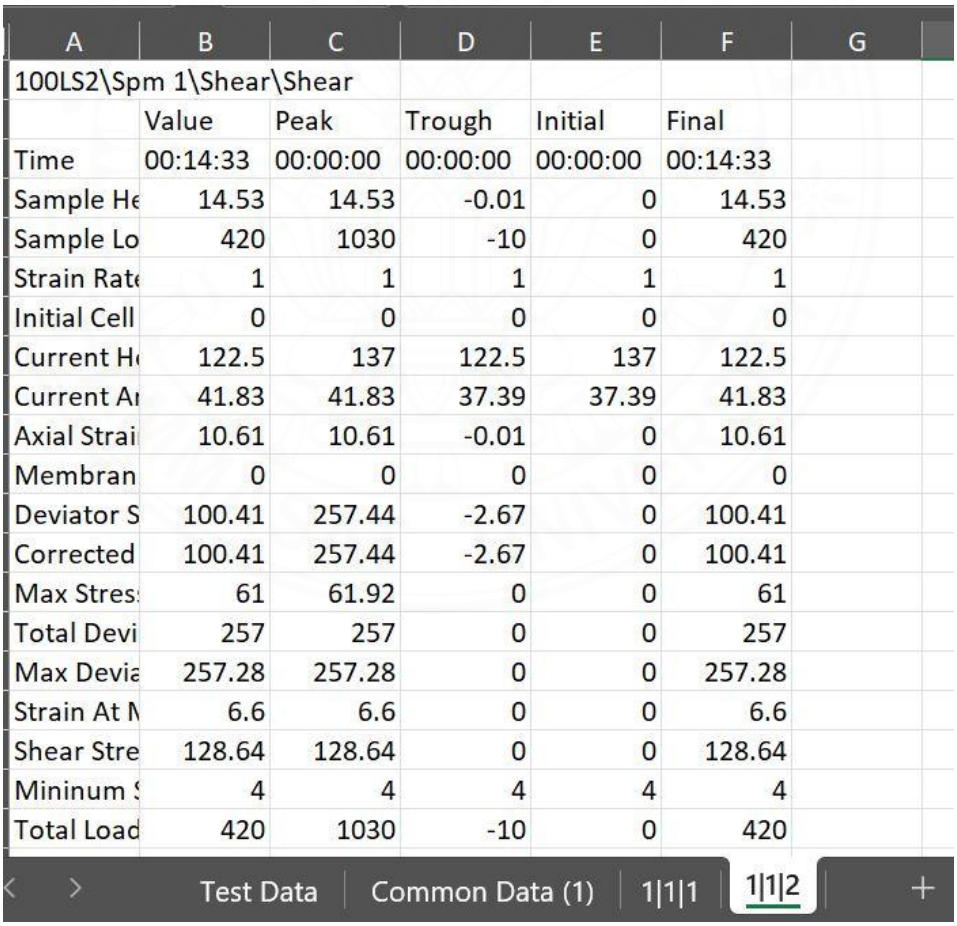

A	B	C	D	E	F	G
100LS2\Spm 1\Shear\Shear						
	Value	Peak	Trough	Initial	Final	
Time	00:14:33	00:00:00	00:00:00	00:00:00	00:14:33	
Sample He	14.53	14.53	-0.01	0	14.53	
Sample Lo	420	1030	-10	0	420	
Strain Rate	1	1	1	1	1	
Initial Cell	0	0	0	0	0	
Current He	122.5	137	122.5	137	122.5	
Current Ar	41.83	41.83	37.39	37.39	41.83	
Axial Strai	10.61	10.61	-0.01	0	10.61	
Membran	0	0	0	0	0	
Deviator S	100.41	257.44	-2.67	0	100.41	
Corrected	100.41	257.44	-2.67	0	100.41	
Max Stres	61	61.92	0	0	61	
Total Devi	257	257	0	0	257	
Max Devia	257.28	257.28	0	0	257.28	
Strain At M	6.6	6.6	0	0	6.6	
Shear Stre	128.64	128.64	0	0	128.64	
Mininum S	4	4	4	4	4	
Total Load	420	1030	-10	0	420	

Test Data | Common Data (1) | 1|1|1 | 1|1|2

Figure A.2 UCS results form in Excel.

Ref. code: 25676522040077WTA

6. California Bearing Ratio

Table A.12 CBR value calculation of Laterite soil.

100 LS (7 Days) UNSOAKED					
Penetration	Standard Stress (MPa)	Stress		CBR (%)	
		Top	Bottom	Top	Bottom
2.54 mm	6.9	0.42	0.43	6.1	6.2
5.08 mm	10.3	0.80	0.69	7.7	6.7

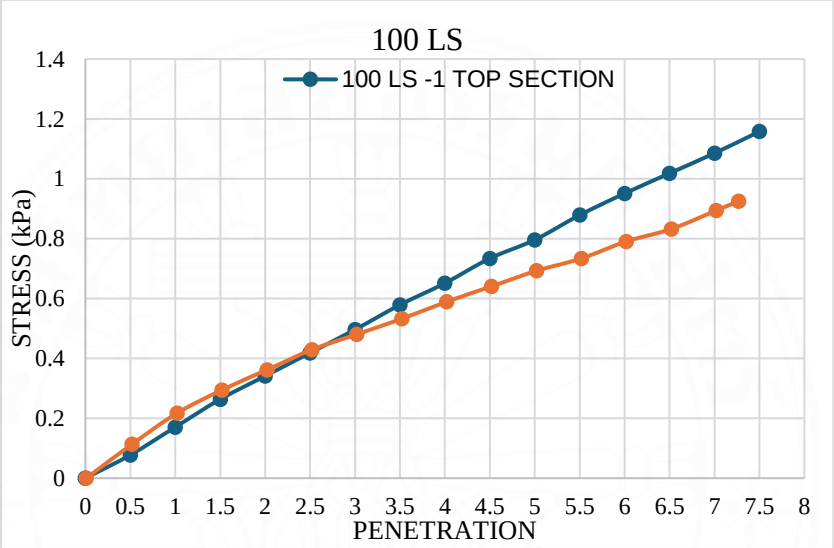

Figure A.3 CBR curve of laterite soil.

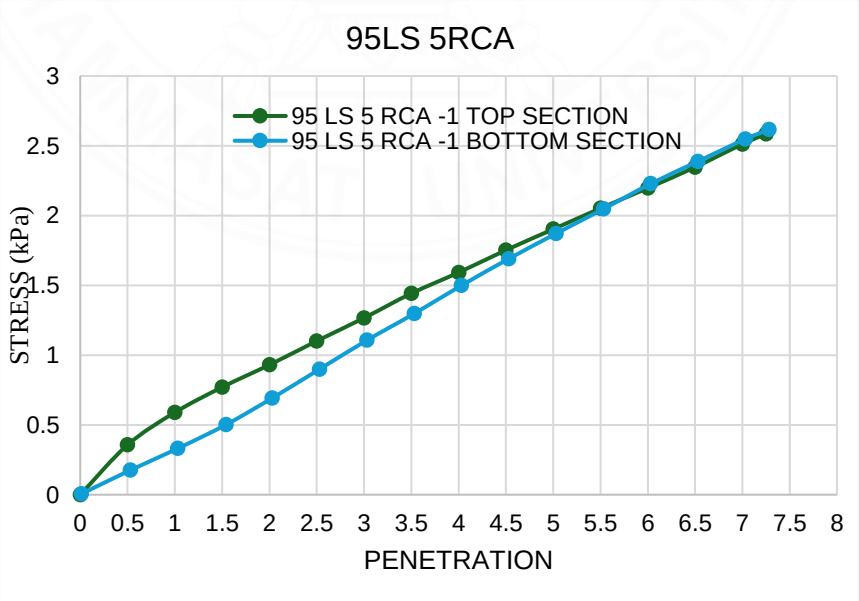

Figure A.4 CBR curve of 95LS5RCA.

Ref. code: 25676522040077WTA

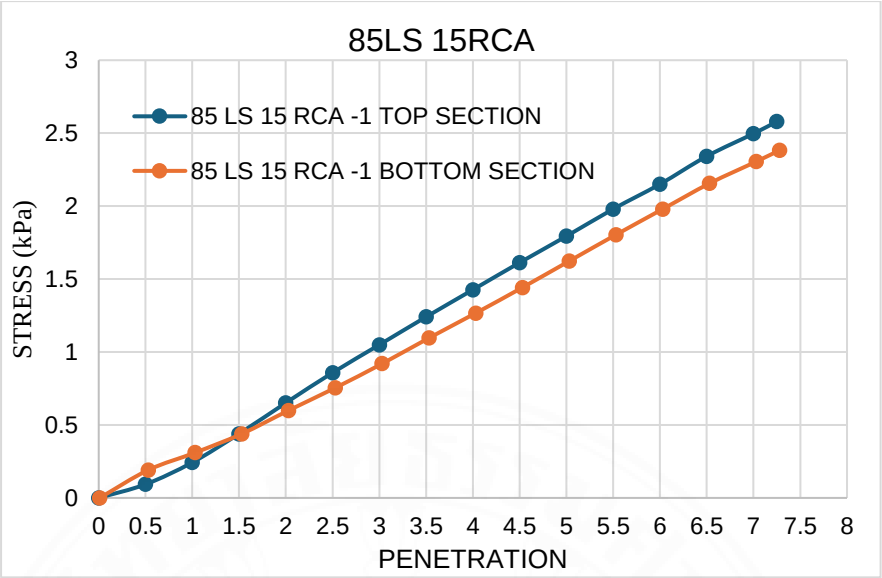

Figure A.5 CBR curve of 85LS15RCA.

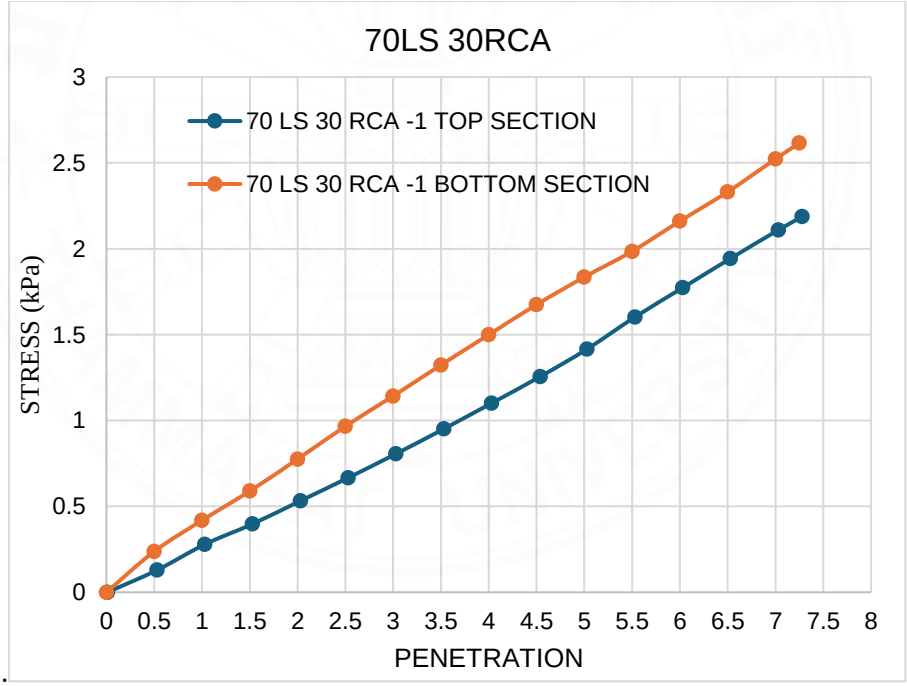

Figure A.6 CBR curve of 70LS30RCA.

Ref. code: 25676522040077WTA

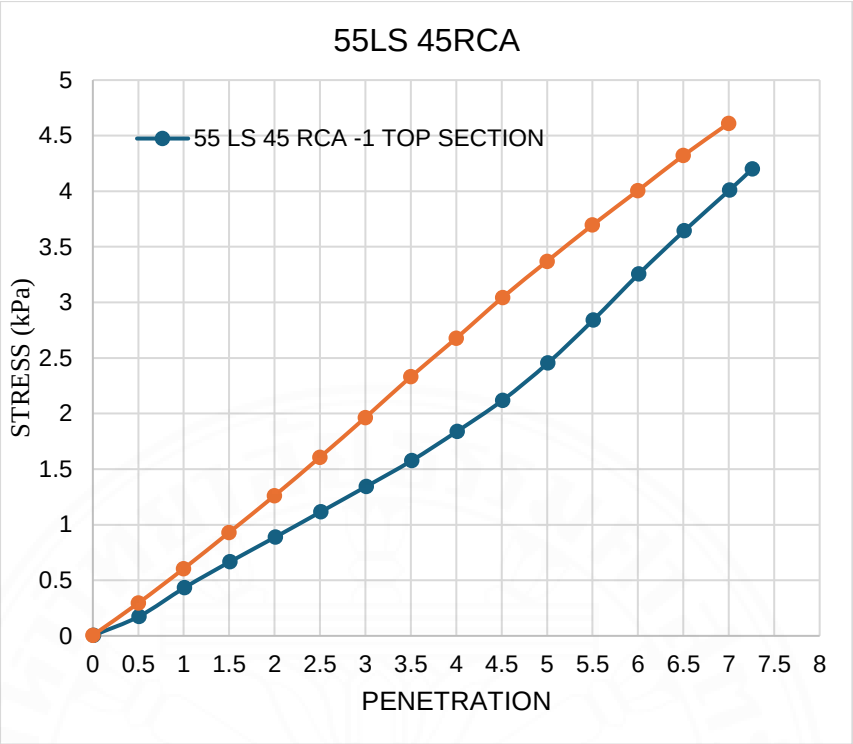

Figure A.7 CBR curve of 55LS45RCA.

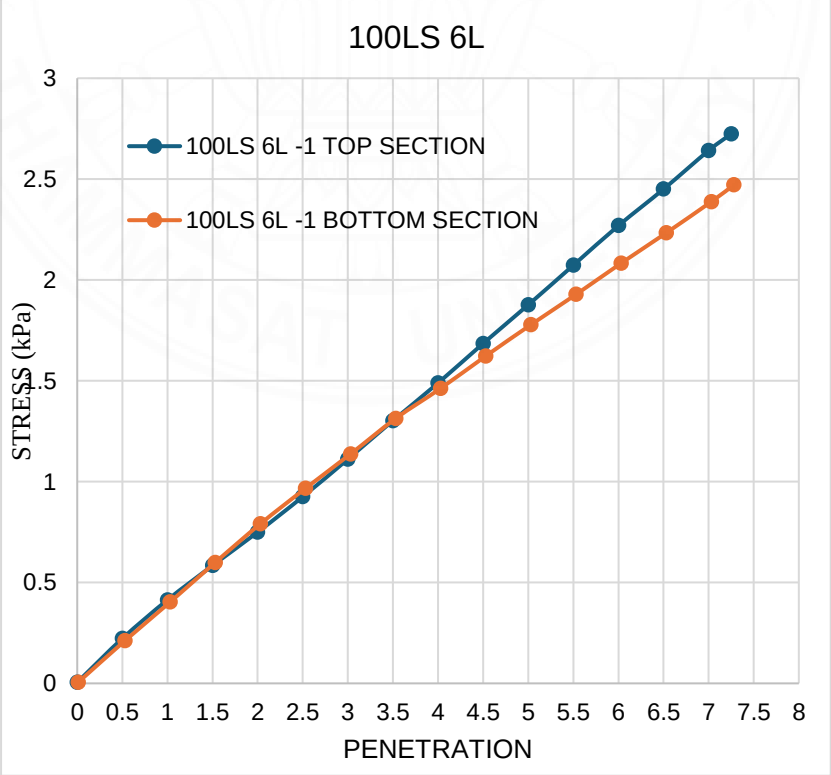

Figure A.8 CBR curve of 100LS6L.

Ref. code: 25676522040077WTA

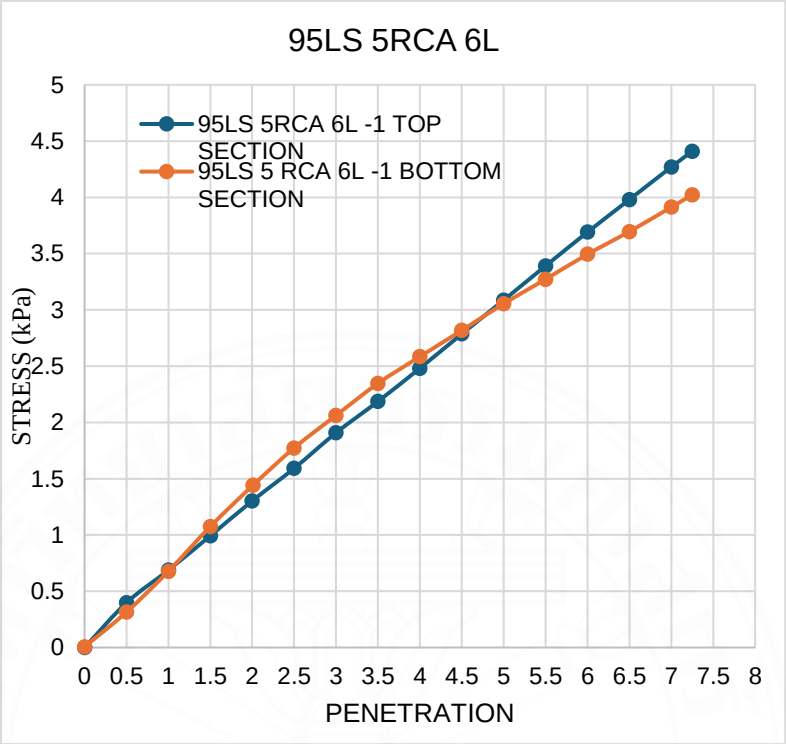

Figure A.9 CBR curve of 95LS5RCA6L.

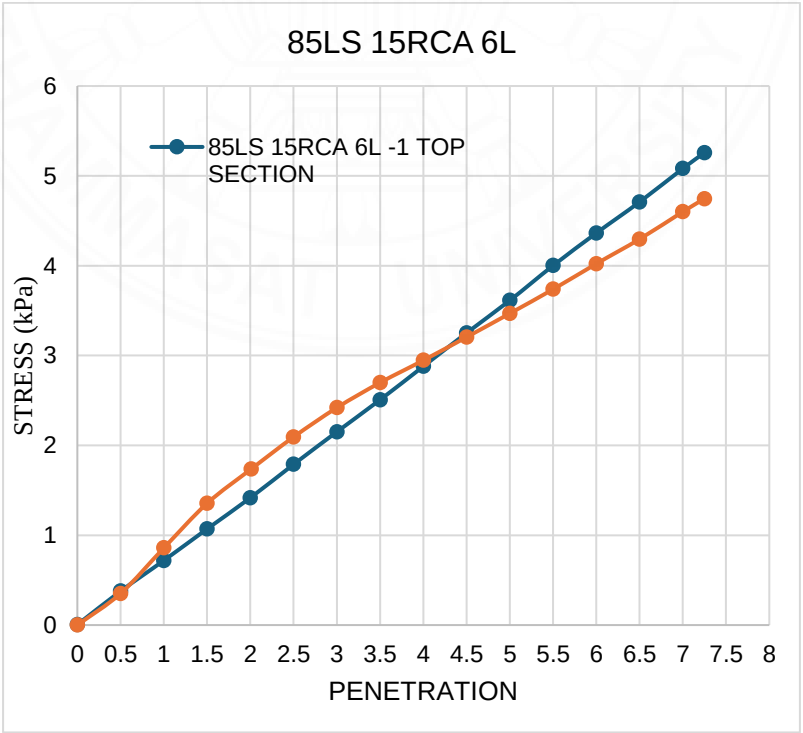

Figure A.10 CBR curve of 85LS15RCA6L.

Ref. code: 25676522040077WTA

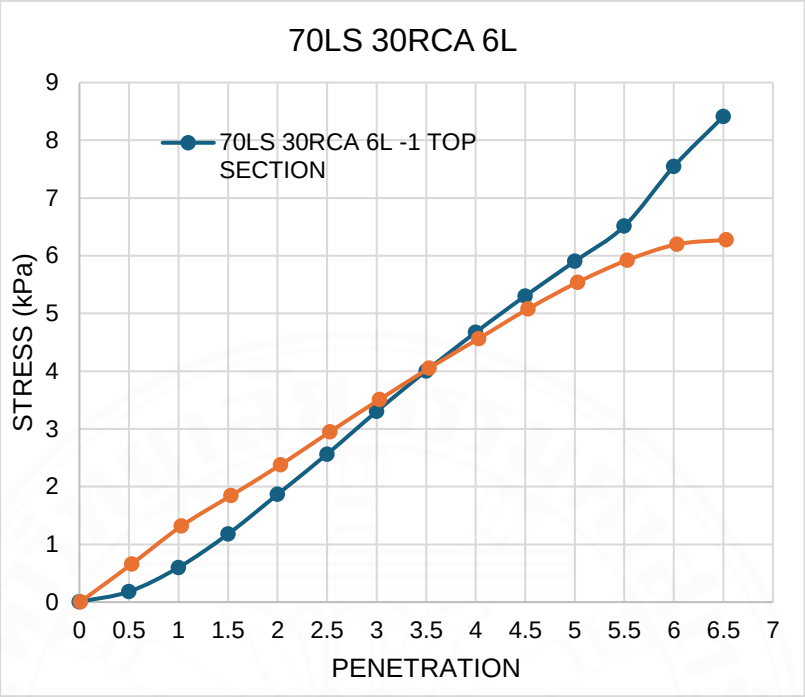

Figure A.11 CBR curve of 70LS30RCA6L.

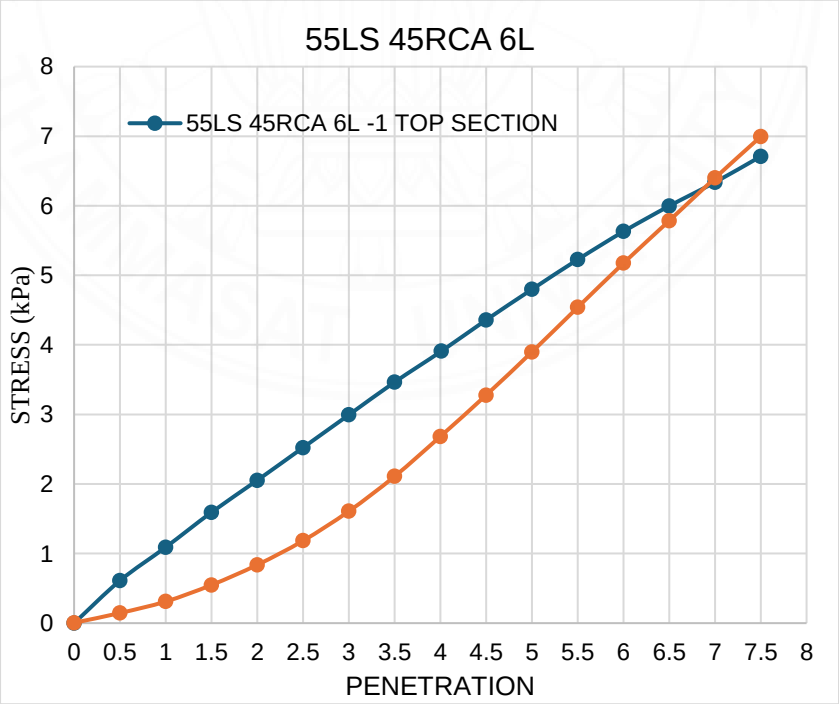

Figure A.12 CBR curve of 55LS45RCA6L.

Ref. code: 25676522040077WTA

7. Direct Shear

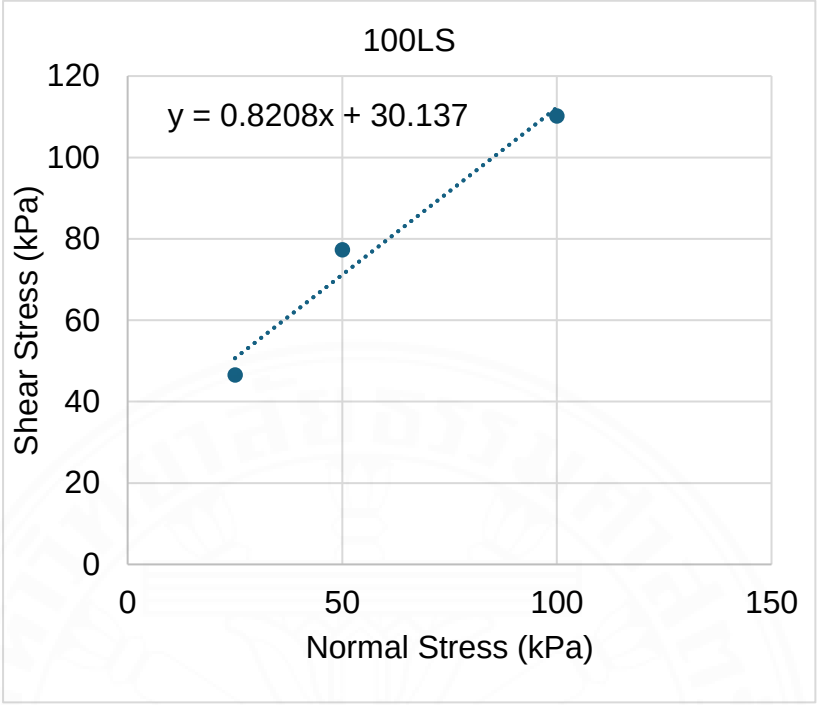

Figure A.13 Relation shear and normal stress of 100LS at 56 days curing period.

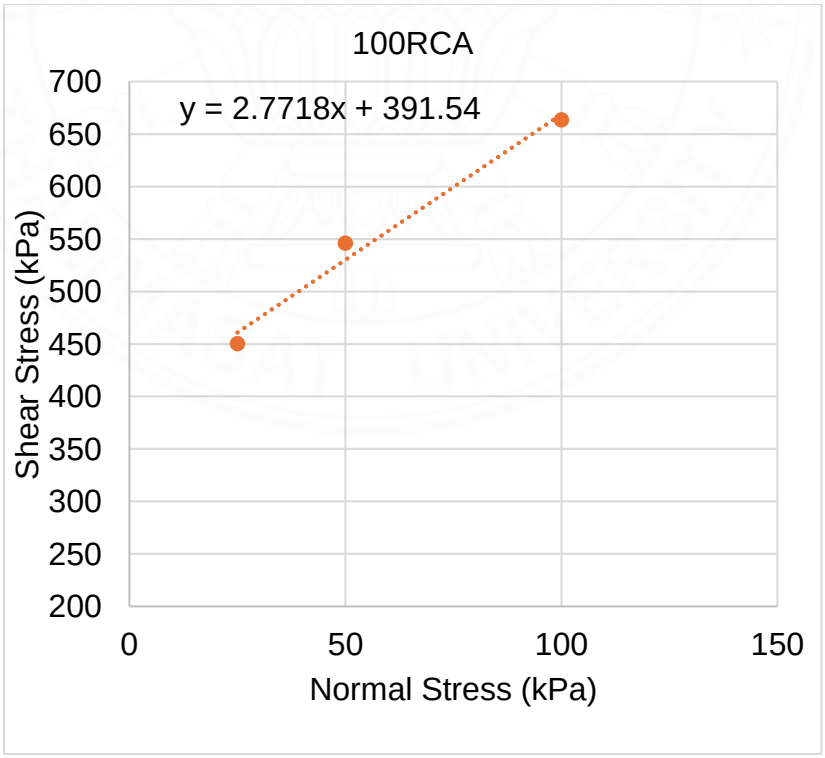

Figure A.14 Relation shear and normal stress of 100RCA at 56 days curing period.

Ref. code: 25676522040077WTA

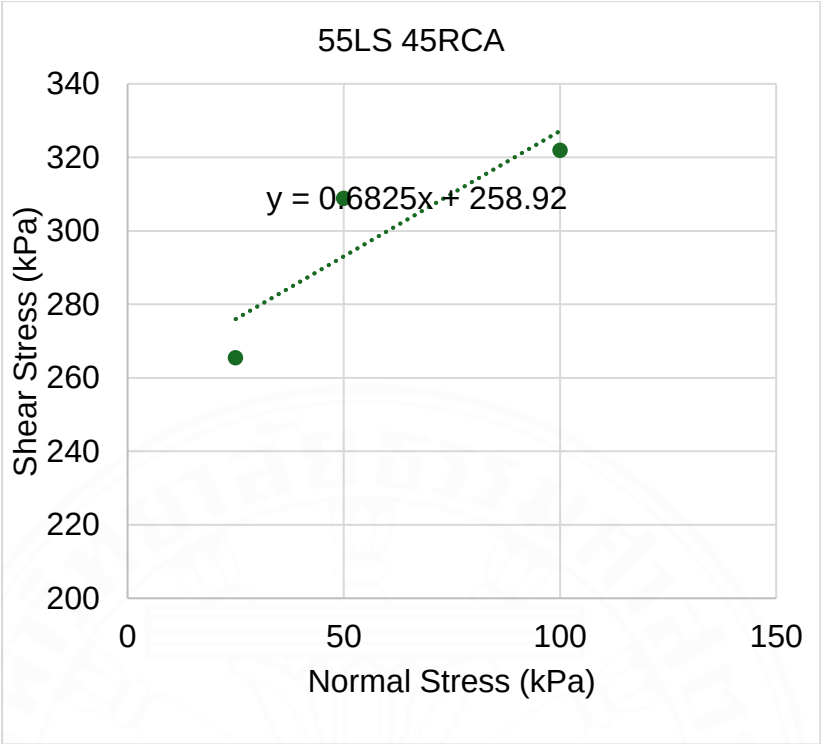

Figure A.15 Relation shear and normal stress of 55LS45RCA at 56 days curing period.

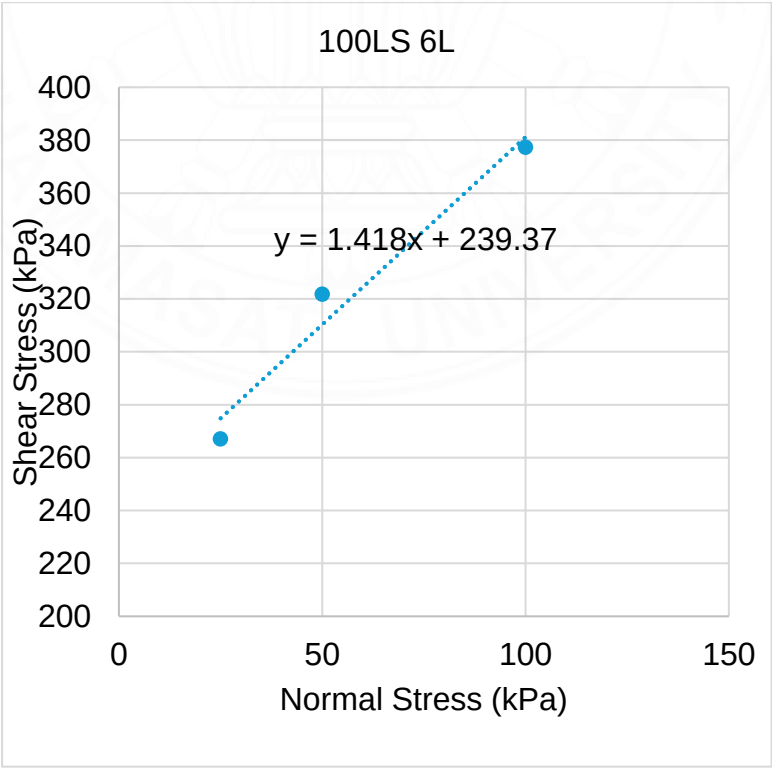

Figure A.16 Relation shear and normal stress of 100LS6L at 56 days curing period.

Ref. code: 25676522040077WTA

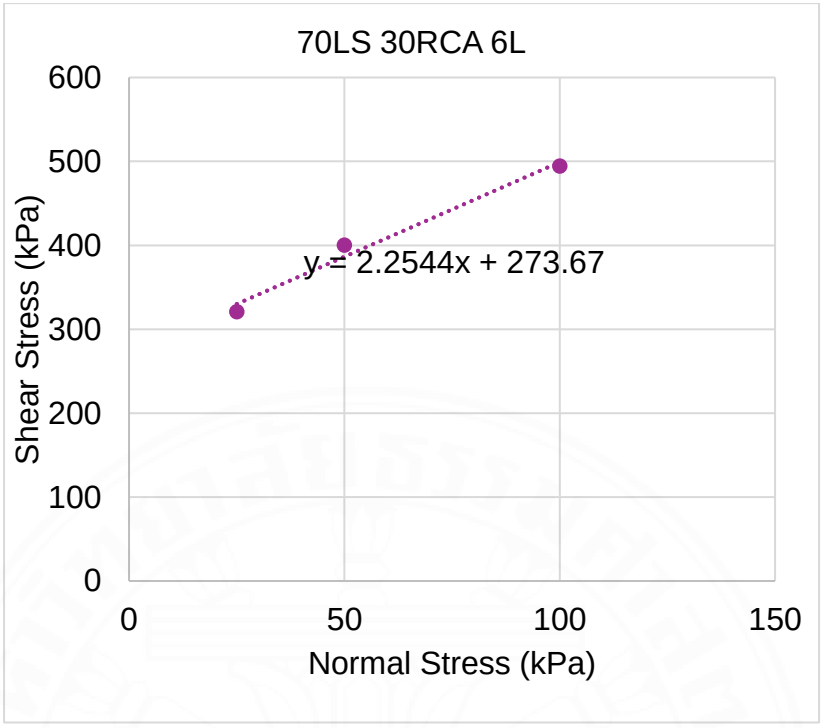

Figure A.17 Relation shear and normal stress of 70LS30RCA6L at 56 days curing period.

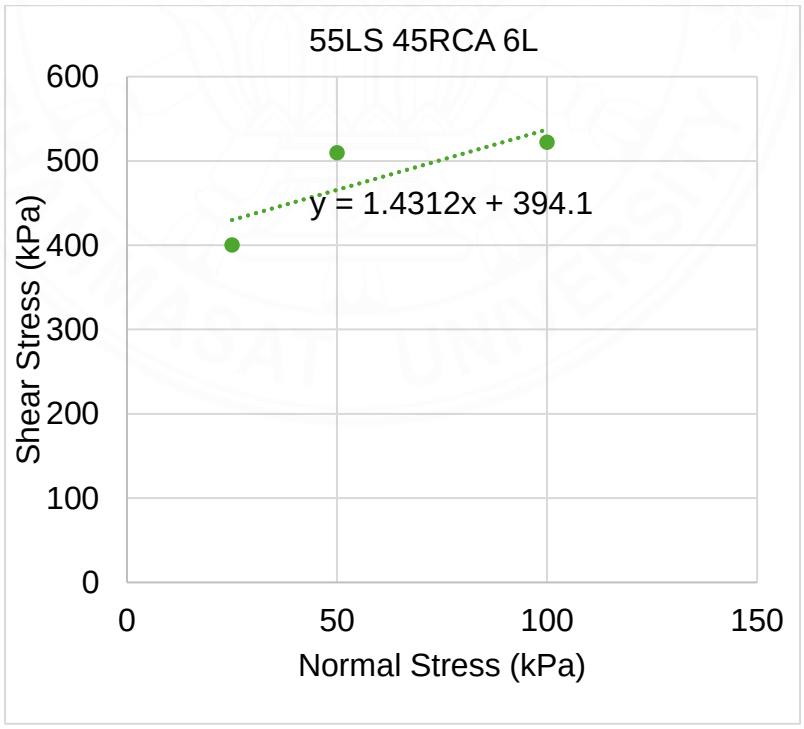

Figure A.18 Relation shear and normal stress of 55LS45RCA6L at 56 days curing period.

Ref. code: 25676522040077WTA

8. Permeability

Table A.13 k values result from different mix designs.

Mix Design	*k* (m/s)	
	28 days	56 days
100 LS	2.58E-08	3.75E-08
100LS 6L	5.29E-08	1.09E-07
70LS 30RCA 6L	5.85E-08	8.25E-08
55LS 45RCA 6L	3.86E-08	4.26E-08
55LS 45RCA	2.27E-07	3.01E-07

Table A.14 Permeability calculation of 55LS45RCA.

Length L, (m)	**D (m)**	**Area (m2)**	**Flow Vol. (m3)**	**Time (Sec)**	**Flow rate (m3/sec)**	**Pressure (kgf/m2) 1 bar = 10197 kgf/m2**	**Hydraulic Conductivity, *k* (m/sec)**	**Average, k (m/s)**
0.08203	0.1	0.007854	5.0272E-06	211.3	2.38E-08	10197	2.39E-07	2.27E-07
0.08203	0.1	0.007854	5.0272E-06	226.51	2.22E-08	10197	2.23E-07	
0.08203	0.1	0.007854	5.0272E-06	226.64	2.22E-08	10197	2.22E-07	
0.08203	0.1	0.007854	5.0272E-06	225.13	2.23E-08	10197	2.24E-07	

Ref. code: 25676522040077WTA

9. XRF (X-ray Fluorescence)

Table A.15 XRF result of laterite soil.

Component	Result	Unit	Component(Org)	Result(Org)	Unit
Na	0.0342	mass%	Na_2O	0.0460	mass%
Mg	0.6486	mass%	MgO	1.0755	mass%
Al	8.9190	mass%	Al_2O_3	16.8521	mass%
Si	32.5580	mass%	SiO_2	69.6519	mass%
P	0.0306	mass%	P_2O_5	0.0701	mass%
S	0.0128	mass%	SO_3	0.0320	mass%
K	2.8780	mass%	K_2O	3.4669	mass%
Ca	0.2952	mass%	CaO	0.4131	mass%
Ti	0.6028	mass%	TiO_2	1.0054	mass%
Cr	0.0126	mass%	Cr_2O_3	0.0184	mass%
Mn	0.0924	mass%	MnO	0.1193	mass%
Fe	4.8945	mass%	Fe_2O_3	6.9978	mass%
Ni	0.0110	mass%	NiO	0.0139	mass%
Cu	0.0062	mass%	CuO	0.0078	mass%
Zn	0.0075	mass%	ZnO	0.0094	mass%
As	0.0058	mass%	As_2O_3	0.0077	mass%
Rb	0.0363	mass%	Rb_2O	0.0397	mass%
Sr	0.0062	mass%	SrO	0.0074	mass%
Y	0.0123	mass%	Y_2O_3	0.0156	mass%
Zr	0.0430	mass%	ZrO_2	0.0581	mass%
Ba	0.0824	mass%	BaO	0.0919	mass%
H-Wax-C	0.1000	mass%			

Table A.16 XRF result of RCA.

Component	Result	Unit	Component(Org)	Result(Org)	Unit
Na	0.1646	mass%	Na_2O	0.2218	mass%
Mg	0.6368	mass%	MgO	1.0558	mass%
Al	1.9815	mass%	Al_2O_3	3.7439	mass%
Si	11.3141	mass%	SiO_2	24.2044	mass%
P	0.0300	mass%	P_2O_5	0.0687	mass%
S	0.8273	mass%	SO_3	2.0658	mass%
Cl	0.0214	mass%	-	-	-
K	1.1224	mass%	K_2O	1.3520	mass%
Ca	44.8949	mass%	CaO	62.8163	mass%
Ti	0.2155	mass%	TiO_2	0.3594	mass%
Cr	0.0166	mass%	Cr_2O_3	0.0243	mass%
Mn	0.0053	mass%	MnO	0.0068	mass%
Fe	2.6386	mass%	Fe_2O_3	3.7726	mass%
Cu	0.0056	mass%	CuO	0.0070	mass%
Zn	0.0351	mass%	ZnO	0.0437	mass%
As	0.0035	mass%	As_2O_3	0.0046	mass%
Rb	0.0196	mass%	Rb_2O	0.0215	mass%
Sr	0.0778	mass%	SrO	0.0920	mass%
Zr	0.0098	mass%	ZrO_2	0.0132	mass%
Ba	0.0938	mass%	BaO	0.1047	mass%
H-Wax-C	0.1000	mass%			

Ref. code: 25676522040077WTA

BIOGRAPHY

Name	Syaifulloh Qoimuddin
Education	2021: Bachelor of Engineering (Civil Engineering)
	Faculty of Engineering
	Universitas Muhammadiyah Yogyakarta

Ref. code: 25676522040077WTA